

People's Democratic Republic of Algeria
Ministry of Higher Education and Scientific Research
Mohamed El Bachir El Ibrahimi University of Borj Bou Arréridj
Faculty of Mathematics and Computer Science
Department of Mathematics



THESIS

In order to obtain the Doctorate degree in LMD (3rd cycle)

Branch : Applied Mathematics

Option : Differential Equations and Applications

THEME

Phase planes and bifurcations in planar linear-quadratic differential systems with a pseudo-focus

By: Meriem Barkat

Publicly defended on: 12/06/2024

In front of the jury composed of:

Dr. Aziza Berbache	University of B.B.A	President
Pr. Rebiha Benterki	University of B.B.A	Supervisor
Pr. Enrique Ponce	University of Sevilla	Co-Supervisor
Pr. Rachid Boukoucha	University of Bejaia	Examiner
Dr. Bilal Ghermoul	University of B.B.A	Examiner
Dr. Abdelkrim kina	University of Ghardaia	Examiner

2023/2024

Acknowledgement

In the name of Allah the Merciful, Praise to Allah, Lord of the Worlds, Praise be to the Lord of all worlds. Prayer and peace be upon our Prophet, Muhammad, his family and all of his companions.

Am sincerely grateful to my thesis advisor, Pr. Rebiha Benterki, from the Mathematics Department at the University Mohamed El Bachir El Ibrahimi of Bordj Bou Arréridj, for her unwavering support, motivation, enthusiasm, and vast knowledge related to my PhD thesis and research. I am also grateful to thank, Pr. Enrique Ponce from Universitat Sevilla of Espana for his comments and suggestions that helped me during this journey. His expertise and insights were instrumental in shaping the direction of my research and enhancing the quality of my work, without forgetting, Pr. Jaume Llibre from Universitat Autonoma de Barcelona, for his valuable guidance in some problems. His expertise and knowledge were instrumental in helping me complete this work.

Additionally, I wish to express heartfelt gratitude towards the members of my thesis committee: Dr. Aziza BERBACHE from the Mathematics Department, University Mohamed El Bachir El Ibrahimi of Bordj Bou Arréridj, Pr. Rachid BOUKOUCHA from the Mathematics Department, University Abderrahmane Mira of Bejaia, and Dr. GHERMOUL Bilal from the Mathematics Department, University Mohamed El Bachir El Ibrahimi of Bordj Bou Arréridj and Dr. Abdelkrim KINA University of Ghardaia.

Dedication

Alhamdulillahirabbil'alamin, praise to Allah for the blessings endowed to me so that I can accomplish this work.

I would like to express my sincerest gratitude to my advisor, Professor Benterki Rebiha, for her guidance during the process of writing this thesis. Her invaluable comments and suggestions have led to improvements of my thesis.

On a personal level, I owe hugely to my dear parents, Barkat Belkacem and Barkat Zoubida. Their permanent love and confidence in me have encouraged me to go ahead in my study.

Some special words of gratitude go to my sisters and my brother who have always been a major source of support. Thanks for always.

I also express my gratitude to my dear husband, Zedam Farid. for his constant understanding and encouragement.

Finally, I would like to dedicate this research to all those who have been affected by the subject matter of this study. It my hope that this work will contribute to the advancement of knowledge and understanding in this field and ultimately lead to positive change and progress.

Thinks you all for your unwavering support and encouragement throughout this research project.

Contents

Introduction	12
1 Basic Concepts and Preliminaries	13
1.1 Discontinuous vector fields	13
1.2 Singular points	15
1.2.1 Types of singular points	15
1.3 First integrals	16
1.4 The Poincaré map	16
1.5 Phase portrait of a vector fields	17
1.6 Poincaré compactification	18
1.7 The averaging theory up to third order	19
2 On the Limit Cycles of the Piecewise Differential systems Formed by a Linear and Hamiltonian Isochronous Center	22
2.1 Statement of the main result	23
2.1.1 Proof of Theorem 2.1	25
Appendix of chapter 2	30
3 Limit Cycles of Discontinuous Picewise Differential Systems Formed by Linear and Cubic Isochronous Centers	34
3.1 Main results	37
3.2 Proof of Theorem 3.1	38
3.3 Proof of Theorem 3.2	42

4	Limit Cycles Bifurcating From Planar Piecewise Differential Systems Formed by Linear and Cubic Centers	47
4.1	Statement of the main result	47
4.2	Proof of Theorem 4.2	49
5	Global Phase Portraits of Piecewise Quadratic Differential Systems with a Pseudo-Focus	61
5.1	Subfamilies with a pseudo-center at the origin	63
5.1.1	Finite and infinite singular points	64
5.2	Main results	73
5.2.1	Linear-quadratic differential system	73
5.2.2	Bi-parametric differential system	76
5.2.3	Quadratic Hamiltonian differential system	80
5.2.4	Reversible quadratic differential system	84
	Conclusion	91
	Bibliography	92

List of Figures

1.1	(a) Escaping, (b) sliding and (c) crossing regions.	14
1.2	Poincaré map of a piecewise differential systems.	17
2.1	(a) The unique limit cycle, (b) the two limit cycles and (c) the three limit cycles for the class of discontinuous piecewise differential system (2.1)-(2.4).	24
2.2	(a) The four limit cycles and (b) the five limit cycles for the class of discontinuous piecewise differential system (2.1)-(2.4).	24
3.1	The two limit cycles of the discontinuous piecewise differential system, (a) for (3.13)-(3.14), (b) for (3.15)-(3.16) and (c) three limit cycles of the discontinuous piecewise differential system (3.17)-(3.18) with <i>conf 2</i>	38
3.2	Three limit cycles of the piecewise differential system, (a) for (3.20)-(3.21), (b) for (3.22)-(3.23) and (c) five limit cycles of the discontinuous piecewise differential system (3.24)-(3.25) with <i>conf 3</i>	43
5.1	The global phase portraits of system (5.6) when (a) $\delta = 0$ and (b) $\delta > 0$	74
5.2	The global phase portraits of system (5.7). The cases (a) and (b) correspond with $\delta = 0$, while the remaining pictures are for $\delta > 0$	77
5.3	The bifurcation set in the plane (d, δ) for system (5.7) when $\delta \geq 0$. The labels in lines or open regions indicate the different global phase portraits, according to Figure 5.2. Note the bifurcation curve given by $d = -3\delta^2$, whose points correspond to the global phase portrait of Figure 5.2(d), separating the ones of Figures 5.2(c) and 5.2(e).	78

5.4	The different global phase portraits of system (5.8). The cases (a)-(c) correspond with $\delta = 0$, while the remaining pictures are for $\delta > 0$ and correspond to the different regions of Figure 5.5.	83
5.5	Bifurcation set of system (5.8) for $\delta > 0$. Note that by using Lemma 5.1(b), it is immediate to deduce the global phase portraits for the portion of the diagram which is symmetric with respect to the dashed main diagonal. . .	83
5.6	According to the bifurcation set of Figure 5.7, for $\delta = 0$ and $d \geq 0$ we have an unbounded periodic annulus. If we except the focus case (not shown), then such periodic annulus is limited from below because of the existence of invariant straight lines. We represent in (a) the singular case $d = 0$, in (b) the node case $0 < d < t^2/4$, and in (c) the improper node case $0 < d = t^2/4$.	85
5.7	Bifurcation set of system (5.9) for $\delta = 0$ in the half-plane (d, t) with $t \geq 0$. We indicate the saddle region R, the node region N, the improper node curve IN and the focus region F.	85
5.8	Some global phase portraits of system (5.10), where we assume $t > 0$, $d < 0$, and $\delta > 0$. The case (a) corresponds to $\delta > 0$, $d < 0$ and $4\delta t + d = 0$ (at the right saddle-node bifurcation straight line of Figure 5.9).	89
5.9	Partial bifurcation set of system (5.10) in the parameter plane $(\tilde{t}, \tilde{d}) = (t/\delta, d/\delta^2)$ when $\delta > 0$. The two thick half-straight lines emanating from the origin are saddle-node bifurcation curves, and we also show two nearby curves where the node becomes a focus. At the vertical axis we have $t = 0$, so that the system becomes piecewise-Hamiltonian, leading to the particular case $d_+ = d_- = d$, which is within the previous family (5.8).	90

List of Articles

- Rebiha Benterki, Meriem Barkat, Limit cycles of discontinuous piecewise differential systems formed by linear and cubic isochronous centers. *J. Math. Comput. Sci.* 12 (2022).
- Meriem Barkat, Rebiha Benterki, Jaume Llibre, The extended 16th Hilbert problem for a class of discontinuous piecewise differential systems. *Nonlinear Dyn* 111. 1475–1484 (2023).
- Meriem Barkat, Rebiha Benterki, Limit cycles of discontinuous piecewise differential systems formed by linear and cubic centers via averaging theory. *Differ Equ Dyn Syst* (2024).
- Meriem Barkat, Rebiha Benterki, Enrique Ponce, Global phase portraits of piecewise quadratic differential systems with a pseudo-center. *International Journal of Bifurcation and Chaos*. Vol. 34, No. 3 (2024).

List of Conferences

International conferences

- The solution of the extended 16th Hilbert problem for a new class of discontinuous piecewise differential systems: International E-conference on pure and applied mathematical sciences. Tunisia, (ICPAMS-2022) 04-07 May 2022.
- Averaging methods for piecewise differential systems formed by a linear focus or center and a cubic weak focus or center: International conference of young mathematician. Ukraine, 01-03 June 2023.

National conferences

- The 16th Hilbert problem for discontinuous piecewise differential centers separated by irregular line: The first national conference on mathematics and its applications. Bordj Bou Arréridj, (CNMA-2021) 13-14 december 2021.
- Crossing limit cycles for a class of piecewise differential system separated by straight line: The second national conference on mathematics and its applications. Bordj Bou Arréridj, (CNMA-2022) 28 september 2022.

Introduction

Within the realm of piecewise differential systems, the family of piecewise linear differential systems plays an important role in modeling many real processes, see for instance [14, 52, 60]. The study of these systems in the plane separated by a straight line goes back to Andronov, Vitt and Khaikin [1] in 1920 and until now such systems have deserved the attention of many researchers.

In the qualitative theory of planar differential systems a *limit cycle* is an isolated periodic orbit in the set of all periodic orbits of such system, this concept was defined at the end of the 19th century by Poincaré which also introduced other fundamental concepts, such as the *phase portrait*, which is a compilation of minimal information enabling to determine the topological structure of the orbits of a differential system, and the notion of a *return map*, commonly recognized as the *Poincaré map*, see [48, 55]. Limit cycles have played and still playing an important role for explaining many phenomena of the real world, as for instance, the one of the Belousov Zhabotinsky model [8] or the motion of the galaxies [22] and the periodicity of oscillations in RLC circuits and the existence of isolated periodic orbits [62].

In general to find an upper bound for the maximum number of limit cycles that a given class of piecewise differential systems can exhibit has remained an open problem until now; this problem is known as the extended 16th Hilbert problem, which states to find an upper bound for the maximum number of limit cycles that the class of polynomial differential systems of a given degree can have, see [35, 36, 38]. The dynamics along the discontinuity curves are defined according to Filippov's conventions [27]. We can exhibit two kinds of limit cycles, the crossing and the sliding ones, in our work we deal with the crossing limit cycle which only contain isolated points on the line of the discontinuity curve.

Several authors have tried to determine the upper bound of limit cycles for the discontinuous piecewise differential systems separated by a straight line. In 2001 Giannakopoulos and Pliete [31] proved the existence of two limit cycles for the discontinuous piecewise linear differential systems with a line of discontinuity. In 2010 Han and Zhang [34] conjectured that discontinuous piecewise linear differential systems in \mathbb{R}^2 separated by a straight line have at most two crossing limit cycles, but in 2012 Llibre and Ponce [46] provided a negative answer to this conjecture by presenting an example illustrate three limit cycles. Braga and Mello [18], Buzzi et al. [19], Liping Li [39], Freire et al. [30], and Llibre et al. [45] obtained also three crossing limit cycles for discontinuous piecewise linear differential systems separated by a straight line. But until now it is unknown whether three is the maximum number of limit cycles in this family.

An additional issue that will be examined is a localized version of the Hilbert problem which requires determining the maximum number of limit cycles of small amplitude that bifurcate from an equilibrium point in the planar polynomial vector field of degree n . This problem is also known as the cyclicity problem, and its solution is essential for understanding the behavior of such vector fields. There are various methods to study the number of limit cycles that can bifurcate from the period orbit. The most important and widely used ones are the Poincaré return map, Melnikov function and the averaging method which are essentially equivalent in the plane. The averaging method has a long history, dating back to the classical works of Lagrange and Laplace, who intuitively justified the process. In 1928, Fatou [26] formalized this theory. Significant practical and theoretical contributions to the averaging method were made in 1930's by Bogoliubov-Krylov [16] and in 1945 by Bogoliubov. This technique, originally created for smooth systems, has recently been applied to research on limit cycle of discontinuous piecewise smooth systems, see [42, 63]. The authors of the articles [33, 44] developed the averaging method for discontinuous piecewise differential systems and showed a relationship between the number of limit cycles of the corresponding differential system and the zeros of the averaged functions of periodic differential equations, see for instance [32, 41].

For the the global dynamics of piecewise differential systems there are some works present the global phase portraits of piecewise linear differential systems. In 2019 Li and Llibre [40] classified the global phase portraits of continuous piecewise linear differential systems separated by a straight line in 2020 Chen et al. [21], provided the global phase portraits of a non-symmetric piecewise linear differential system with three zones. Recently, [58, 59, 66] studied the global phase portraits of planar refracting piece-

wise linear differential systems with FS (The system with two regions has a focus and a saddle), and the more interesting case of planar discontinuous piecewise linear differential systems of the focus-center type [65]. However, there are few works that have completely classified the global phase portraits of planar piecewise smooth nonlinear differential systems, and even for smooth differential systems, only a few families have been completely studied see for instant [56].

Regarding piecewise quadratic differential systems, the situation is more unsatisfactory. As indicated in [3] the number of parameters of a quadratic system is essentially five, but when considering piecewise quadratic such a number, roughly speaking, is multiplied by two. Thus, to afford a complete analysis, any contribution in this area needs to consider specific families with a lower number of parameters, see [3, 64] and references therein. In fact obtaining normal forms which simplify the expression of the vector field for discontinuous piecewise differential systems is an intricate issue, due to the presence of different vector fields separated by a common boundary. The iterative changes of variables must be selected based on the region where the vector fields are defined. Additionally, the points of the discontinuity line must be invariant under the different changes of variables to ensure topological equivalence between the initial and reduced vector fields. Therefore, the standard theory of normal forms cannot be applied to study the dynamical behavior of discontinuous piecewise smooth vector fields in the neighborhood of a pseudo-equilibrium point. However, some papers have proposed normal forms and limit cycle bifurcation from piecewise smooth vector fields, including those with a pseudo-focus, see for example [24].

Summarizing, this work consists five chapters. The first Chapter we present some preliminaries, terminology to clarify this work.

In the second chapter, we solve the second part of 16th Hilbert problem for a planar discontinuous piecewise differential systems formed by a linear center and a class of Hamiltonian isochronous global center separated by straight line.

In Chapter three we study the existence and the upper bound of limit cycles for discontinuous planar piecewise differential systems formed by linear and three families of isochronous cubic centers separated by irregular line. We provide the maximum number of limit cycles that these classes of discontinuous piecewise differential systems can exhibit.

In the fourth chapter and by using the averaging method up to third order, we are

interested in determining an upper bound for the maximum number of limit cycles bifurcating from the periodic orbits for the discontinuous piecewise differential systems formed by a linear focus or center and a cubic weak focus or center separated by one straight line. More specifically, at each order of the averaging theory from order one to order three we give the maximum number of limit cycles for a given discontinuous piecewise differential systems.

And finally, in the fifth chapter we are interesting in providing the global phase portraits and the bifurcation sets for some specific families of discontinuous piecewise quadratic differential systems, characterized by having a singular point at the origin, which belongs to the discontinuity manifold. More precisely, the origin is assumed to be a special pseudo-focus, with a double invisible tangency surrounded by crossing periodic orbits forming a periodic annulus. In short, the origin is a pseudo-center.

Basic Concepts and Preliminaries

In this chapter we introduce some fundamental concepts and results for the development of the study of discontinuous vector fields defined in two or more zones. We discuss some definitions related with our work such as: discontinuous piecewise differential system, singular points, phase portraits, limit cycles, . . . , etc.

We also define the averaging method, which involves of finding the number of limit cycles that appear after the perturbation of a differential system.

Section 1.1 Discontinuous vector fields

DEFINITION 1.1 (Piecewise smooth vector field) *A discontinuous piecewise differential system on \mathbb{R}^2 is a pair of C^k differential systems with $k \geq 1$, separated by a smooth curve Σ . The discontinuity manifold Σ is obtained by considering $\Sigma = f^{-1}(0)$, where $f : \mathbb{R}^2 \rightarrow \mathbb{R}$ is a smooth function having 0 as a regular value. Usually, a piecewise smooth vector field is written as*

$$N(\mathbf{x}) = \begin{cases} X(x, y), & \text{if } f(x, y) \geq 0, \\ Y(x, y), & \text{if } f(x, y) \leq 0. \end{cases} \quad (1.1)$$

For more details see [17].

For any point $(x, y) \in \Sigma$, that is, fulfilling $f(x, y) = 0$, these transversal components are easily computed by considering the orbital derivatives of the function f , namely $Xf(x_0) = \langle \nabla f(x, y), X(x, y) \rangle$. We can divide the discontinuity line into two important

subsets:

(a) Crossing set $\Sigma^c = \{x_0 \in \Sigma : Xf(x_0) \cdot Yf(x_0) > 0\}$,

(b) Sliding set $\Sigma^s = \{x_0 \in \Sigma : Xf(x_0) \cdot Yf(x_0) \leq 0\}$.

Furthermore, within the sliding set, it is usual to consider its attractive part

$$\Sigma^{as} = \{x_0 \in \Sigma : Xf(x_0) < 0 \text{ and } Yf(x_0) > 0\},$$

and its repulsive part

$$\Sigma^{rs} = \{x_0 \in \Sigma : Xf(x_0) > 0 \text{ and } Yf(x_0) < 0\},$$

sometimes referred as the *escaping set*.

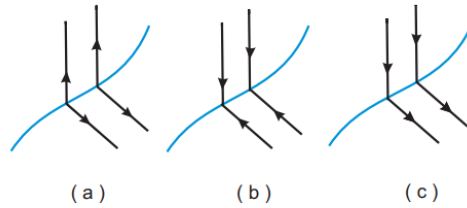


Figure 1.1: (a) Escaping, (b) sliding and (c) crossing regions.

If $x_0 \in \Sigma$ and $Xf(x_0) = 0$ or $(Yf(x_0) = 0)$ we say that x_0 is a tangency point of X or (Y) . Furthermore, we say that the point x_0 is a visible (invisible) tangency point if the local flow of $X(x_0)$ remains in the region $f(x, y) > 0$ ($f(x, y) < 0$). We can argue in an analogous way for tangency points regarding Y .

For points $q \in \Sigma^{as} \cup \Sigma^{rs}$, the so-called sliding vector field is given by

$$g(q) = \frac{Yf(q)X(q) - Xf(q)Y(q)}{Yf(q) - Xf(q)}. \quad (1.2)$$

Any point $p \in \Sigma^s$ satisfying $g(p) = 0$ acts in some sense as an equilibrium point of our system and it will be called pseudo-equilibrium point. See [17]

A pseudo-focus or fused focus is a double invisible tangency point with close orbits spiraling around it. When a pseudo-focus is surrounded by crossing periodic orbits filling in a certain neighborhood of the point, it is called a pseudo-center.

A stable pseudo-node is formed when a pseudo-equilibrium is present in the attractive part of the sliding set with $g'(q) < 0$. While a pseudo-saddle is formed if $g'(q) > 0$. Similarly, a unstable pseudo-node is formed when a pseudo-equilibrium is present in the repulsive part with $g'(q) > 0$, while a pseudo-saddle is formed if $g'(q) < 0$. For more details see [47].

Section 1.2 Singular points

Consider the autonomous equation

$$\dot{x} = F(x), \tag{1.3}$$

with $F : \mathcal{D} \rightarrow \mathbb{R}^n$ be a continuous function in an open set $\mathcal{D} \subset \mathbb{R}^n$.

The set \mathcal{D} is called the phase space of the differential equation (1.3).

DEFINITION 1.2 (Singular points)

A point $x_0 \in \mathbb{R}^n$ satisfying $F(x_0) = 0$ is called an equilibrium point (or a singular point) of (1.3). If there are no equilibrium point in the neighbourhood of the equilibrium point other than x_0 , then x_0 is called an isolated singularity. See [54].

DEFINITION 1.3 (Singular points of piecewise vector field)

A point $x_0 \in \mathbb{R}^2 \setminus \Sigma$ is called real (virtual) singularity or equilibrium of X if $X(x_0) = 0$ and $f(x_0) > 0$ ($f(x_0) < 0$). Similarly, a point x_0 is called real (virtual) singularity or equilibrium of Y if $Y(x_0) = 0$ and $f(x_0) < 0$ ($f(x_0) > 0$). For more details see [39].

1.2.1 Types of singular points

DEFINITION 1.4 The local behavior of the flow near a singular point x_0 of a planar C^k vector field $\mathcal{X} = (P, Q)$ is intricate, as evidenced by the diverse classes of behavior exhibited by linear systems, even for local topological equivalence.

The linear part of the vector field \mathcal{X} at x_0 written as

$$D\mathcal{X}(x_0) = \begin{pmatrix} \frac{\partial P}{\partial x}(x_0) & \frac{\partial P}{\partial y}(x_0) \\ \frac{\partial Q}{\partial x}(x_0) & \frac{\partial Q}{\partial y}(x_0) \end{pmatrix}.$$

The equilibrium points of a differential system in \mathbb{R}^2 are classified into *hyperbolic*, *semi-hyperbolic*, *nilpotent* and *linearly zero*.

The *hyperbolic* ones are the equilibrium points with all eigenvalues have nonzero real part. The *semi-hyperbolic* points are the ones having a unique eigenvalue equal to zero. The *nilpotent* singular points have a linear part is not identically zero with both zero eigenvalues. Finally when the linear component is identically zero we talking about *linearly zero* singular points which studies their local phase portraits by using the so-called Blow-ups, see for instance chapter 2 and 3 of [23].

Section 1.3 First integrals

For a given polynomial differential systems of the form

$$\frac{dx}{dt} = P(x, y), \quad \frac{dy}{dt} = Q(x, y), \quad (1.4)$$

where the degree of the systems is defined as $m = \max\{\deg P, \deg Q\}$ with a vector field $\mathcal{X} = (P, Q)$. System (1.4) is integrable on an open subset U of \mathbb{R}^n if there exists a non constant analytic function $H : U \rightarrow \mathbb{R}$ called a first integral of the system on U , with $H(x(t), y(t)) = \text{constant}$. See [51].

Section 1.4 The Poincaré map

The Poincaré map is a one of the best important tools for studying the behavior of dynamical systems in the neighborhood of periodic orbits. Let F be a locally Lipschitz vector field $F : U \rightarrow \mathbb{R}^n$ with U is an open set of \mathbb{R}^n and let $\phi(t, x)$ be the flow defined of the differential equation (1.3). Take a point $p \in L \cap U$ with L is a hypersurface in \mathbb{R}^n if $F(p)$ is not contained in the tangent space to L at the point p we say that the flow ϕ is transverse to L at point p , and p is called a contact point of the flow with L if $F(p) \in T_p L$. The flow ϕ is transverse to L at V if it is transverse to L at every point in the open subset

V .

Consider now two points $p_1 \in L_1 \cap U$ and $p_2 \in L_2 \cap U$ with L_1, L_2 are two open hypersurfaces such that $p_2 = \phi(p_1, s_1)$. There exist a function $\tau : V_1 \rightarrow R$ satisfying $\tau(p_1) = s_1$ and $\phi(q, \tau(q)) \in V_2$ for every $q \in V_1$, with V_1 is a neighborhood of p_1 in $L_1 \cap U$ and V_2 is a neighborhood of p_2 in $L_2 \cap U$. We define the Poincaré map in this case as the map $\pi : V_1 \rightarrow V_2$ given by $\pi(q) = \phi(q, \tau(q))$, for every $q \in V_1$.

When the vector field is globally Lipschitz, C^r with $r \geq 1$ or analytic, the Poincaré map π is also continuous, C^r with $r \geq 1$ or analytic, we conclude that the Poincaré map is invertible by reversing the sense of the flow and its inverse map π^{-1} is continuous, C^r with $r \geq 1$ or analytic, respectively. In the case that $L_1 = L_2$ the Poincaré map π will be called a return map. For more details see [50].

REMARK 1 *When we consider the piecewise differential systems the Poincaré map consists of two half return maps that are defined by using orbits in either side of the switching manifold.*

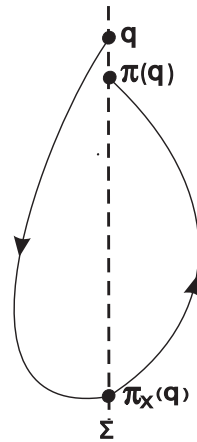


Figure 1.2: Poincaré map of a piecewise differential systems.

Section 1.5 Phase portrait of a vector fields

It is very difficult to determine explicitly the solutions of a differential system, but it is important to get information about these solutions this can be done by describing the phase portrait of the differential equation.

DEFINITION 1.5 A phase portraits or the phase plane of the vector field given by (1.3) is the set of all trajectories of the system. See for instance [61].

DEFINITION 1.6 (Periodic solutions) Let $\varphi(t, x)$ be a solution of (1.3). If there exists a finite time $T > 0$ such that $\varphi(t+T, x) = \varphi(t, x)$ for $t \in \mathbb{R}$, then $\varphi(t, x)$ is a periodic solution of (1.3) of period T . See for instance [61].

DEFINITION 1.7 (Limit cycle) A limit cycle is an isolated periodic trajectory of a differential system. In other word, for small arbitrarily neighborhood of the periodic trajectory there are no other periodic trajectory. See for instance [61].

Section 1.6 Poincaré compactification

In this section we give some basic results for studying the behavior of the trajectories of a polynomial differential systems in \mathbb{R}^2 near infinity.

Consider a planar vector field

$$\mathcal{X} = P(x_1, x_2) \frac{\partial}{\partial x_1} + Q(x_1, x_2) \frac{\partial}{\partial x_2}, \quad (1.5)$$

where $P(x_1, x_2)$, $Q(x_1, x_2)$ are polynomials of degree n in the variables x_1 and x_2 . We consider the phase plane \mathbb{R}^2 as the plane in \mathbb{R}^3 defined by $(y_1, y_2, y_3) = (x_1, x_2, 1)$, so that it becomes tangent to the Poincaré sphere

$$\mathbb{S}^2 = \{y = (y_1, y_2, y_3) \in \mathbb{R}^3 : y_1^2 + y_2^2 + y_3^2 = 1\}.$$

Using central projection, we can induce a vector field on \mathbb{S}^2 getting two copies of the flow on \mathbb{R}^2 , one for each hemisphere. We denote by $p(\mathcal{X})$ the Poincaré compactification of \mathcal{X} on \mathbb{S}^2 , being

$$\mathbb{S}^1 = \{(y_1, y_2, y_3) \in \mathbb{R}^3 : y_1^2 + y_2^2 + y_3^2 = 1, y_3 = 0\}$$

the equator of \mathbb{S}^2 , which captures all the points at infinity. As usual, we can consider the six local charts $U_i = \{y \in \mathbb{S}^2 : y_i > 0\}$ and $V_i = \{y \in \mathbb{S}^2 : y_i < 0\}$ for the calculation of the expression of $p(\mathcal{X})$, with $i = 1, 2, 3$. We use the same notation (u, v) for variables in

every local chart, even if its meaning depends on the specific chart under consideration. For instance, in U_1 and V_1 we have $(u, v) = (x_2/x_1, 1/x_1)$, while in U_2 and V_2 we have $(u, v) = (x_1/x_2, 1/x_2)$.

As shown in [23], the expression for the extension of $p(\mathcal{X})$ in the local chart U_1 , which allows the analysis of the singularities at the equator, is given by

$$\begin{cases} \dot{u} = v^n \left[-uP\left(\frac{1}{v}, \frac{u}{v}\right) + Q\left(\frac{1}{v}, \frac{u}{v}\right) \right], \\ \dot{v} = -v^{n+1}P\left(\frac{1}{v}, \frac{u}{v}\right), \end{cases} \quad (1.6)$$

while when considering the local chart U_2 , we get

$$\begin{cases} \dot{u} = v^n \left[P\left(\frac{u}{v}, \frac{1}{v}\right) - uQ\left(\frac{u}{v}, \frac{1}{v}\right) \right], \\ \dot{v} = -v^{n+1}Q\left(\frac{u}{v}, \frac{1}{v}\right). \end{cases} \quad (1.7)$$

Note that the expression for the corresponding differential system in the local chart V_j is the same than in the chart U_j multiplied by $(-1)^{n-1}$, for $j = 1, 2$. See Chapter 5 in [23].

THEOREM 1.1 *Two phase portraits of the two polynomial differential systems $p(\mathcal{X})$ and $p(\mathcal{Y})$ are topologically equivalent if there exists a homeomorphism that sends orbits of $p(\mathcal{X})$ to orbits of $p(\mathcal{Y})$ either preserving or reversing the orientation of all orbits. See [12].*

Section 1.7 The averaging theory up to third order

The averaging theory is a powerful tool for studying the number of limit cycles of differential systems. This method has been used to study limit cycle and determine the the upper bound of limit cycles that can be bifurcated from the periodic orbits of a given system.

By introducing the main result, we aim to apply this theory to effectively study and understand the behavior of such systems.

We consider the following discontinuous differential system

$$\dot{r}(\theta) = \begin{cases} F^+(\theta, r, \varepsilon), \\ F^-(\theta, r, \varepsilon). \end{cases} \quad \theta \in \mathcal{S}^1, \quad (1.8)$$

where $F^\pm(\theta, r, \varepsilon) = \sum_{i=0}^3 \varepsilon^i F_i^\pm(\theta, r) + \varepsilon^4 R^\pm(\theta, r, \varepsilon)$, $\theta \in S^1$ and $r \in D$ where D is an open interval of \mathbb{R}^+ .

A fundamental inquiry in the investigation of discontinuous differential system (1.8) revolves around comprehending which periodic orbits of the unperturbed system $\dot{r}(\theta) = F^\pm(\theta, r)$ persists for $|\varepsilon|$ sufficiently small. To address this, we introduce a set of functions $f_i : D \rightarrow \mathbb{R}$, for $i = 1, 2, \dots, k$, called averaged functions, such that their simple zeros provide the existence of isolated periodic solutions of the differential system (1.8). In [43] it was proved that these averaged functions are given by $f_i = \frac{y_i(2\pi, r)}{i!}$ where $y_i : \mathbb{R} \times D \rightarrow \mathbb{R}$, are defined by the following integrals

$$\begin{aligned} y_1^\pm(s, r) &= \int_0^s F_1^\pm(t, r) dt, \\ y_2^\pm(s, r) &= \int_0^s \left(2F_2^\pm(t, r) + 2\partial F_1^\pm(t, r) y_1^\pm(t, r) \right) dt, \\ y_3^\pm(s, r) &= \int_0^s \left(6F_3^\pm(t, r) + 6\partial F_2^\pm(t, r) y_1^\pm(t, r) + 3\partial^2 F_1^\pm(t, r) y_1^\pm(t, r)^2 + 3\partial F_1^\pm(t, r) y_2^\pm(t, r) \right) dt. \end{aligned}$$

Also, we have the functions

$$\begin{aligned} f_1^\pm(r) &= \int_0^{\pm\pi} F_1^\pm(t, r) dt, \\ f_2^\pm(r) &= \int_0^{\pm\pi} \left(F_2^\pm(t, r) dt + \partial F_1^\pm(t, r) y_1^\pm(t, r) \right) dt, \\ f_3^\pm(r) &= \int_0^{\pm\pi} \left(F_3^\pm(t, r) dt + \partial F_2^\pm(t, r) y_1^\pm(t, r) + \frac{1}{2} \partial^2 F_1^\pm(t, r) y_1^\pm(t, r)^2 + \frac{1}{2} \partial F_1^\pm(t, r) y_2^\pm(t, r) \right) dt. \end{aligned}$$

For more details see [37].

The function $f_k(r) = f_k^+(r) + f_k^-(r)$ called the averaged function of order k . The simple positive real roots of the functions $f_{l+1}(r)$ which satisfy $f_l(r) = 0$ for every $l \in \{1, 2\}$ but $f_{l+1}(r) \neq 0$, provide limit cycles of the piecewise differential system (1.8).

In order to know the number of zeros of a real polynomial, we are going to use the following Lemma.

LEMMA 1.1 Consider $p + 1$ linearly independent functions $f_i : U \subset \mathbb{R} \rightarrow \mathbb{R}$, $i = 0, 1, \dots, p$

(i) Given p arbitrary values $x_i \in U$, $i = 1, \dots, p$ there exist $p + 1$ constants C_i , $i =$

$0, 1, \dots, p$ such that

$$f(x) := \sum_{i=0}^p C_i f_i(x) \tag{1.9}$$

is not the zero function and $f(x_i) = 0$ for $i = 0, 1, \dots, p$.

- (ii) If all f_i are analytical functions on U and there exists $j \in \{1, \dots, p\}$ such that $f_j|_U$ has constant sign, it is possible to get an f given by (1.9), such that it has at least p simple zeroes in U .

See Proposition 1 of [48].

On the Limit Cycles of the Piecewise Differential systems Formed by a Linear and Hamiltonian Isochronous Center

This chapter is devoted to study the extended 16th Hilbert problem of two families of planar differential systems, the first one is a linear center and the second one is a family of Hamiltonian isochronous global center. By using the first integrals, we prove a sharp upper bound for the maximum number of crossing limit cycles that these classes of discontinuous piecewise differential systems can exhibit.

The following lemma provides a normal form for a linear differential center.

LEMMA 2.1 *Through a linear change of variables and a rescaling of the independent variable every linear differential center in \mathbb{R}^2 can be written as*

$$\begin{aligned} \dot{x} &= b - ax - \frac{a^2 + \omega^2}{d}y, \\ \dot{y} &= c + dx + ay, \text{ with } \omega > 0 \text{ and } d > 0, \end{aligned} \quad (2.1)$$

its first integral is

$$H_1(x, y) = \omega^2 y^2 + (ay + dx)^2 - 2d(by - cx). \quad (2.2)$$

For a proof of Lemma 2.1 see [49].

We consider the class of Hamiltonian isochronous global center of the form

$$\dot{x} = -(\delta nxy^{n-1} + \delta^2 ny^{2n-1} + y), \quad \dot{y} = \delta y^n + x, \quad (2.3)$$

with $n \in \mathbb{N}$ and $\delta \neq 0$. The first integral of system (2.3) is given by

$$H(x, y) = \frac{1}{2}((\delta y^n + x)^2 + y^2).$$

For more details on the Hamiltonian system (2.3) see Theorem B of [53] and Theorem 2.3 of [57].

The Hamiltonian isochronous global center (2.3) after an affine change of variables

We present the expression of the class of Hamiltonian isochronous global center (2.3) and its first integral after a general affine change of variables $(x, y) \rightarrow (a_1x + b_1y + c_1, \alpha_1x + \beta_1y + \gamma_1)$, with $b_1\alpha_1 - a_1\beta_1 \neq 0$.

The Hamiltonian isochronous global center (2.3) is given as

$$\begin{aligned} \dot{x} &= \frac{-1}{(b_1\alpha_1 - a_1\beta_1)}(-b_1(a_1x + b_1y + c_1 + (\gamma_1 + x\alpha_1 + y\beta_1)^n\delta) - \frac{1}{(\gamma_1 + x\alpha_1 + y\beta_1)} \\ &\quad (\beta_1((x\alpha_1 + y\beta_1 + \gamma_1)^2 + n(a_1x + b_1y + c_1)(\gamma_1 + x\alpha_1 + y\beta_1)^n\delta + n(x\alpha_1 + y\beta_1 \\ &\quad + \gamma_1)^{2n}\delta^2))), \\ \dot{y} &= \frac{-1}{(b_1\alpha_1 - a_1\beta_1)}(a_1(a_1x + b_1y + c_1 + (x\alpha_1 + y\beta_1 + \gamma_1)^n\delta) + \frac{1}{(\gamma_1 + x\alpha_1 + y\beta_1)} \\ &\quad (\alpha_1((\gamma_1 + x\alpha_1 + y\beta_1)^2 + n(a_1x + b_1y + c_1)(\gamma_1 + x\alpha_1 + y\beta_1)^n\delta + n(\gamma_1 + x\alpha_1 + y \\ &\quad \beta_1)^{2n}\delta^2))), \end{aligned} \quad (2.4)$$

with its first integral

$$H_2(x, y) = \frac{1}{2}((x\alpha_1 + y\beta_1 + \gamma_1)^2 + (a_1x + b_1y + c_1 + (y\beta_1 + \gamma_1 + x\alpha_1)^n\delta)^2).$$

Section 2.1 Statement of the main result

Our objective is to provide the maximum number of limit cycles with two points on the line of discontinuity $x = 0$ for a class of discontinuous planar differential system formed by a linear center and a class of Hamiltonian isochronous global center. First, we solved the problem for $n = 1$ to $n = 6$, and then we tried to solve it for an arbitrary n .

Our main result is the following.

THEOREM 2.1 *The maximum number of limit cycles of discontinuous piecewise differential system (2.1)-(2.3) after an arbitrary affine change of variables separated by the straight line $x = 0$ is*

- (a) zero for $n = 1$;
- (b) at most one for $n = 2$, and this maximum is reached, see Figure 2.1(b);
- (c) at most two for $n = 3$, and this maximum is reached, see Figure 2.1(c);
- (d) at most three for $n = 4$, and this maximum is reached, see Figure 2.1(d);
- (e) at most four for $n = 5$, and this maximum is reached, see Figure 2.2(a);
- (f) at most five for $n \geq 6$, and this maximum is reached, see Figure 2.2(b).

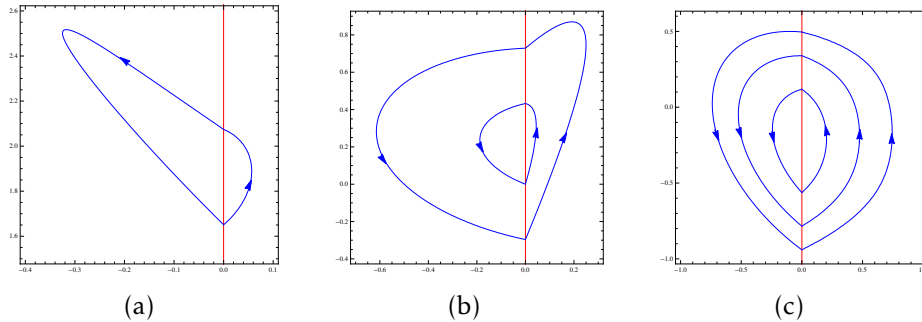


Figure 2.1: (a) The unique limit cycle, (b) the two limit cycles and (c) the three limit cycles for the class of discontinuous piecewise differential system (2.1)-(2.4).

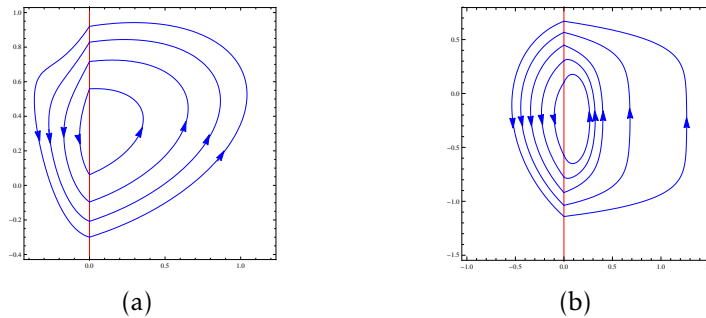


Figure 2.2: (a) The four limit cycles and (b) the five limit cycles for the class of discontinuous piecewise differential system (2.1)-(2.4).

2.1.1 Proof of Theorem 2.1

We shall prove that the maximum number of crossing limit cycles in the family of system formed by a linear center and a class of Hamiltonian isochronous global center is at most five.

Proof.

The statement (a) of Theorem 2.1 has already been proved in Theorem 4 of [49] and in Theorem 3 of [45].

In one region, we consider the linear differential center (2.1) with its first integral $H_1(x, y)$. In the other region, we consider the Hamiltonian isochronous global center (2.4) with its first integral $H_2(x, y)$.

Our objective is to prove that the discontinuous piecewise differential system formed by system (2.1)-(2.4) have limit cycles intersecting the line of discontinuity $x = 0$ in two points $(0, y)$ and $(0, Y)$, with $y \neq Y$. We know that these two points must satisfy the system of equations

$$\begin{aligned} e_1 &= H_1(0, y) - H_1(0, Y) = -(y - Y)(-(a^2 + w^2)(y + Y) + 2bd) = 0, \\ e_2 &= H_2(0, y) - H_2(0, Y) = \frac{1}{2}(y - Y)Q_i(y, Y) = 0, \end{aligned} \quad (2.5)$$

with $i \in \{1, 2, 3, 4, 5\}$. Since $y \neq Y$, then by solving $e_1 = 0$ we know that $Y = \frac{2bd}{a^2 + w^2} - y = f(y)$. Substituting the expression of Y in $Q_i(y, Y) = 0$, we obtain an equation $G_i(y) = 0$ in the variable y .

Proof of statement (b) of Theorem 2.1. For $n = 2$, the solutions of system (2.5) are equivalently the solutions of the quadratic equation $G_1(y) = 0$, where

$$\begin{aligned} G_1(y) &= \frac{1}{(a^2 + w^2)^3} (2((a^2 + w^2)(b_1 \delta(-2b\beta_1 d(a^2 + w^2)(\beta_1 y - 2\gamma_1) + (a^2 + w^2)^2 \gamma_1^2 + \beta_1^2 y^2) \\ &\quad + 4b^2 \beta_1^2 d^2) + b_1 c_1 (a^2 + w^2)^2) + \beta_1 \gamma_1 (a^2 + w^2) + b\beta_1 d)(2\delta^2(-2b\beta_1 d(a^2 + w^2)(\beta_1 y \\ &\quad - \gamma_1) + (a^2 + w^2)^2 \gamma_1^2 + \beta_1^2 y^2) + 2b^2 \beta_1^2 d^2) + 2c_1 \delta (a^2 + w^2)^2 + (a^2 + w^2)^2) + bb_1^2 d (a^2 \\ &\quad + w^2)^2)). \end{aligned}$$

This equation has at most two real solutions y_1 and y_2 . Consequently, system (2.5) has at most two real solutions namely $(y_1, f(y_1))$ and $(y_2, f(y_2))$. The two solutions are symmetric in the sense that $(y_1, f(y_1)) = (f(y_2), y_2)$. Then both solutions provide the same limit cycle for the

discontinuous piecewise differential system (2.1)-(2.4).

Now we provide an example of a discontinuous piecewise differential system (2.1)-(2.4) with one limit cycle. Then, in the half plane $R_1 = \{(x, y) : x > 0\}$ and by taking $(a, b, c, d, w) \simeq (-1, 4, \frac{5}{2}, 7.91671, 4)$, we obtain a linear differential center in the form (2.1) with its first integral $H_1(x, y)$. In the half plane $R_2 = \{(x, y) : x < 0\}$ we choose the following parameters $(\alpha_1, \beta_1, \gamma_1, a_1, b_1, c_1, \delta) \simeq (3, \frac{2}{5}, -\frac{11}{2}, 5, -9, -6, 1)$, then we obtain a Hamiltonian isochronous global center in the form (2.4) with its first integral $H_2(x, y)$. Thus, the unique real solution of system (2.5) is $(y, Y) \simeq (1.65085, 2.07466)$. So, the discontinuous piecewise differential system (2.1)-(2.4) has one limit cycle shown in Figure 2.1(a).

Proof of statement (c) of Theorem 2.1. For $n = 3$, the solutions of system (2.5) are equivalently the ones of the quartic equation $G_2(y) = 0$, where

$$G_2(y) = \frac{1}{(a^2 + w^2)^5} (2\beta_1(c_1\delta(a^2 + w^2))^3(-2b\beta_1d(a^2 + w^2))\beta_1y - 3\gamma_1) + (a^2 + w^2)^2(3\gamma_1^2 + \beta_1^2y^2) + 4b^2\beta_1^2d^2) + \delta^2(\gamma_1(a^2 + w^2) + b\beta_1d)(-2b\beta_1d(a^2 + w^2))(3\beta_1y - \gamma_1) + (a^2 + w^2)^2(\gamma_1^2 + 3\beta_1^2y^2) + 4b^2\beta_1^2d^2)(-2b\beta_1d(a^2 + w^2))\beta_1y - 3\gamma_1) + (a^2 + w^2)^2(3\gamma_1^2 + \beta_1^2y^2) + 4b^2\beta_1^2d^2) + (a^2 + w^2)^4(\gamma_1(a^2 + w^2) + b\beta_1d)) + (a^2 + w^2)^2(b_1\delta(-4b^2(a^2 + w^2)\beta_1^2d^2)(2\beta_1y - 3\gamma_1) + 2b\beta_1d(a^2 + w^2))^2(3\gamma_1^2 + 2\beta_1^2y^2 - 3\beta_1\gamma_1y) + \gamma_1(a^2 + w^2)^3(\gamma_1^2 + 3\beta_1^2y^2) + 8b^3\beta_1^3d^3) + b_1c_1(a^2 + w^2)^3) + bb_1^2da^2 + w^2)^4).$$

The equation $G_2(y) = 0$ has at most four real solutions, symmetric in the sense stated in the proof of statement (b). Therefore system (2.5) has at most two real solutions. Hence the discontinuous piecewise differential system (2.1)-(2.4) has at most two limit cycles.

To complete the proof of statement (c) we build an example with exactly two limit cycles. Then in the half plane R_1 and by considering $(\alpha_1, \beta_1, \gamma_1, a_1, b_1, c_1, \delta) \simeq (\frac{1}{2}, -0.232929, 1.68341, 4, -2, 2, -1)$, we obtain a Hamiltonian isochronous global center in the form (2.4), with its first integral $H_2(x, y)$. Now by considering $(a, b, c, d, w) \simeq (1, 2, -1, 4, 6)$ we obtain in the half plane R_2 a linear differential center in the form (2.1) and its corresponding first integral $H_1(x, y)$.

The discontinuous piecewise differential system (2.1)-(2.4) has at most two limit cycles shown in Figure 2.1(b), because the system of equations (2.5) has the two real solutions $(y, Y) \simeq \{\frac{2}{37}(4 - 3\sqrt{10}), \frac{2}{37}(4 + 3\sqrt{10}), (0, \frac{16}{37})\}$.

Proof of statement (d) of Theorem 2.1. For $n = 4$, the solutions of system (2.5) are equiva-

lently the solutions of the sextic equation $G_3(y) = 0$, where

$$\begin{aligned}
G_3(y) = & \frac{1}{(a^2 + w^2)^7} (2((a^2 + w^2)^3(b_1 \delta(-8b^3 \beta_1^3 d^3(a^2 + w^2)(3\beta_1 y - 4\gamma_1) + 8b^2 \beta_1^2 d^2(a^2 + w^2)^2 \\
& (3\gamma_1^2 + 2\beta_1^2 y^2 - 4\beta_1 \gamma_1 y) - 4b\beta_1 d(a^2 + w^2)^3(-2\gamma_1^3 + \beta_1^3 y^3 - 4\beta_1^2 \gamma_1 y^2 + 3\beta_1 \gamma_1^2 y) + (a^2 \\
& + w^2)^4(\gamma_1^4 + \beta_1^4 y^4 + 6\beta_1^2 \gamma_1^2 y^2) + 16b^4 \beta_1^4 d^4) + b_1 c_1 (a^2 + w^2)^4) + \beta_1(\gamma_1(a^2 + w^2) + b\beta_1 \\
& d)(4c_1 \delta(a^2 + w^2)^4(-2b\beta_1 d(a^2 + w^2)(\beta_1 y - \gamma_1) + (a^2 + w^2)^2(\gamma_1^2 + \beta_1^2 y^2) + 2b^2 \beta_1^2 d^2) \\
& + 4\delta^2(-2b\beta_1 d(a^2 + w^2)(\beta_1 y - \gamma_1) + (a^2 + w^2)^2(\gamma_1^2 + \beta_1^2 y^2) + 2b^2 \beta_1^2 d^2)(-16b^3 \beta_1^3 d^3 \\
& (a^2 + w^2)(\beta_1 y - \gamma_1) + 12b^2 \beta_1^2 d^2(a^2 + w^2)^2(\gamma_1 - \beta_1 y)^2 - 4b\beta_1 d(a^2 + w^2)^3(\beta_1 y - \gamma_1)^3 \\
& + (a^2 + w^2)^4(\gamma_1^4 + \beta_1^4 y^4 + 6\beta_1^2 \gamma_1^2 y^2) + 8b^4 \beta_1^4 d^4) + (a^2 + w^2)^6 + bb_1^2 da^2 + w^2)^6).
\end{aligned}$$

This equation has at most six real solutions, which provide after the symmetry only three real solutions of system (2.5). Therefore the discontinuous piecewise differential system (2.1)-(2.4) has at most three limit cycles.

To reach the result of this statement we give an example of a discontinuous piecewise differential system (2.1)-(2.4) with exactly three limit cycles. In the half plane R_1 , we consider the Hamiltonian isochronous global center (2.4) and its corresponding first integral $H_2(x, y)$, with $(\beta_1, \delta, c_1, \gamma_1, b_1, \alpha_1, a_1) \simeq (-4.72646, -0.00991602, -1.3326, -1, -\frac{1}{5}, \frac{1}{2}, -4)$.

In the half plane R_2 , we consider the linear differential center (2.1) and its first integral $H_1(x, y)$, with $(a, b, c, d, w) \simeq (3, -2, -1, 5, 6)$. Then, for these system the three real solutions of system (2.5) are $(y, Y) \simeq \{(\frac{1}{45}(-10 - \sqrt{1045}), \frac{1}{45}(-10 - \sqrt{1045})), (\frac{2}{45}(-5 - 4\sqrt{10}), \frac{2}{45}(-5 + 4\sqrt{10})), (\frac{1}{45}(-10 - \sqrt{235}), \frac{1}{45}(-10 + \sqrt{235}))\}$. Thus the three crossing limit cycles of the discontinuous piecewise differential system (2.1)-(2.4) are shown in Figure 2.1(c).

Proof of statement (e) of Theorem 2.1. For $n = 5$, the solutions of system (2.5) are the ones of the polynomial equation of degree eight $G_4(y) = 0$. Due to the big expression of $G_4(y)$ we will not provide it, and we conclude immediately that the maximum number of crossing limit cycles of the discontinuous piecewise differential system (2.1)-(2.4) is at most four.

To prove that this upper bound is attached, we provide an example with exactly four limit cycles. In the half plane R_1 and by considering $(a, b, c, d, w) \simeq (-2, 3, 1, 3, 5)$ we obtain a linear differential center in the form (2.1) and its corresponding first integral $H_1(x, y)$. Now by taking $(\alpha_1, \gamma_1, b_1, \delta, \beta_1, c_1, a_1) \simeq (\frac{1}{2}, -1, -1.03433, -0.977806, 0, -0.656806, 3)$, we obtain in the half plane R_2 a Hamiltonian isochronous global center in the form (2.4) with its first integral $H_2(x, y)$. It results that the discontinuous piecewise differential system (2.1)-(2.4)

has exactly four crossing limit cycles intersecting the straight line $x = 0$ at the points $(y, Y) \simeq \left\{ \left(\frac{1}{29}(9 - \sqrt{313}), \frac{1}{29}(9 + \sqrt{313}) \right), \left(\frac{1}{29}(9 - \sqrt{226}), \frac{1}{29}(9 + \sqrt{226}) \right), \left(\frac{1}{29}(9 - \sqrt{134}), \frac{1}{29}(9 + \sqrt{134}) \right) \right.$ and $\left. \left(\frac{1}{29}(9 - 2\sqrt{13}), \frac{1}{29}(9 + 2\sqrt{13}) \right) \right\}$. These limit cycles are shown in Figure 2.2(a).

We need to use the following technical Proposition and lemma 1.1 in chapter 1 to prove the statement (f) of Theorem 2.1.

PROPOSITION 2.1 *Let f_0, \dots, f_n be analytic functions defined on an open interval $I \subset \mathbb{R}$. If f_0, \dots, f_n are linearly independent, then there exists $s_1, \dots, s_n \in I$ and $\lambda_0, \dots, \lambda_n \in \mathbb{R}$ such that for every $j \in \{1, \dots, n\}$ we have $\sum_{i=0}^n \lambda_i f_i(s_j) = 0$.*

For a proof of this result see for instance Proposition 1 of the Appendix of [48].

Proof of statement (f) of Theorem 2.1. For $n = 6$ solving system (2.5) is equal to solving the algebraic equation $G_6(y) = 0$ of degree 10, where

$$G_6(y) = A_0 + A_1y + A_2y^2 + A_3y^3 + A_4y^4 + A_5y^5 + A_6y^6 + A_7y^7 + A_8y^8 + A_9y^9 + A_{10}y^{10},$$

and the A_i 's for $i = 0, \dots, 10$, are given in the appendix.

Since the rank of the Jacobian matrix of the function $\mathcal{A} = (A_0, \dots, A_{10})$ with respect to its twelve parameters: $a, b, c, d, \alpha_1, \beta_1, \gamma_1, c_1, a_1, b_1, \delta, \omega$, is six of the functions A_i , with $i = 0, \dots, 10$, this means that they are linearly independent. So according to Lemma 1.1, it follows that the equation $G_6(y) = 0$ has at most ten real solutions. Thus the system of equations (2.5) has at most five real solutions, which provide at most five limit cycles of the discontinuous piecewise differential system (2.1)-(2.4).

We complete the proof of this statement by providing an example with exactly five limit cycles of the discontinuous piecewise differential system (2.1)-(2.4). So in the half plane R_2 we consider $(a, b, c, d, w) \simeq (1, -1, -2, 4, 4)$, and we obtain a linear differential center in the form (2.1) with its first integral $H_1(x, y)$. Now in the half plane R_1 , we consider the Hamiltonian isochronous global center (2.4) with $(\alpha_1, \gamma_1, \beta_1, c_1, b_1, \delta, a_1) \simeq \left(\frac{1}{50}, 0.379849, 1.61436, -0.399469, 0, 0.494401, 4 \right)$, with its first integral $H_2(x, y)$. Hence the discontinuous piecewise differential system (2.1)-(2.4) has exactly five crossing limit cycles intersecting the straight line $x = 0$ at the points $(y, Y) \simeq \left\{ \left(\frac{1}{17}(-4 - \sqrt{237}), \frac{1}{17}(-4 + \sqrt{237}) \right), \left(\frac{1}{17}(-4 - \sqrt{186}), \frac{1}{17}(-4 + \sqrt{186}) \right), \left(\frac{1}{17}(-4 - 3\sqrt{15}), \frac{1}{17}(-4 + 3\sqrt{15}) \right), \left(\frac{2}{17}(-2 - \sqrt{21}), \frac{2}{17}(-2 + \sqrt{21}) \right), \left(\frac{1}{17}(-4 - \sqrt{33}), \frac{1}{17}(-4 + \sqrt{33}) \right) \right\}$. These limit cycles are shown in Figure 2.2(b). This completes the proof of statement

(f) of Theorem 2.1 for $n = 6$.

In the general case for $n > 6$, we consider the linear differential center (2.1) with its first integral $H_1(x, y)$ in the half-plane R_2 , and the Hamiltonian isochronous global center (2.4) with its first integral $H_2(x, y)$, in the half-plane R_1 . If a limit cycle exists for the discontinuous piecewise differential system (2.1)-(2.4) it must intersect the discontinuity line $x = 0$ in two points $(0, y)$ and $(0, Y)$, with $y \neq Y$. These two points must satisfy the system

$$\begin{aligned} H_1(0, y) - H_1(0, Y) &= (y - Y)P_1(y, Y) = 0, \\ H_2(0, y) - H_2(0, Y) &= (y - Y)Q_n(y, Y) = 0, \end{aligned} \quad (2.6)$$

where $Q_n(y, Y)$ is a polynomial of degree less than or equal $2n - 1$. From $P_1(y, Y) = 0$ we get $Y = \frac{2bd}{a^2 + w^2} - y = f(y)$. By replacing $y = f(Y)$ in equation $Q_n(y, Y) = 0$, we obtain again a polynomial $D(y)$ of degree at most $2n - 1$ in the variable y . Assume that the degree of $D(Y)$ is $2n - 1$, if the degree is smaller we can use the same arguments for proving that the discontinuous piecewise differential system has at most five limit cycles. So we write

$$D(y) = C_0 + C_1y + C_2y^2 + \dots + C_{2n-1}y^{2n-1}.$$

Let $M_{(2n) \times 12}$ be the Jacobian matrix of the function $\mathcal{C} = (C_0, \dots, C_{2n-1})$ with respect to its twelve parameters

$$M_{(2n) \times 12} = \begin{pmatrix} \frac{\partial C_0}{\partial a} & \frac{\partial C_0}{\partial b} & \dots & \frac{\partial C_0}{\partial \omega} \\ \frac{\partial C_1}{\partial a} & \frac{\partial C_1}{\partial b} & \dots & \frac{\partial C_1}{\partial \omega} \\ \vdots & \vdots & \ddots & \vdots \\ \frac{\partial C_{2n-1}}{\partial a} & \frac{\partial C_{2n-1}}{\partial b} & \dots & \frac{\partial C_{2n-1}}{\partial \omega} \end{pmatrix}.$$

We know that the rank of this matrix for $n > 6$ is at most 12. In view of lemma 1.1 we conclude that the maximum number of real solutions of the equation $D(y) = 0$ is at most eleven, and it results immediately that the maximum number of real solutions of system (2.6) is at most 5. Then the maximum number of crossing limit cycles of the discontinuous piecewise differential system (2.1)-(2.4) for $n > 6$ is at most 5. ■

Appendix of Chapter 2

Here we provide the expressions A_i , with $i = 0, \dots, 10$, that appear in the proof of Theorem 2.1.

$$\begin{aligned}
 A_0 = & \frac{1}{(a^2 + \omega^2)^{11}} (b_1 c_1 a^{22} + \beta_1 \gamma_1 a^{22} + 11 b_1 c_1 \omega^2 a^{20} + b d \beta_1^2 a^{20} + b b_1^2 d a^{20} + 11 \omega^2 \beta_1 a^{20} \\
 & + 55 b_1 c_1 \omega^4 a^{18} + 10 b b_1^2 d \omega^2 a^{18} + 10 b d \omega^2 \beta_1^2 a^{18} + 55 \omega^4 \beta_1 \gamma_1 a^{18} + 165 b_1 c_1 \omega^6 a^{16} + (a^2 \\
 & + \omega^2)^5 (32 b^5 d^5 (2 b b_1 d + c_1 (a^2 + \omega^2)) \beta_1^6 + 45 b b_1^2 d \omega^4 a^{16} + 165 \omega^6 \beta_1 \gamma_1 a^{16} 2 + \omega^{22} \beta_1 \gamma_1 \\
 & + 462 b_1 c_1 \omega^{10} a^{12} + 330 b_1 c_1 \omega^8 a^{14} + 120 b b_1^2 d \omega^6 a^{14} + 120 b d \omega^6 \beta_1^2 a^{14} + 462 \omega^{10} \beta_1 \gamma_1 \\
 & + 330 \omega^8 \beta_1 \gamma_1 a^{14} + 210 b b_1^2 d \omega^8 a^{12} + 210 b d \omega^8 \beta_1^2 a^{12} + 462 b_1 c_1 \omega^{12} a^{10} + 55 b_1 c_1 \omega^{18} a^4 \\
 & + b b_1^2 d \omega^{20} + 462 \omega^{12} \beta_1 \gamma_1 a^{10} + 252 b b_1^2 d \omega^{10} a^{10} + 330 b_1 c_1 \omega^{14} a^8 + 210 b b_1^2 d \omega^{12} a^8 c_1 \\
 & + 210 b d \omega^{12} \beta_1^2 a^8 + 330 \omega^{14} \beta_1 \gamma_1 a^8 + 165 b_1 c_1 \omega^{16} a^6 + 252 b d \omega^{10} \beta_1^2 a^{10} + 45 b d \omega^{16} \beta_1^2 \\
 & + 3072 b^{10} d^{10} (a^2 + \omega^2) \gamma_1 \beta_1^{10} + 55 \omega^{18} \beta_1 \gamma_1 a^4 + 11 b_1 c_1 \omega^{20} a^2 + 10 b b_1^2 d \omega^{18} a^2 + 6 (a^2 \\
 & + \omega^2)^5 (2 b b_1 d + c_1 (a^2 + \omega^2)) \gamma_1^5 \beta_1 + b_1 (a^2 + \omega^2)^6 \gamma_1^6 \delta + b d \omega^{20} \beta_1^2 + 11 \omega^{20} \beta_1 \gamma_1 a^2 b \beta_1 \\
 & + 10 b d \omega^{18} \beta_1^2 a^2 + 8448 b^9 d^9 (a^2 + \omega^2)^2 \gamma_1^2 \beta_1^9 + 14080 b^8 d^8 (a^2 + \omega^2)^3 \gamma_1^3 \beta_1^8 + 30 b d (a^2 \\
 & + \omega^2)^4 (2 b b_1 d + c_1 (a^2 + \omega^2)) \gamma_1^4 \beta_1^2 + 15840 b^7 d^7 (a^2 + \omega^2)^4 \gamma_1^4 \beta_1^7 + 12672 b^6 d^6 c_1 \omega_1^{12} (a^2 \\
 & + \omega^2)^5 \gamma_1^5 \beta_1^6 + 7392 b^5 d^5 (a^2 + \omega^2)^6 \gamma_1^6 \beta_1^5 + 3168 b^4 d^4 (a^2 + \omega^2)^7 \gamma_1^7 \beta_1^4 + 990 b^3 c_1 \beta_1^2 d^3 (a^2 \\
 & + \omega^2)^8 \gamma_1^8 \beta_1^3 + 220 b^2 d^2 (a^2 + \omega^2)^9 \gamma_1^9 \beta_1^2 + 33 b d (a^2 + \omega^2)^{10} \gamma_1^{10} \beta_1 + 3 (a^2 + \omega^2)^{11} \gamma_1^{11} \delta \\
 & + 96 b^4 d^4 (a^2 + \omega^2) (2 b b_1 d + c_1 (a^2 + \omega^2)) \gamma_1 \beta_1^5 + 120 b^3 d^3 (a^2 + \omega^2)^2 (2 b b_1 d + c_1 b \gamma_1^2 (a^2 \\
 & + \omega^2)) \gamma_1^2 \beta_1^4 + 80 b^2 d^2 (a^2 + \omega^2)^3 (2 b b_1 d + c_1 (a^2 + \omega^2)) \gamma_1^3 \beta_1^3),
 \end{aligned}$$

$$\begin{aligned}
 A_1 = & -\frac{1}{(a^2 + \omega^2)^{10}} (2 b d \beta_1^2 \delta (5 \gamma_1^3 (22 \beta_1 \delta \gamma_1^6 + 3 b_1 \gamma_1 + 4 c_1 \beta_1) a^{18} + 5 \gamma_1^2 (9 \gamma_1 (22 \beta_1 \delta \gamma_1^6 + 3 b_1 \\
 & + 4 c_1 \beta_1) \omega^2 + 2 b d \beta_1 (99 \beta_1 \delta \gamma_1^6 + 8 b_1 \gamma_1 + 6 c_1 \beta_1)) a^{16} + 4 \gamma_1 (45 \gamma_1^2 (22 \beta_1 \delta \gamma_1^6 + 3 b_1 \gamma_1 c_1 a^2 \\
 & + 4 c_1 \beta_1) \omega^4 + 20 b d \beta_1 \gamma_1 (99 \beta_1 \delta \gamma_1^6 + 8 b_1 \gamma_1 + 6 c_1 \beta_1) \omega^2 + 9 b^2 d^2 \beta_1^2 (5 b_1 \gamma_1 + 2 \beta_1 (66 \delta \gamma_1^6 \\
 & + c_1))) a^{14} + 4 (105 \gamma_1^3 (22 \beta_1 \delta \gamma_1^6 + 3 b_1 \gamma_1 + 4 c_1 \beta_1) \omega^6 + 70 b d \beta_1 \gamma_1^2 (99 \beta_1 \delta \gamma_1^6 + 8 b_1 \gamma_1 + 2 \\
 & (66 \delta \gamma_1^6 + c_1)) \omega^2 + 8 b^3 d^3 \beta_1^3 (462 \beta_1 \delta \gamma_1^6 + 6 b_1 \gamma_1 + c_1 \beta_1)) a^{12} + 6 c_1 \beta_1 \omega^4 + 63 b^2 d^2 \beta_1^2 \gamma_1 \\
 & (5 b_1 \gamma_1 + 2 (315 \gamma_1^3 (22 \beta_1 \delta \gamma_1^6 + 3 b_1 \gamma_1 + 4 c_1 \beta_1) \omega^8 + 280 b d \beta_1 \gamma_1^2 \omega^6 (99 \beta_1 \delta \gamma_1^6 + 8 b_1 \gamma_1
 \end{aligned}$$

$$\begin{aligned}
& +6c_1\beta_1) + 378b^2d^2\beta_1^2\gamma_1(5b_1\gamma_1 + 2\beta_1(66\delta\gamma_1^6 + c_1))\omega^4 + 96\omega^2b^3d^3\beta_1^3(462\beta_1\delta\gamma_1^6 + 6 \\
& b_1\gamma_1) + 40b^4d^4\beta_1^4(396\beta_1\delta\gamma_1^5 + b_1)a^{10} + 70b\gamma_1^2d\beta_1\gamma_1^2(99\beta_1\delta\gamma_1^6 + 8b_1\gamma_1 + 6c_1\beta_1)\omega^8 \\
& + 10(63\gamma_1^3(22\beta_1\delta\gamma_1^6 + 3b_1\gamma_1 + 4c_1\beta_1)\omega^{10} + 126b^2d^2\beta_1^2\gamma_1(5b_1\gamma_1 + 2\beta_1(66\delta\gamma_1^6 + c_1)) \\
& \omega^6 + 48b^3d^3\beta_1^3(462\beta_1\delta\gamma_1^6 + 6b_1\gamma_1 + c_1\beta_1)\omega^4 + 20\omega^{12}(21\gamma_1^3(22\beta_1\delta\gamma_1^6 + 3b_1\gamma_1 + 4c_1 \\
& \beta_1) + 40b^4d^4\beta_1^4(396\beta_1\delta\gamma_1^5 + b_1)\omega^2 + 4752b^5d^5\beta_1^6\gamma_1^4\delta)a^8 + 28bd\beta_1\gamma_1^2(99\beta_1\delta\gamma_1^6 + 8b_1 \\
& \gamma_1 + 6c_1\beta_1)\omega^{10} + 63b^2d^2\beta_1^2\gamma_1(5b_1\gamma_1 + 2\beta_1(66\delta\gamma_1^6 + c_1))\omega^8 + 32b^3d^3(462\beta_1\delta\gamma_1^6 + c_1 \\
& \beta_1 + 6b_1\gamma_1)\omega^6 + 40b^4d^4\beta_1^4(396\beta_1\delta\gamma_1^5 + b_1)\omega^4 + 9504b^5d^5\beta_1^6\gamma_1^4\delta\omega^2 + 2464b^6d^6\beta_1^7\gamma_1^3 \\
& \delta)a^6 + 4(45\gamma_1^3(22\beta_1\delta\gamma_1^6 + 3b_1\gamma_1 + 4c_1\beta_1)\omega^{14} + 70bd\beta_1\gamma_1^2(99\beta_1\delta\gamma_1^6 + 8b_1\gamma_1 + 6c_1\beta_1) \\
& \omega^{12} + 189b^2d^2\beta_1^2\gamma_1(5b_1\gamma_1 + 2\beta_1(66\delta\gamma_1^6 + c_1))\omega^{10} + 120b^3d^3\beta_1^3(462\beta_1\delta\gamma_1^6 + 6b_1\gamma_1 \\
& \delta c_1^7\omega^2 + c_1\beta_1)\omega^8 + 200b^4d^4\beta_1^4(396\beta_1\delta\gamma_1^5 + b_1)\omega^6 + 71280b^5d^5\beta_1^6\gamma_1^4\delta\omega^4 + 36960b^6d^6 \\
& \beta_1^7\gamma_1^3 + 5\omega^{18}(22\beta_1\delta\gamma_1^6 + 3b_1\gamma_1 + 4c_1\beta_1) + 8448b^7d^7\beta_1^8\gamma_1^2\delta)a^4(45\gamma_1^3 + (22\beta_1\delta\gamma_1^6 + 3b_1 \\
& \gamma_1 + 4c_1\beta_1)\omega^{16} + 80bd\beta_1\gamma_1^2(99\beta_1\delta\gamma_1^6 + 8b_1\gamma_1 + 6c_1\beta_1)\omega^{14} + 252b^2d^2\beta_1^2\gamma_1(5b_1\gamma_1 + 2 \\
& \beta_1(66\delta\gamma_1^6 + c_1))\omega^{12} + 192b^3d^3\beta_1^3(462\beta_1\delta\gamma_1^6 + 6b_1\gamma_1 + c_1\beta_1)\omega^{10} + 400b^4d^4\beta_1^4(396\beta_1 \\
& \delta + b_1)\omega^8 + 190080b^5d^5 + \beta_1^6\gamma_1^4\delta\omega^6 + 147840b^6d^6\beta_1^7\gamma_1^3\delta\omega^4 + 67584b^7d^7\beta_1^8\gamma_1^2\delta\omega^2a^2 \\
& + 2560b^9 + 13824b^8d^8\beta_1^9\gamma_1\delta)(d^9\beta_1^{10}\delta + 47520b^5d^5\omega^8\beta_1^6\gamma_1^4\delta) + 49280b^6d^6\omega^6\beta_1^7\gamma_1^3\delta \\
& + 33792b^7d^7\omega^4\beta_1^8\gamma_1^2\delta + (396\beta_1\delta\gamma_1^5 + b_1)13824b^8d^8\omega^2\beta_1^9\gamma_1\delta + 80b^4d^4\omega^{10}\beta_1^4 + (8b_1 \\
& + 99\beta_1\delta\gamma_1^6 + 6c_1\beta_1)10bd\omega^{16}\beta_1\gamma_1^2 + 32b^3d^3\omega^{12}\beta_1^3 + 6b_1\gamma_1 + c_1\beta_1)(5b_1\gamma_1 + 2\beta_1(66\delta\gamma_1^6 \\
& + c_1))(462\beta_1\delta\gamma_1^6 + 36b^2d^2\omega^{14}\beta_1^2\gamma_1), \\
A_2 = & \frac{1}{(a^2 + \omega^2)^9}(\beta_1^2\delta(5\gamma_1^3(22\beta_1\delta\gamma_1^6 + 3b_1\gamma_1 + 4c_1\beta_1)a^{18} + 5\gamma_1^2(9\gamma_1\omega^2(22\beta_1\delta\gamma_1^6 + 3b_1\gamma_1 \\
& + 4c_1\beta_1) + 2bd\beta_1(99\beta_1\delta\gamma_1^6 + 8b_1\gamma_1 + 6c_1\beta_1))a^{16} + 4\gamma_1(45\gamma_1^2\omega^4(22\beta_1\delta\gamma_1^6 + 3b_1\gamma_1 \\
& + 4c_1\beta_1) + 20bd\beta_1\gamma_1(99\beta_1\delta\gamma_1^6 + 8b_1\gamma_1 + 6c_1\beta_1)\omega^2 + 12b^2d^2\beta_1^2(5b_1\gamma_1 + 2\beta_1(66\delta\gamma_1^6 \\
& + c_1)))a^{14} + 28(15\gamma_1^3(22\beta_1\delta\gamma_1^6 + 3b_1\gamma_1 + 4c_1\beta_1)\omega^6 + 10\omega^4bd\beta_1\gamma_1^2(99\beta_1\delta\gamma_1^6 + 8b_1\gamma_1 \\
& + 6c_1\beta_1) + 12b^2d^2\beta_1^2\gamma_1(5b_1\gamma_1 + 2\beta_1(66\delta\gamma_1^6 + c_1))\omega^2 + 2b^3d^3\beta_1^3(462\beta_1\delta\gamma_1^6 + 6b_1\gamma_1 \\
& + c_1\beta_1))a^{12} + 2(315\gamma_1^3(22\beta_1\delta\gamma_1^6 + 3b_1\gamma_1 + 4c_1\beta_1)\omega^8 + 280bd\beta_1\gamma_1^2(99\beta_1\delta\gamma_1^6 + 8b_1\gamma_1) \\
& + 6c_1\beta_1)\omega^6 + 504b^2d^2\beta_1^2\gamma_1(5b_1\gamma_1 + 2\beta_1(66\delta\gamma_1^6 + c_1))\omega^4 + 168b^3d^3\beta_1^3(462\beta_1\delta\gamma_1^6c_1\beta_1 \\
& + 6b_1\gamma_1)\omega^2 + 88b^4d^4\beta_1^4(396\beta_1\delta\gamma_1^5 + b_1))a^{10} + 10(63\gamma_1^3(22\beta_1\delta\gamma_1^6 + 3b_1\gamma_1 + 4c_1\beta_1)\omega^{10} \\
& + 70bd\beta_1\gamma_1^2(99\beta_1\delta\gamma_1^6 + 8b_1\gamma_1 + 6c_1\beta_1)\omega^8 + 168b^2d^2\beta_1^2\gamma_1(5b_1\gamma_1 + 2\beta_1(66\delta\gamma_1^6 + c_1))
\end{aligned}$$

$$\begin{aligned}
& \omega^6 + 84b^3d^3\beta_1^3(462\beta_1\delta\gamma_1^6 + 6b_1\gamma_1 + c_1\beta_1)\omega^4 + 88b^4d^4\beta_1^4(396\beta_1\delta\gamma_1^5 + b_1) + d^5\beta_1^6\gamma_1^4) \\
& + 12672b^5a^8 + 20(21\gamma_1^3(22\beta_1\delta\gamma_1^6 + 3b_1\gamma_1 + 4c_1\beta_1)\omega^{12} + 28bd\beta_1\gamma_1^2(99\beta_1\delta\gamma_1^6 + 8b_1\gamma_1 \\
& + 6c_1\beta_1)\omega^{10} + 84b^2d^2\beta_1^2\gamma_1(5b_1\gamma_1 + 2\beta_1(66\delta\gamma_1^6 + c_1))\omega^8 + 56b^3d^3\beta_1^3(462\beta_1\delta\gamma_1^6 + 6b_1 \\
& + c_1\beta_1)\omega^6 + 88b^4d^4\beta_1^4(396\beta_1\delta\gamma_1^5 + b_1)\omega^4 + 25344b^5d^5\beta_1^6\gamma_1^4\delta\omega^2 + 7744b^6d^6\beta_1^7\gamma_1^3\delta) \\
& a^6 + 4(45\gamma_1^3(22\beta_1\delta\gamma_1^6 + 3b_1\gamma_1 + 4c_1\beta_1)\omega^{14} + 70bd\beta_1\gamma_1^2(99\beta_1\delta\gamma_1^6 + 8b_1\gamma_1 + 6c_1\beta_1) \\
& \omega^{12} + 252b^2d^2\beta_1^2\gamma_1(5b_1\gamma_1 + 2\beta_1(66\delta\gamma_1^6 + c_1))\omega^{10} + 210b^3d^3\beta_1^3(462\beta_1\delta\gamma_1^6 + 6b_1\gamma_1 \\
& + c_1\beta_1)\omega^8 + 440b^4d^4\beta_1^4(396\beta_1\delta\gamma_1^5 + b_1)\omega^6 + 190080b^5d^5\beta_1^6\gamma_1^4\delta\omega^4 + 116160b^6d^6\beta_1^7 \\
& + \gamma_1^3\delta\omega^2 + 30624b^7d^7\beta_1^8\gamma_1^2\delta)a^4 + (45\gamma_1^3(22\beta_1\delta\gamma_1^6 + 3b_1\gamma_1 + 4c_1\beta_1)\omega^{16} + 80bd\beta_1\gamma_1^2\omega^9 \\
& (99\beta_1\delta\gamma_1^6 + 8b_1\gamma_1 + 6c_1\beta_1) + 336b^2d^2\beta_1^2\gamma_1(5b_1\gamma_1 + 2\beta_1(66\delta\gamma_1^6 + c_1))\omega^{12} + 336b^3d^3 \\
& (462\beta_1\delta\gamma_1^6 + 6b_1\gamma_1 + c_1\beta_1)\omega^{10} + 880b^4d^4\beta_1^4(396\beta_1\delta\gamma_1^5 + b_1)\omega^8 + 506880b^5d^5\beta_1^6\gamma_1^4\delta \\
& + 464640b^6d^6\beta_1^7\gamma_1^3\delta\omega^4 + 244992b^7d^7\beta_1^8\gamma_1^2\delta\omega^2 + 56832b^8d^8\beta_1^9\gamma_1\delta)a^2 + 11776b^9d^9 \\
& + 126720b^5d^5\omega^8\beta_1^6\gamma_1^4\delta + 154880b^6d^6\omega^6\beta_1^7\gamma_1^3\delta + 122496b^7d^7\omega^4\beta_1^8\gamma_1^2\delta + 56832b^8d^8 \\
& + \beta_1^9\gamma_1\delta + 176b^4d^4\omega^{10}\beta_1^4(396\beta_1\delta\gamma_1^5 + b_1) + 5\omega^{18}\gamma_1^3(22\beta_1\delta\gamma_1^6 + 3b_1\gamma_1 + 4c_1\beta_1)(99\beta_1 \\
& + 8b_1 + \gamma_1 + 6c_1\beta_1) + 10bd\omega^{16}\beta_1\gamma_1^2\delta\gamma_1^6 + 56b^3d^3\omega^{12}\beta_1^3(462\beta_1\delta\gamma_1 + c_1\beta_1) + 48b^2d^2\omega^4 \\
& + 6b_1(5b_1\gamma_1 + 2\beta_1(66\delta\gamma_1^6 + c_1))), \\
A_3 = & -\frac{1}{(a^2 + \omega^2)^8}(4b\beta_1^4d\delta(15a^{14}b_1\gamma_1^2 + 6a^{14}\beta_1c_1\gamma_1 + 36a^{12}bb_1\beta_1\gamma_1d + 6a^{12}b\beta_1^2c_1d + 105 \\
& (a^{12}b_1\gamma_1^2\omega^2 + 42a^{12}\beta_1c_1\gamma_1\omega^2) + 26a^{10}b^2b_1\beta_1^2d^2 + 216a^{10}bb_1\beta_1\gamma_1\omega^2 + 36a^{10}b\beta_1^2c_1d \\
& + 315a^{10}\omega^2b_1\gamma_1^2\omega^4 + 126a^{10}\beta_1c_1\gamma_1\omega^4 + 130a^8b^2b_1\beta_1^2d^2\omega^2 + 540a^8bb_1\beta_1\gamma_1d\omega^4 + 90 \\
& a^8b\beta_1^2c_1d\omega^4 + 525a^8b_1\gamma_1^2\omega^6 + 210a^8\beta_1c_1\gamma_1\omega^6 + 260a^6b^2b_1\beta_1^2d^2\omega^4 + 525a^6b_1\gamma_1^2 \\
& + \omega^{8720}a^6bb_1\beta_1\gamma_1d\omega^6 + 120a^6b\beta_1^2c_1d\omega^6 + 210a^6\beta_1c_1\gamma_1\omega^8 + 260a^4b^2b_1\beta_1^2d^2\omega^6 \\
& + 540a^4bb_1\beta_1\gamma_1d\omega^8 + 90a^4b\beta_1^2c_1d\omega^8 + 315a^4b_1\gamma_1^2\omega^{10} + 126a^4\beta_1c_1\gamma_1\omega^{10} + 4\beta_1\delta \\
& (43b^6 + \beta_1^6\gamma_1d^6(a^2 + \omega^2) + 130a^2b^2b_1\beta_1^2d^2\omega^8 + \gamma_1^3d^4(a^2 + \omega^2)^38184b^5\beta_1^5\gamma_1^2d^5b^4(a^2 \\
& + \omega^2)^28800\beta_1^4 + 5940b^3\beta_1^3\gamma_1^4d^3(a^2 + \omega^2)^4 + 2574b^2\beta_1^2\gamma_1^5d^2(a^2 + \omega^2)^5 + 693b\beta_1\gamma_1^6d(a^2 \\
& + \omega^2)^6 + 99\gamma_1^7(a^2 + \omega^2)^7 + 2574 + 1024b^7\beta_1^7d^7) + 216a^2bb_1\beta_1\gamma_1d\omega^{10}b\beta_1^2c_1d\omega^{10} + 36 \\
& a^2 + 105a^2b_1\gamma_1^2 + 42a^2\beta_1c_1\gamma_1\omega^{12} + 26b^2b_1\beta_1^2d^2\omega^{10} + 36bb_1\beta_1\gamma_1d\omega^{12} + 15b_1\gamma_1^2 + 6b \\
& \beta_1^2c_1d\omega^{12} + 6\beta_1c_1\gamma_1\omega^{14}),
\end{aligned}$$

$$\begin{aligned}
A_4 = & -\frac{1}{(a^2 + \omega^2)^7} (\beta_1^4 \delta (15a^{14} b_1 \gamma_1^2 + 6a^{14} \beta_1 c_1 \gamma_1 + 36a^{12} b b_1 \beta_1 \gamma_1 d + 6a^{12} b \beta_1^2 c_1 d + 6\beta_1 c_1 \gamma_1) \\
& b_1 \gamma_1^2 \omega^2 + 42a^{12} \beta_1 c_1 \gamma_1 \omega^2 + 36a^{10} b^2 b_1 \beta_1^2 d^2 + 216a^{10} b b_1 \beta_1 \gamma_1 d \omega^2 + 36a^{10} b \beta_1^2 c_1 d \omega^2 \\
& 315a^{10} b_1 \gamma_1^2 \omega^4 + 126a^{10} \beta_1 c_1 \gamma_1 \omega^4 + 180a^8 b^2 b_1 \beta_1^2 d^2 \omega^2 + 540a^8 b b_1 \beta_1 \gamma_1 d \omega^4 b^6 \beta_1^6 \gamma_1 d^6 \\
& + (a^2 + \omega^2) + 22704b^5 \beta_1^5 \gamma_1^2 d^5 (a^2 + \omega^2)^2 + 20240b^4 \beta_1^4 \gamma_1^3 d^4 (a^2 + \omega^2)^3 + 10890b^3 \beta_1^3 \gamma_1^4 \\
& (a^2 + \omega^2)^4 + 3564b^2 \beta_1^2 \gamma_1^5 d^2 (a^2 + \omega^2)^5 + 693b \beta_1 \gamma_1^6 d (a^2 + \omega^2)^6 + 99\gamma_1^7 (a^2 + \omega^2)^7 \\
& + 3824b^7 + \beta_1^7 d^7) + 42a^2 \beta_1 c_1 \gamma_1 \omega^{12} + 90a^8 b \beta_1^2 c_1 d \omega^4 + 525a^8 b_1 \gamma_1^2 \omega^6 + 4\beta_1 \delta b^2 + 360 \\
& a^6 b^2 b_1 \beta_1^2 d^2 \omega^4 (14208 + 216a^2 b b_1 \beta_1 \gamma_1 d \omega^{10} + 36a^2 b \beta_1^2 c_1 d \omega^{10} + 105a^2 b_1 \gamma_1^2 \omega^{12} + 36b^2 \\
& b_1 \beta_1^2 d^2 \omega^{10} + 36b b_1 \beta_1 \gamma_1 d \omega^{12} + 6b \beta_1^2 c_1 d \omega^{12} + 15b_1 \gamma_1^2 \omega^{14} + 720a^6 b b_1 \beta_1 \gamma_1 d \omega^6 + 120 \\
& a^6 b \beta_1^2 c_1 d \omega^6 + 525a^6 b_1 \gamma_1^2 \omega^8 + 210a^6 \beta_1 c_1 \gamma_1 \omega^8 + 360a^4 b^2 b_1 \beta_1^2 d^2 \omega^6 + 90a^4 b \beta_1^2 + 540 \\
& a^4 b b_1 \beta_1 \gamma_1 d \omega^8 + c_1 d \omega^8 + 315a^4 b_1 \gamma_1^2 \omega^{10} + 126a^4 \beta_1 c_1 \gamma_1 \omega^{10} + 180a^2 b^2 b_1 d^2 \omega^8), \\
A_5 = & -\frac{1}{(a^2 + \omega^2)^6} (2b \beta_1^6 d \delta (-(a^2 + \omega^2)((a^2 + \omega^2)(44\beta_1 \gamma_1^2 \delta (340b^2 \beta_1^2 \gamma_1 d^2 (a^2 + \omega^2) + 27\gamma_1^3 \\
& (a^2 + \omega^2)^3 + 135b \beta_1 \gamma_1^2 d (a^2 + \omega^2)^2 + 480b^3 \beta_1^3 d^3) + 3b_1 (a^2 + \omega^2)^3) - 5024b^5 \beta_1^6 d^5 \delta) \\
& + 15936b^4 \beta_1^5 \gamma_1 d^4 \delta)), \\
A_6 = & -\frac{1}{(a^2 + \omega^2)^5} (12480b^4 \beta_1^5 \gamma_1 d^4 \delta + 4736b^5 \beta_1^6 d^5 \delta + \beta_1^6 \delta ((a^2 + \omega^2)((a^2 + \omega^2)(44\beta_1 \gamma_1^2 \delta \\
& (160b^2 \beta_1^2 \gamma_1 d^2 (a^2 + \omega^2 + 45b \beta_1 \gamma_1^2 d (a^2 + \omega^2)^2 + 9\gamma_1^3 (a^2 + \omega^2)^3 + 300b^3 \beta_1^3 d^3) + b_1 (a^2 \\
& + \omega^2)^3))), \\
A_7 = & -\frac{1}{(a^2 + \omega^2)^4} (-80b \beta_1^9 d \delta^2 (42b^2 \beta_1^2 \gamma_1 d^2 (a^2 + \omega^2) + 33b \beta_1 \gamma_1^2 d (a^2 + \omega^2)^2 + 11\gamma_1^3 (a^2 \\
& + \omega^2)^3 + 20b^3 \beta_1^3 d^3)), \\
A_8 = & \frac{1}{(a^2 + \omega^2)^3} (10\beta_1^9 \delta^2 (60b^2 \beta_1^2 \gamma_1 d^2 (a^2 + \omega^2) + 33b \beta_1 \gamma_1^2 d (a^2 + \omega^2)^2 + 11\gamma_1^3 (a^2 + \omega^2)^3 \\
& + 38b^3 \beta_1^3 d^3)), \\
A_9 = & -\frac{1}{(a^2 + \omega^2)^2} (60b \beta_1^{11} d \delta^2 (\gamma_1 a^2 + \omega^2 \gamma_1) + b \beta_1 d), \\
A_{10} = & \frac{1}{a^2 + \omega^2} (6\beta_1^{11} \delta^2 (a^2 \gamma_1 + \omega^2 \gamma_1) + b \beta_1 d).
\end{aligned}$$

Limit Cycles of Discontinuous Piecewise Differential Systems Formed by Linear and Cubic Isochronous Centers

Here we deal with the piecewise differential system defined by

$$F(\mathbf{x}) = \begin{cases} F^-(\mathbf{x}) = (F_1^-(x, y), F_2^-(x, y)) & (x, y) \in \Sigma^-, \\ F^+(\mathbf{x}) = (F_1^+(x, y), F_2^+(x, y)) & (x, y) \in \Sigma^+, \end{cases} \quad (3.1)$$

where $\Sigma = \Gamma_1 \cup \Gamma_2$ such that $\Gamma_1 = \{(x, y) \in \mathbb{R}^2 : x = 0 \text{ and } y \geq 0\}$, $\Gamma_2 = \{(x, y) \in \mathbb{R}^2 : x \geq 0 \text{ and } y = 0\}$, where the separation curve $\Sigma^+ = \{(x, y) \in \mathbb{R}^2 : x > 0, y > 0\}$ and $\Sigma^- = \{(x, y) \in \mathbb{R}^2 : x \geq 0, y < 0\} \cup \{(x, y) \in \mathbb{R}^2 : x < 0\}$.

In the literature we find many papers interesting in solving the second part of the sixteenth Hilbert problem for linear discontinuous piecewise differential systems, but few papers devoted to solve this problem for the nonlinear ones.

In 2020 Benterki and Llibre [10], studied the sixteenth Hilbert problem for discontinuous piecewise differential systems separated by a straight line, when these differential system are linear centers or three families of cubic isochronous centers, and they proved that the maximum number of limit cycles varies from 0, 1 and 2 depending on the chosen class.

In our work we study the maximum number of limit cycles for discontinuous planar piecewise differential systems formed by linear centers and three classes of isochronous cubic centers separated by irregular line. We provide a sharp upper bound for the max-

imum number of crossing limit cycles that these classes of discontinuous piecewise differential systems can exhibit.

We consider the following four classes of isochronous linear and cubic centers.

LEMMA 3.1 *After applying a linear change of variables and rescaling the independent variable every linear center in \mathbb{R}^2 can be written as*

$$\dot{x} = -Ax - y(A^2 + \omega^2) + B, \quad \dot{y} = x + Ay + C, \quad (3.2)$$

with $\omega > 0, A, B, C \in \mathbb{R}$ and $A \neq 0$.

The first integral of this system is

$$H(x, y) = (x + Ay)^2 + 2(Cx - By) + \omega^2 y^2. \quad (3.3)$$

Or we can define the linear differential center as follows

$$\dot{x} = -Ax - (A^2 + \omega^2)y, \quad \dot{y} = x + Ay, \quad (3.4)$$

with $\omega > 0, A \in \mathbb{R} - \{0\}$, and its corresponding first integral is

$$H_1(x, y) = (Ay + x)^2 + y^2 \omega^2. \quad (3.5)$$

For a proof of Lemma 3.1 see [49].

Now we give the three classes of isochronous cubic differential centers.

I) The first class is given by

$$\dot{x} = y(2K_1 x + 2K_2 x^2 - 1), \quad \dot{y} = K_1(y^2 - x^2) + 2K_2 x y^2 + x,$$

which has the first integral $H_2(x, y) = \frac{x^2 + y^2}{1 - 2x(K_1 + K_2 x)}$.

(II) The second class is

$$\dot{x} = y\left(\frac{8x}{3} - \frac{32y^2}{9} - 1\right), \quad \dot{y} = x - \frac{4y^2}{3},$$

and its first integral is $H_3(x, y) = (3x - 4y^2)^2 + 9y^2$.

(III) The last class is

$$\dot{x} = -y(1-x)(1-2x), \quad \dot{y} = 2x^3 - 2x^2 + x + y^2,$$

and its corresponding first integral is $H_4(x, y) = \frac{(x-1)^2(x^2+y^2)}{(2x-1)^2}$.

For a proof, see [20].

Cubic isochronous centers after an affine change of variables

We present the expression of the three families of the cubic isochronous centers (I), (II) and (III) after doing the general affine change of variables of the form $(x, y) \rightarrow (ax + by + c, \alpha x + \beta y + \gamma)$, with $b\alpha - a\beta \neq 0$. Thus, system (I) become

$$\begin{aligned} \dot{x} &= \frac{1}{\alpha b - a\beta} (b(-a^2 K_1 x^2 + d(-2a K_1 x + 2K_2 + 2K_2(\beta y \gamma + \alpha x))(-\beta y + \gamma + \alpha x)) + ax \\ &\quad (2K_2(\beta y + \gamma + \alpha x)(-\beta y \gamma + \alpha x)) + ax - d^2 K_1 + (K_1 \gamma + K_1 \alpha x + K_1 \beta y)(\gamma + \alpha x \\ &\quad - \beta y)) + b^2 y(-2a K_1 x - 2d K_1 + 2K_2(\gamma + \alpha x)(\gamma + \alpha x + \beta y) + 2K_2 - \beta(2ax + 2d) \\ &\quad (K_2(ax + d) + K_1) - \beta(\gamma + \alpha x + \beta y) - b^3 K_1 y^2), \\ \dot{y} &= \frac{1}{\alpha b - a\beta} (a^3 K_1 x^2 - a^2 x(-2b K_1 y - 2d K_1 + 2K_2(\gamma + \beta y)(\gamma + \alpha x + \beta y) + 1) + a \\ &\quad (b^2 K_1 y^2 + d(-2(K_2(\gamma + \beta y))^2 - b K_1 y) + 2a^2 K_2 x^2 - 1) - 2b K_2 y(\gamma - \alpha x + \beta y) \\ &\quad (\gamma + \alpha x + \beta y) - by + d^2 K_1 + K_1(-\gamma + \alpha x - \beta y)(\gamma + \alpha x + \beta y)) + \alpha(2(by + d) \\ &\quad (K_2(by + d) + K_1) - 1)(\gamma + \alpha x + \beta y)), \end{aligned} \quad (3.6)$$

with its first integral

$$\tilde{H}_2(x, y) = \frac{(ax + by + d)^2 + (\gamma + \alpha x + \beta y)^2}{1 - 2(ax + by + d)(K_2(ax + by + d) + K_1)}. \quad (3.7)$$

The system (II) written as

$$\begin{aligned} \dot{x} &= \frac{1}{9\alpha b - 9a\beta} (3b(3ax + 3d - 4(\gamma + \alpha x + \beta y)(\gamma + \alpha x + 3\beta y)) + \beta(\gamma + \alpha x + \beta y) \\ &\quad (-24ax - 24d + 32(\gamma + \alpha x + \beta y)^2 + 9) + 9b^2 y), \\ \dot{y} &= \frac{1}{-9\alpha b + 9a\beta} (9a^2 x + 3a(3by + 3d - 4(\alpha x + \beta y + \gamma)(\gamma + 3\alpha x + \beta y)) + \alpha(\gamma + \alpha x \\ &\quad + \beta y)(-24by - 24d + 32(\alpha x + \beta y + \gamma)^2 + 9)), \end{aligned} \quad (3.8)$$

where its first integral is

$$\tilde{H}_3(x, y) = (3(ax + by + d) - 4(\gamma + \alpha x + \beta y)^2)^2 + 9(\gamma + \alpha x + \beta y)^2. \quad (3.9)$$

System (III) is given by

$$\begin{aligned}
\dot{x} &= \frac{1}{\alpha b - a\beta} (b^2 y (6a^2 x^2 + 4d(3ax - 1) - 4ax + 6d^2 + 2\beta y(\gamma + \alpha x + \beta y) + 1) + b \\
&\quad (2a^3 x^3 + d(6a^2 x^2 - 4ax + 4\beta y(\gamma + \alpha x + \beta y) + 1) - 2a^2 x^2 + d^2(6ax - 2) + ax \\
&\quad (4\beta y(\gamma + \alpha x + \beta y) + 1) + 2d^3 + (\gamma + \alpha x + \beta y)(\gamma + \alpha x - 2\beta y)) + 2b^3 y^2 (3ax \\
&\quad + 3d - 1) + \beta(ax + d - 1)(2ax + 2d - 1)(\gamma + \alpha x + \beta y) + 2b^4 y^3), \\
\dot{y} &= \frac{-1}{\alpha b - a\beta} (2a^4 x^3 + 2a^3 x^2 (3by + 3d - 1) + a^2 x (6b^2 y^2 + 4d(3by - 1) - 4by + 6d^2 \\
&\quad + 2ax(\gamma + \alpha x + \beta y) + 1) + a(2b^3 y^3 + d(6b^2 y^2 - 4by + 4ax(\gamma + \alpha x + \beta y) + 1) \\
&\quad - 2b^2 y^2 + d^2(6by - 2) + by(4ax(\gamma + \alpha x + \beta y) + 1) + 2d^3 - (-\gamma + 2ax - \beta y) \\
&\quad (\gamma + \alpha x + \beta y)) + \alpha(by + d - 1)(2by + 2d - 1)(\gamma + \alpha x + \beta y)),
\end{aligned} \tag{3.10}$$

and its corresponding first integral is

$$\tilde{H}_4(x, y) = \frac{(ax + by + d - 1)^2 ((ax + by + d)^2 + (\gamma + \alpha x + \beta y)^2)}{(2(ax + by + d) - 1)^2}. \tag{3.11}$$

Section 3.1 Main results

In this chapter we study the existence and the upper bound of limit cycles that intersect the irregular separation line Σ in two points, where we will find two possible configurations of limit cycles. The first configuration denoted by *conf 1* is when the limit cycles have two intersection points with Γ_1 or Γ_2 . But to study the limit cycles which intersect Γ_1 or Γ_2 in two point is equivalent to study the piecewise differential systems separated by one straight line. It was proved by Benterki and Llibre in Theorem 1 of [10] that the maximum number of limit cycles of this configuration varies from 0, 1 and 2.

The second configuration denoted by *conf 2*, is when the limit cycles have two intersection points with the irregular line Σ , such that one point is situated in Γ_1 and the second point is located in Γ_2 , i.e., the first point of intersection is $(x_1, 0) \in \Gamma_1$ and the second point is $(0, y_2) \in \Gamma_2$. We notice that when we combine the two configurations *conf 1* and *conf 2* we obtain another configuration that have a combination between the two kinds of limit cycles and we will denoted it by *conf 3*.

We restrict our analysis to study the maximum number of limit cycles of *conf 2* and *conf 3*.

The first main result of the present chapter is the following.

THEOREM 3.1 *The maximum number of limit cycles of discontinuous piecewise differential system separated by the irregular line Σ and formed by linear differential center (3.4) in the regions Σ^- and an arbitrary cubic isochronous center in the regions Σ^+ after an affine change of variables is:*

- (i) *at most two for system of type (I)-(3.4), and there are example with exactly two limit cycles, see Fig 3.1(a);*
- (ii) *at most two for system of type (II)-(3.4), and there are example with exactly two limit cycles, see Fig 3.1(b);*
- (iii) *at most three for system of type (III)-(3.4), and there are example with exactly three limit cycles, see Fig 3.1(c).*

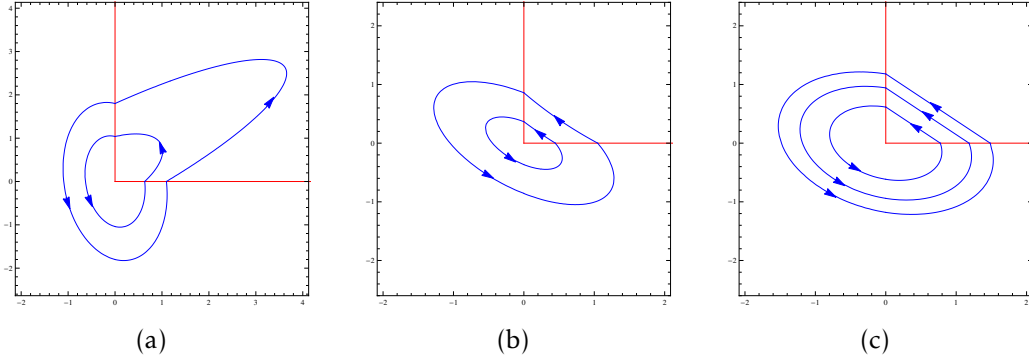


Figure 3.1: The two limit cycles of the discontinuous piecewise differential system, (a) for (3.13)-(3.14), (b) for (3.15)-(3.16) and (c) three limit cycles of the discontinuous piecewise differential system (3.17)-(3.18) with *conf 2*.

Section 3.2 Proof of Theorem 3.1

In the region Σ^- we consider the linear differential center (3.4) with its first integral $H_1(x, y)$ given by (3.5). In the region Σ^+ we consider one of the three families of cubic isochronous systems with its corresponding first integral $\tilde{H}_i(x, y)$ with $i = 2, 3, 4$. If the discontinuous piecewise differential system (3.4)-(2m), with $m \in \{3, 4, 5\}$ has a limit cycle, which intersects the separation line Σ in two distinct points $(0, y_1) \in \Gamma_1$ and $(x_1, 0) \in \Gamma_2$. These two points must satisfy the system of equations

$$\begin{aligned}
e_1 &= H_1(x_1, 0) - H_1(0, y_1) = P_1(x_1, y_1) = 0, \\
e_2 &= \tilde{H}_i(x_1, 0) - \tilde{H}_i(0, y_1) = P_i(x_1, y_1) = 0, \text{ with } i = 2, 3, 4.
\end{aligned} \tag{3.12}$$

By solving $P_1(x_1, y_1) = 0$, we get $x_1 = g(y_1) = Dy_1$, with $D = \sqrt{A^2 + \omega^2}$, and by substituting x_1 in $P_i(x_1, y_1) = 0$ we obtain an equation in the variable y_1 , and we distinguish three cases according to the expression of the first integral $\tilde{H}_i(x, y)$.

Proof.

Proof of statement (i) of Theorem 3.1. For $i = 2$, the corresponding isochronous cubic system is (3.6) with its first integral $\tilde{H}_2(x, y)$ given in (3.7), the solutions of the equation $P_2(g(y_1), y_1) = 0$ are equivalent to the solutions of the quartic equation $F_1(y_1) = 0$ such that

$$\begin{aligned}
F_1(y_1) &= y_1(2b(K_1(D^2y_1^2(a^2 + \alpha^2) + \gamma^2) - d^2K_1 + d(2K_2(\gamma^2 + \alpha^2D^2y_1^2) + 1)) - a^2D^2y_1(-2dK_1 \\
&\quad + 2K_2(\gamma + \beta y_1)^2 + 1) + b^2y_1(-2aDK_1y_1 - 2dK_1 + 2K_2(\gamma + \alpha Dy_1)^2 + 1) + 2aD(d^2K_1 \\
&\quad - d(2K_2(\gamma^2 + \beta^2y_1^2) + 1) - K_1(\gamma^2 + \beta^2y_1^2)) + (2d(dK_2 + K_1) - 1)(\alpha D - \beta)(2\gamma + \alpha Dy_1 \\
&\quad + \beta y_1)) + 4\gamma Dy_1^2(2dK_2 + K_1)(\alpha b - a\beta).
\end{aligned}$$

This equation has at most four real solutions. Therefore system (3.12) has at most four real solutions, which can easily be proved that they are symmetric. These two solutions provide at most two limit cycles for the discontinuous piecewise differential system (3.4)-(3.6).

Now we prove that the result of statement (i) is reached by giving an example of discontinuous piecewise differential system (3.4)-(3.6) with exactly two limit cycles.

In the region Σ^+ we consider the cubic isochronous differential center

$$\begin{aligned}
\dot{x} &\simeq x^2(0.29088 - 0.234119y) + x((0.389428y - 0.210984y^2) + 0.673442) \\
&\quad + 0.2x^3 + (-0.594058y - 1.39526)y + 0.0801447, \\
\dot{y} &\simeq x(0.69824y - 0.234119y^2) + 0.788391x + 0.2yx^2 - 0.152264x^2 + y \\
&\quad ((-0.210984y - 0.191014)y - 0.289442) + 0.251744,
\end{aligned} \tag{3.13}$$

with the first integral

$$\tilde{H}_2(x, y) \simeq \frac{(x + 0.596858y + 0.4)^2 + (x - 1.76745y + 0.2)^2}{1 - 2(0.1(x - 1.76745y + 0.2) + 0.2)(0.2 + x - 1.76745y)}.$$

In the region Σ^- we consider the linear differential center

$$\dot{x} = -\left(\frac{1}{10}x + \frac{37}{100}\right), \quad \dot{y} = \frac{1}{10}y + x, \tag{3.14}$$

which has the first integral $H_1(x, y) = \frac{9}{25}y^2 + (x + \frac{1}{10}y)^2$.

The real solutions of system (3.12) are $(x_1, y_1) \simeq \{(1.09545, 1.8009), (0.632456, 1.03975)\}$. Then the two crossing limit cycles of system (3.13)-(3.14) corresponding to these solutions are shown in Figure 3.1(a).

Proof of statement (ii) of Theorem 3.1. For $i = 3$, the isochronous cubic system is (3.8), where its first integral is $\tilde{H}_3(x, y)$ given in (3.9). To obtain the number of real solutions of system (3.12), we have to solve the equation $P_3(g(y_1), y_1) = 0$ which has the same solutions as the quartic equation $F_2(y_1) = 0$, such that

$$F_2(y_1) = 3y_1^2(-3a^2D^2 + 16a\alpha\gamma D^2 + 3b^2 - 16\beta b\gamma - (3 + 32\gamma^2 - 8d)(-\beta + \alpha D)(\alpha D + \beta)) - 2y_1(3aD(-4\gamma^2 + 3d) + 12\gamma^2b - 9db - \gamma(24d - 32\gamma^2 - 9)(\alpha D - \beta)) + 8y_1^3(3a\alpha^2 D^3 - 3b\beta^2 + 8(\gamma\beta^3 - \gamma\alpha^3 D^3)) + 16y_1^4(\beta^4 - \alpha^4 D^4).$$

Its clear that this equation has at most four real solutions, and due to the fact that these solutions are symmetric, we know that system (3.12) has at most two distinct real solutions. Consequently, the discontinuous piecewise differential system (3.4)-(3.8) has at most two limit cycles.

To reach our result we shall give an example of discontinuous piecewise differential system (3.4)-(3.8) with exactly two limit cycles.

In the region Σ^+ we consider the cubic isochronous differential center

$$\begin{aligned} \dot{x} &\simeq y(y(0.195657 - 0.011447y) - 0.071458) + 0.011447x^3 + x^2(-0.0343434y - 0.071009) + xy(0.034343y - 0.124647) - 6.3691 - 1.44776x, \\ \dot{y} &\simeq y(y(0.0623236 - 0.011447y) + 1.44776) + 0.011447x^3 + x^2(-0.034343y - 0.204343) + xy(0.034343y + 0.14202)y + 5.20374 + 0.138904x, \end{aligned} \quad (3.15)$$

with the first integral

$$\tilde{H}_3(x, y) \simeq (3(0.210589 + 0.1xy + 1.22182) + 4(-0.1y + 0.1x - 0.22)^2)^2 - 9(-0.22 + 0.1x - 0.1y)^2.$$

In region Σ^- we consider the linear differential center

$$\dot{x} = -\left(\frac{7}{10}x + \frac{149}{100}y\right), \quad \dot{y} = \frac{7}{10}y + x, \quad (3.16)$$

which has the first integral $H_1(x, y) = \left(x + \frac{7}{10}y\right)^2 + y^2$.

The discontinuous piecewise differential system (3.15)-(3.16) has exactly two crossing limit

cycles, because system (3.12) has the two solutions $(x_1, y_1) \simeq \{(1.04881, 0.859218), (0.447214, 0.366372)\}$. These limit cycles are shown in Figure 3.1(b).

Proof of statement (iii) of Theorem 3.1. For $i = 4$, the first integral for the cubic isochronous system (3.10) is $\tilde{H}_4(x, y)$ given in (3.11). We are interesting in finding the solutions y_1 of the equation $P_4(g(y_1), y_1) = 0$ which has the same solutions as the equation of degree six $F_3(y_1) = 0$ such that

$$\begin{aligned}
F_3(y_1) = & y_1^2(a^2D^2(3\gamma^2 - 2d(2\gamma^2 + 5d((2d - 4)d + 15d - 5) + 2d + 4a\gamma(2d - 1)D(\alpha(2d \\
& - 1)(1 - d)D - 2\beta(d - 1)) + b^2(-3\gamma^2 + 2d(2\gamma^2 + 5d(2d(d - 2) + 3) - 25d + 1) + 4b \\
& \gamma(2d - 1)(1 - d)(\beta - 2\beta d + 2\alpha(d - 1)D) + (d - 1)^2((-1 + 2d)^2)(\alpha D - \beta)(\beta + \alpha D)) \\
& + 4a^2b^2D^2y_1^6(-D^2(a^2 + \alpha^2) + b^2 + \beta^2) - 2y_1^3(b(2a^2D^2(\gamma^2 + (2d - 1)^3) - 8a\gamma(-2d \\
& + 1)(-1 + d)D(\alpha D - \beta) + (d - 1)(2d - 1)(\beta^2(1 - 2d) + 2\alpha^2(d - 1)D^2)) + aD(a^2(2d \\
& - 1)^3D^2 + a\gamma D(\alpha(1 - 2d)^2D - 4\beta(d - 1)^2) + (d - 1)(2d - 1)(\alpha^2(2d - 1)D^2 - 2\beta^2(1 \\
& - d))) - b^2(2aD(\gamma^2 + (2d - 1)^3) + \gamma(\beta - 4(1 - d)(\beta d + D(\alpha - \alpha d)))) - b^3(2d - 1)^3 \\
& - 4abDy_1^5(b(2a^2(2d - 1)D^2 + 2a\gamma D(\alpha D - \beta) + \beta^2(1 - 2d) - 2\alpha^2(-d + 1)D^2) + D^3 \\
& (a^2 + \alpha^2)a(2d - 1) + 2ab^2(1 - 2d)D - 2a\beta^2(d - 1)D + b^3(1 - 2d)) + y_1^4(8abD(a\gamma D \\
& (2\beta(d - 1) + D(\alpha - 2\alpha d)) - (2d - 1)(a^2(2d - 1)D^2 + (d - 1)(\alpha D - \beta)(\beta + \alpha D))) + a^2 \\
& D^2(4\beta^2(1 - d)^2 - (1 - 2d)^2D^2(a^2 + \alpha^2)) + 8ab^3(1 - 2d)^2D - b^2(\beta - 2\beta d + 2\alpha(d \\
& - 1)D)(8a\gamma D + \beta(2d - 1) + 2\alpha(d - 1)D) + b^4(1 - 2d)^2) + 2(d - 1)(2d - 1)dy_1(2d \\
& (1 - d) + dy_1(b - aD) + \gamma^2(b - aD) + (-2d\gamma + \gamma)(1 - d)(\alpha D - \beta)).
\end{aligned}$$

The equation $F_3(y_1) = 0$ has at most six real solutions. Therefore, system (3.12) has at most three real non-symmetric solutions, which provide at most three limit cycles for the discontinuous piecewise differential system (3.4)-(3.10).

To complete the proof of this statement we shall provide an example of discontinuous piecewise differential system formed by an arbitrary linear center and a cubic isochronous center of type (3.10) with exactly three limit cycles.

In the region Σ^+ , we consider the cubic isochronous differential center

$$\begin{aligned}
\dot{x} \simeq & -0.0333565x^3 + 0.0251109x^2y + 325.854x^2 - x((-0.220905y^2 + 1633.64y) \\
& - 1.31696 \times 10^6) - y((2564.66 - 0.171752y)y - 1.1617 \times 10^7) - 1.43102, \\
& \times 10^{10} \\
\dot{y} = & x^2(1293.86 - 0.139931y) + x(y(1299.6 - 0.0250305y) - 7.36102 \times 10^6) \\
& - 0.0689903x^3 + y((0.0526109y - 409.335)y - 1.31566 \times 10^6) + 1.13904 \\
& \times 10^{10},
\end{aligned} \tag{3.17}$$

which has the first integral

$$\tilde{H}_4(x, y) \simeq \frac{1}{((0.4x + 0.0502352y - 324.994) - 1)^2} ((0.3x - 0.376965y + 0.2)^2 - (-1625.97 + 0.2x + 0.251176y)^2 (-0.2x + 1624.97 - 0.251176y)^2).$$

In Σ^- , we consider the linear differential center

$$\dot{x} = -\left(\frac{3}{10}x + \frac{1973}{1250}y\right), \quad \dot{y} = \frac{3}{10}y + x, \quad (3.18)$$

and its corresponding first integral is

$$H_1(x, y) = \left(\frac{3}{10}y + x\right)^2 + \frac{3721}{2500}y^2. \quad \blacksquare$$

The three solutions of system (3.12) for these systems are $(x_1, y) \simeq \{(1.48324, 1.1806), (1.18322, 0.941793), (0.774597, 0.616548)\}$. Then the three crossing limit cycles for the discontinuous piecewise differential system (3.17)-(3.18) are shown in Figure 3.1(c).

THEOREM 3.2 *The maximum number of limit of discontinuous piecewise differential system separated by the irregular line Σ and formed by an arbitrary linear differential center (3.2) in the regions Σ^- and an arbitrary cubic isochronous center in the regions Σ^+ after an affine change of variables with **conf 1** and **conf 2** is*

- (i) *at most three for system of type (I)-(3.2), and there are example with exactly three limit cycles, see Figure 3.2(a);*
- (ii) *at most three for system of type (II)-(3.2), and there are example with exactly three limit cycles, see Figure 3.2(b);*
- (iii) *at most five for system of type (III)-(3.2), and there are example with exactly five limit cycles, see Figure 3.2(c).*

Section 3.3 Proof of Theorem 3.2

In order to have limit cycles of **conf 1** and **conf 2** simultaneously, the limit cycles of **conf 1** which intersect the separation line Γ_1 in two points must satisfy the equations

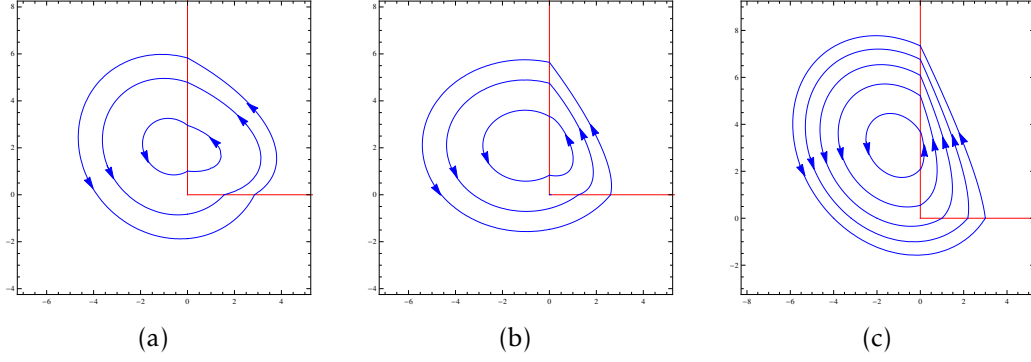


Figure 3.2: Three limit cycles of the piecewise differential system, (a) for (3.20)-(3.21), (b) for (3.22)-(3.23) and (c) five limit cycles of the discontinuous piecewise differential system (3.24)-(3.25) with *conf 3*.

$$\begin{aligned}
 E_1 &= H(0, y_1) - H(0, y_2) = (y_1 - y_2)(-2B + (y_1 + y_2)(A^2 + \omega^2)) = 0, \\
 E_2 &= \tilde{H}_i(0, y_1) - \tilde{H}_i(0, y_2) = P_i(y_1, y_2) = 0,
 \end{aligned} \tag{3.19}$$

where $\tilde{H}_i(x, y)$ for $i = 2, 3, 4$, are the first integrals given by (3.7), (3.9), (5.39). On the other hand the two intersection points of limit cycles of *conf 2* with the irregular separation line Σ must satisfy system (3.12). Then we have the following results.

Proof.

Proof of statement (i) of Theorem 3.2.

In what follows we give an example of discontinuous piecewise differential system formed by an arbitrary linear center (3.2) and the cubic isochronous center (3.6), which has one limit cycle of *conf 1* and two limit cycles of *conf 2*, i.e., has three limit cycles of *conf 3*.

In the region Σ^+ we consider the cubic isochronous center

$$\begin{aligned}
 \dot{x} &\simeq x^2(0.103711 - 0.006568y) - 0.00592118x^3 + x((0.0124892y + 0.189279)y \\
 &\quad - 0.755639) - (0.118324y + 1.2791)y + 2.88432, \\
 \dot{y} &\simeq x(0.112022y - 0.006568y^2) + 0.445381x + x^2(-0.00592118y - 0.0323263) \\
 &\quad - y(0.143181 + (-0.0124892y - 0.0949698)y) - 0.122119,
 \end{aligned} \tag{3.20}$$

with the first integral

$$\tilde{H}_2(x, y) \simeq \frac{(-0.1x - 0.210924y + 0.4)^2 + (-0.1x + 0.1y - 0.2)^2}{1 + 2(-0.296059(-0.1x + 0.1y - 0.2) - 0.680186)(0.2 + 0.1x - 0.1y)}.$$

In the region Σ^- we consider the linear differential center

$$\dot{x} = -\left(\frac{1}{10}x - 2 + \frac{101}{100}y\right), \quad \dot{y} = \frac{5}{10} + x + \frac{1}{10}y, \quad (3.21)$$

which has the first integral

$$H(x, y) = \left(x + \frac{1}{10}y\right)^2 + (x - 4y) + y^2.$$

For the discontinuous piecewise differential system (3.20)–(3.21), system (3.19) has the unique solution $(y_1, y_2) \simeq (1.00506, 2.95533)$, which provide one limit cycle intersecting Γ_1 in the two points $(0, y_1)$ and $(0, y_2)$, and system (3.12) has the two solutions $(x_3, y_3) \simeq (1.56155, 4.78761)$ and $(x_4, y_4) = (2.8541, 5.82887)$, which provide the four intersecting points $(x_i, 0), (0, y_i)$ with $i = 3, 4$ of the two limit cycles with the separation irregular line Σ . Then the discontinuous piecewise differential system (3.20)–(3.21) has exactly three limit cycles, see Figure 3.2(a).

Proof of statement (ii) of Theorem 3.2. In what follows we give an example of discontinuous piecewise differential system formed by an arbitrary linear center (3.2) and the cubic isochronous center (3.8), which has one limit cycle of **conf 1** and two limit cycles of **conf 2**, i.e, has three limit cycles of **conf 3**.

In the region Σ^+ we consider the cubic isochronous center

$$\begin{aligned} \dot{x} &\simeq 0.169221x^2 - 0.246893yx^2 + x(1.03113y - 0.292023y^2) - 0.914334x \\ &\quad + y((0.982871 - 0.115134y)y - 3.20465) - 0.0695791x^3 + 3.31428, \\ \dot{y} &\simeq 0.0588262x^3 + x^2(0.208737y + 0.082386) + x((0.246893y - 0.338442)y \\ &\quad + 0.983531) - 0.716136 + y(0.097340y - 0.515564)y + 0.914334y, \end{aligned} \quad (3.22)$$

and its first integral is

$$\begin{aligned} \tilde{H}_3(x, y) &\simeq (0.16x^2 + (0.378493y + 0.149387)x + 0.469133 + (0.223839y - 1.27391)y \\ &\quad + 1.48034)^2 - 9(0.236558y + 0.2x)^2. \end{aligned}$$

In the region Σ^- we consider the linear differential center

$$\dot{x} = -\left(\frac{14401}{10000}y - 3 + \frac{x}{100}\right), \quad \dot{y} = 1 + x + \frac{y}{100}, \quad (3.23)$$

which has the first integral

$$H(x, y) = \left(x + \frac{1}{100}y\right)^2 + 2(x - 3y) + \frac{36}{25}y^2.$$

For the discontinuous piecewise differential system (3.22)–(3.23), system (3.19) has the unique solution $(y_1, y_2) \simeq (0.833353, 3.33302)$. which provide one limit cycle intersecting Γ_1 in the two points $(0, y_1)$ and $(0, y_2)$, and system (3.12) has the two solutions $(x_3, y_3) \simeq (1.23607, 4.75101)$ and $(x_4, y_4) \simeq (2.60555, 5.64302)$, which provide the four intersecting points $(x_i, 0)$, $(0, y_i)$ with $i = 3, 4$ of the two limit cycles with the separation irregular line Σ . Then the discontinuous piecewise differential system (3.22)–(3.23) has exactly three limit cycles, see Figure 3.2(b).

Proof of statement (iii) of Theorem 3.2. In what follows we give an example of discontinuous piecewise differential system formed by an arbitrary linear center (3.2) and the cubic isochronous center (3.10), which has two limit cycles of **conf 1** and three limit cycles of **conf 2**, i.e, has five limit cycles of **conf 3**.

In the region Σ^+ we consider the cubic isochronous center

$$\begin{aligned} \dot{x} &\simeq -0.048133x^3 - 0.121939x^2y - 0.426587x^2 + x((-0.095040y - 0.972986) \\ &\quad y + 0.995223) + y((-0.023526y - 0.581449)y + 1.46708) + 1.15725, \\ \dot{y} &\simeq 0.0367839x^3 + 0.093016x^2y + 0.59027x^2 + x((0.072423y + 1.42865) \\ &\quad y + 0.128844) + 0.794241 + y((0.017915y + 0.892226)y - 0.037402), \end{aligned} \quad (3.24)$$

with the first integral

$$\begin{aligned} \tilde{H}_4(x, y) &\simeq \frac{1}{(2(0.037796x + 0.023059y + 0.77109) - 1)^2} ((0.037796x + 0.023059y \\ &\quad + 0.77109)^2 + (0.339871x + 0.447685y + 0.5)^2)(0.037797x + 0.023051y \\ &\quad - 0.23891)^2. \end{aligned}$$

In Σ^- we consider the linear differential center

$$\dot{x} = -\left(\frac{2}{10}x + \frac{26}{25}y\right), \quad \dot{y} = x + \frac{5}{10} + \frac{2}{10}y, \quad (3.25)$$

and its first integral is

$$H(x, y) = y^2 + \left(x + \frac{2}{10}y\right)^2 + (x - 6y).$$

For the discontinuous piecewise differential system (3.24)–(3.25), system (3.19) has the two solution $(y_1, y_2) \simeq (2.09171, 3.67752)$ and $(y_3, y_4) \simeq (0.553009, 5.21622)$, which provide the

two limit cycles intersecting Γ_1 in the four points $(0, y_i)$ with $i = 1, 2, 3, 4$, and system (3.12) has the three solutions $(x_5, y_5) \simeq (1, 6.08525)$, $(x_6, y_6) = (2.19258, 6.76428)$ and $(x_7, y_7) = (3, 7.34101)$, which provide the six intersecting points $(x_i, 0), (0, y_i)$ with $i = 5, 6, 7$ of the three limit cycles with the separation line Σ . Then the discontinuous piecewise differential system (3.24)–(3.25) has exactly five limit cycles of **conf 3** shown in Figure 3.2(c). ■

Limit Cycles Bifurcating From Planar Piecewise Differential Systems Formed by Linear and Cubic Centers

The objective of this chapter is to study the limit cycles that can bifurcate from the discontinuous piecewise differential systems separated by the straight line $y = 0$ and formed by a linear differential system having a center or focus of the form

$$\dot{x} = \gamma + \alpha x + \beta y, \quad \dot{y} = \delta - \beta x + \alpha y. \quad (4.1)$$

defined in the half-plane $y \geq 0$, where α, β, γ , and $\delta \in \mathbb{R}$, and by an arbitrary cubic weak focus or center located at the origin given by

$$\begin{aligned} \dot{x} &= -cxy - y - ax^2 - zy^2 - kx^3 - mx^2y - pxy^2 - hy^3, \\ \dot{y} &= x + by^2 + dxy + gx^2 + ly^3 + nxy^2 + qx^2y + wx^3. \end{aligned} \quad (4.2)$$

defined in the half-plane $y \leq 0$, where all the parameters of the system are real.

Section 4.1 Statement of the main result

The main goal of our chapter focuses on studying the simple zeros of the averaged functions. Here we shall use the averaging theory up to the third order for studying the number of limit cycles that can bifurcate from the discontinuous piecewise differential systems formed by (4.1) for $y \geq 0$, when we perturb it inside the class of all polynomial

differential systems of degree 1 as follows

$$\dot{x} = \sum_{i=1}^3 \varepsilon^i P_{1i}(x, y), \dot{y} = \sum_{i=1}^3 \varepsilon^i Q_{1i}(x, y), \quad (4.3)$$

and by the differential system (4.2) for $y \leq 0$ when we perturb it inside the class of all polynomial differential systems of degree 3 as follows

$$\dot{x} = \sum_{i=1}^3 \varepsilon^i P_{3i}(x, y), \dot{y} = \sum_{i=1}^3 \varepsilon^i Q_{3i}(x, y). \quad (4.4)$$

Here $\varepsilon > 0$ is a small parameter, $i = 1, \dots, 3$, P_{1i} and Q_{1i} , are real polynomials of degree 1 in the variables x and y , and P_{3i} , Q_{3i} are real polynomials of degree 3 in the variables x and y .

We need to use the following Descartes Theorem and Lemma 1.1 in chapter 1 in order to demonstrate our results regarding the number of zeros in a real polynomial.

THEOREM 4.1 (Descartes Theorem) *Consider the real polynomial $r(x) = a_{i_1}x^{i_1} + a_{i_2}x^{i_2} + \dots + a_{i_r}x^{i_r}$ with $0 = i_1 < i_2 < \dots < i_r$ and $a_{i_j} \neq 0$ real constants for $j \in \{1, \dots, r\}$. When $a_{i_j}a_{i_{j+1}} < 0$, we say that a_{i_j} have a variation of the sign. If the number of variations of signs is m , then $r(x)$ has at most m positive real roots. Moreover, it is always possible to choose the coefficients of $r(x)$ in such a way that $r(x)$ has exactly $r - 1$ positive real roots.*

For more details see [15].

Our main result is the following.

THEOREM 4.2 *For $|\varepsilon| \neq 0$ sufficiently small and by using the averaging theory up to third order the maximum number of limit cycles of the discontinuous piecewise differential systems formed by linear differential focus or center (4.1) and the cubic weak focus or center (4.2) is at most seven. There are examples with exactly seven limit cycles bifurcating from the periodic orbits of these system.*

Section 4.2 Proof of Theorem 4.2

In order to apply the averaging method for studying the limit cycles for ε sufficiently small, we need to write the tow systems in the standard form. So we have developed the parameters of the differential systems until the third order in ε . To ensure that the origin of system (4.1) is a center, we must add -1 with regard to the growth of β . Then in $y \geq 0$ we have the following system

$$\dot{x} = -y + \alpha x + \beta y + \gamma, \quad \dot{y} = x - \beta x + \alpha y + \delta,$$

with

$$\begin{aligned} \alpha &= \alpha_1 \varepsilon + \alpha_2 \varepsilon^2 + \alpha_3 \varepsilon^3, & \beta &= -1 + \beta_1 \varepsilon + \beta_2 \varepsilon^2 + \beta_3 \varepsilon^3, \\ \gamma &= \gamma_1 \varepsilon + \gamma_2 \varepsilon^2 + \gamma_3 \varepsilon^3, & \delta &= \delta_1 \varepsilon + \delta_2 \varepsilon^2 + \delta_3 \varepsilon^3. \end{aligned}$$

Then the perturbed system of system (4.1) is given by

$$\begin{aligned} \dot{x} &= \varepsilon(\alpha_1 x + \beta_1 y + \gamma_1) + \varepsilon^2(\alpha_2 x + \beta_2 y + \gamma_2) + \varepsilon^3(\alpha_3 x + \beta_3 y + \gamma_3) - 2y, \\ \dot{y} &= 2x + \varepsilon(-\beta_1 x + \alpha_1 y + \delta_1) + \varepsilon(-\beta_2 x + \alpha_2 y + \delta_2) + \varepsilon^3(-\beta_3 x + \alpha_3 y + \delta_3). \end{aligned} \quad (4.5)$$

According to system (4.3) we know that

$$\begin{aligned} P_{11}(x, y) &= \gamma_1 + \alpha_1 x + \beta_1 y, & P_{12}(x, y) &= \gamma_2 + \alpha_2 x + \beta_2 y, & P_{13}(x, y) &= \gamma_3 + \alpha_3 x + \beta_3 y, \\ Q_{11}(x, y) &= -\beta_1 x + \alpha_1 y + \delta_1, & Q_{12}(x, y) &= -\beta_2 x + \alpha_2 y + \delta_2, & Q_{13}(x, y) &= -\beta_3 x + \alpha_3 y + \delta_3. \end{aligned}$$

In $y \leq 0$ we have the differential system

$$\begin{aligned} \dot{x} &= -cxy - y - ax^2 - zy^2 - kx^3 - mx^2y - pxy^2 - hy^3, \\ \dot{y} &= by^2 + dxy + gx^2 + ly^3 + nxy^2 + qx^2y + wx^3 + x. \end{aligned}$$

Where

$$\begin{aligned} a &= a_1 \varepsilon + a_2 \varepsilon^2 + a_3 \varepsilon^3, & c &= c_1 \varepsilon + c_2 \varepsilon^2 + c_3 \varepsilon^3, & p &= p_1 \varepsilon + p_2 \varepsilon^2 + p_3 \varepsilon^3, \\ z &= z_1 \varepsilon + z_2 \varepsilon^2 + z_3 \varepsilon^3, & k &= k_1 \varepsilon + k_2 \varepsilon^2 + k_3 \varepsilon^3, & m &= m_1 \varepsilon + m_2 \varepsilon^2 + m_3 \varepsilon^3, \\ h &= h_1 \varepsilon + h_2 \varepsilon^2 + h_3 \varepsilon^3, & g &= g_1 \varepsilon + g_2 \varepsilon^2 + g_3 \varepsilon^3, & d &= d_1 \varepsilon + d_2 \varepsilon^2 + d_3 \varepsilon^3, \\ b &= b_1 \varepsilon + b_2 \varepsilon^2 + b_3 \varepsilon^3, & w &= w_1 \varepsilon + w_2 \varepsilon^2 + w_3 \varepsilon^3, & q &= q_1 \varepsilon + q_2 \varepsilon^2 + q_3 \varepsilon^3, \\ n &= n_1 \varepsilon + n_2 \varepsilon^2 + n_3 \varepsilon^3, & l &= l_1 \varepsilon + l_2 \varepsilon^2 + l_3 \varepsilon^3. \end{aligned}$$

Then the perturbed system of system (4.2) is given by

$$\begin{aligned} \dot{x} &= -y + \varepsilon(-a_1 x^2 - c_1 xy - z_1 y^2 - k_1 x^3 - m_1 x^2 y - p_1 xy^2 - h_1 y^3) + \varepsilon^2(-a_2 x^2 \\ &\quad - c_2 xy - z_2 y^2 - k_2 x^3 - m_2 x^2 y - p_2 xy^2 - h_2 y^3) + \varepsilon^3(-a_3 x^2 - c_3 xy - z_3 y^2 \end{aligned}$$

$$\begin{aligned}
& -k_3x^3 - m_3x^2y - p_3xy^2 - h_3y^3), \\
\dot{y} = & x + \varepsilon(b_1y^2 + d_1xy + g_1x^2 + l_1y^3 + n_1xy^2 + q_1x^2y + w_1x^3) + \varepsilon^2(b_2y^2 + d_2xy \\
& + g_2x^2 + l_2y^3 + n_2xy^2 + q_2x^2y + w_2x^3) + \varepsilon^3(b_3y^2 + d_3xy + g_3x^2 + l_3y^3 + n_3xy^2 \\
& + q_3x^2y + w_3x^3). \tag{4.6}
\end{aligned}$$

According to system (4.4) we know that

$$\begin{aligned}
P_{31}(x, y) &= -a_1x^2 - c_1xy - z_1y^2 - k_1x^3 - m_1x^2y - p_1xy^2 - h_1y^3, \\
P_{32}(x, y) &= -a_2x^2 - c_2xy - z_2y^2 - k_2x^3 - m_2x^2y - p_2xy^2 - h_2y^3, \\
P_{33}(x, y) &= -a_3x^2 - c_3xy - z_3y^2 - k_3x^3 - m_3x^2y - p_3xy^2 - h_3y^3, \\
Q_{31}(x, y) &= b_1y^2 + d_1xy + g_1x^2 + l_1y^3 + n_1xy^2 + q_1x^2y + w_1x^3, \\
Q_{32}(x, y) &= b_2y^2 + d_2xy + g_2x^2 + l_2y^3 + n_2xy^2 + q_2x^2y + w_2x^3, \\
Q_{33}(x, y) &= b_3y^2 + d_3xy + g_3x^2 + l_3y^3 + n_3xy^2 + q_3x^2y + w_3x^3.
\end{aligned}$$

We compute the averaged functions $f_i(r)$, for $i = 1$ we get

$$f_1(r) = \frac{1}{8}\pi r^3(-3k_1 + 3l_1 - p_1 + q_1) - \frac{2}{3}r^2(2b_1 - c_1 + g_1) + \pi\alpha_1r + 2\delta_1.$$

By using Descartes Theorem we know that the polynomial $f_1(r)$ can have at most three positive real roots, which provide three limit cycles for the discontinuous piecewise differential system (4.1)–(4.2).

In order to apply the averaging theory of the second order, we need that $f_1(r) \equiv 0$. So we must take $c_1 = 2b_1 + g_1$, $p_1 = -3k_1 + 3l_1 + q_1$, $\delta_1 = 0$ and $\alpha_1 = 0$. Computing the function $f_2(r)$ we get

$$\begin{aligned}
f_2(r) = & \frac{1}{16}\pi r^5(h_1(q_1 - 3k_1) + k_1(-m_1 + n_1 + 3w_1) + 2l_1m_1 - 2l_1n_1 + m_1q_1 - n_1q_1 - q_1w_1) \\
& + \frac{2}{15}r^4(a_1(3k_1 - 4l_1 - 3q_1) - 4b_1m_1 + 4b_1n_1 - 3d_1k_1 + 2d_1l_1 + 2d_1q_1 + g_1(-2h_1 - 3m_1 \\
& + 2n_1 + 3w_1) + 6k_1z_1 - 2q_1z_1) + \frac{1}{8}\pi r^3(2a_1b_1 + 3a_1g_1 - b_1d_1 - d_1g_1 + g_1z_1 - 3k_2 + 3l_2 \\
& - p_2 + q_2) - \frac{2}{3}r^2(2b_2 - c_2 + g_2) + \pi\alpha_2r + 2\delta_2.
\end{aligned}$$

This polynomial can have at most five positive real roots, which provide at most five limit cycles for the discontinuous piecewise differential system (4.1)–(4.2).

In order to apply the averaging theory of third order we need to have $f_2(r) \equiv 0$, for that we must take

$$\begin{aligned}
w_1 = & -\frac{1}{g_1(3k_1 - q_1)}((3k_1 - q_1)(a_1(3k_1 - 4l_1 - 3q_1) - 4b_1m_1 + 4b_1n_1 + d_1(2(l_1 + q_1) - 3k_1) \\
& - 3g_1m_1 + 2g_1n_1 + 6k_1z_1 - 2q_1z_1) + 2g_1(m_1 - n_1)(k_1 - 2l_1 - q_1)),
\end{aligned}$$

$$c_2 = 2b_2 + g_2, p_2 = a_1(2b_1 + 3g_1) - d_1(b_1 + g_1) + g_1z_1 - 3k_2 + 3l_2 + q_2, \alpha_2 = 0,$$

$$h_1 = -\frac{1}{g_1(3k_1 - q_1)}(a_1(3k_1 - q_1)(3k_1 - 4l_1 - 3q_1) - 12b_1k_1m_1 + 12b_1k_1n_1 + 4b_1m_1q_1 - 4b_1n_1q_1 - d_1(3k_1 - q_1)(3k_1 - 2(l_1 + q_1)) - 6g_1k_1m_1 + 3g_1k_1n_1 - 6g_1l_1m_1 + 6g_1l_1n_1 + g_1n_1q_1 + 2z_1(q_1 - 3k_1)^2), \delta_2 = 0.$$

For w_1 and h_1 we considered four cases $g_1(3k_1 - q_1) \neq 0$, or $(g_1 = 0, (3k_1 - q_1) \neq 0)$, or $(g_1 \neq 0, 3k_1 - q_1 = 0)$ or $(g_1 = 0, 3k_1 - q_1 = 0)$. We start with the first case $g_1(3k_1 - q_1) \neq 0$.

Case 1. $g_1(3k_1 - q_1) \neq 0$. Computing the function $f_3(r)$ we obtain

$$f_3(r) = A_1r^7 + A_2r^6 + A_3r^5 + A_4r^4 + A_5r^3 - \frac{2}{3}(2b_3 - c_3 + g_3)r^2 + \pi\alpha_3r + 2\delta_3.$$

Where

$$A_1 = \frac{1}{64g_1(3k_1 - q_1)}(\pi(k_1 - 5l_1 - 2q_1)((3k_1 - q_1)(m_1 - n_1)(a_1(3k_1 - 4l_1 - 3q_1) - 4b_1m_1 + 4b_1n_1 + d_1(-3k_1 + 2l_1 + 2q_1) + 6k_1z_1 - 2q_1z_1) + g_1(k_1(6l_1q_1 + 12m_1n_1 - 6m_1^2 - 6n_1^2 + q_1^2) - 3k_1^2(3l_1 + 2q_1) + 9k_1^3 - l_1(-8m_1n_1 + 4m_1^2 + 4n_1^2 + q_1^2))),$$

$$A_2 = \frac{1}{105g_1(q_1 - 3k_1)^2}(2((297k_1^4 - 36(9l_1 + 7q_1)k_1^3 + 3(72l_1^2 + 132q_1l_1 - 32m_1^2 - 32n_1^2 + 23q_1^2 + 64m_1n_1)k_1^2 - 6(24q_1l_1^2 + 2(4m_1^2 - 8n_1m_1 + 4n_1^2 + 13q_1^2)l_1 + q_1(-8m_1^2 - 8n_1^2 + 16n_1m_1 + q_1^2))k_1 + 4l_1(6l_1(2m_1^2 - 4n_1m_1 + 2n_1^2 + q_1^2) + q_1(12m_1^2 - 24n_1m_1 + 12n_1^2 + 5q_1^2)))g_1^2 + 4(m_1 - n_1)(3k_1 - q_1)(d_1(-15k_1^2 + 33l_1k_1 + 24q_1k_1 - 6q_1^2 - 10l_1q_1) + a_1(12k_1^2 - 3(13l_1 + 8q_1)k_1 + q_1(11l_1 + 6q_1)) + 2(3k_1 - q_1)(3k_1 - 4l_1 - 3q_1)z_1)g_1 - 48b_1^2(m_1 - n_1)^2(q_1 - 3k_1)^2 + 2(q_1 - 3k_1)^2(2(3l_1 + q_1)(3k_1 - 4l_1 - 3q_1)a_1^2 + ((3k_1 - q_1)(3k_1 + 8l_1 + q_1)z_1 - d_1(9k_1 - 8l_1 - 7q_1)(3l_1 + q_1))a_1 + 2(q_1 - 3k_1)^2z_1^2 + d_1^2(3l_1 + q_1)(3k_1 - 2(l_1 + q_1)) - d_1(3k_1 + 4l_1)(3k_1 - q_1)z_1) + 2b_1(q_1 - 3k_1)^2(g_1(27k_1^2 - 3(12l_1 + 5q_1)k_1 + 2(-12m_1^2 + 24n_1m_1 - 12n_1^2 + 6l_1q_1 + q_1^2)) + 2(m_1 - n_1)(-9d_1k_1 + 12z_1k_1 + 12d_1l_1 + 8d_1q_1 + a_1(9k_1 - 24l_1 - 13q_1) - 4q_1z_1))))),$$

$$A_3 = \frac{1}{16g_1(3k_1 - q_1)}(\pi(2(3k_1 - q_1)(b_1(3k_1 - 4l_1 - 3q_1) + g_1(8k_1 - 11l_1 - 8q_1))a_1^2 + (-8(m_1 - n_1)(3k_1 - q_1)b_1^2 + (4(z_1(q_1 - 3k_1))^2 + g_1(-20k_1m_1 - 2l_1m_1 + 6q_1m_1 + 17k_1n_1 + 2l_1n_1 - 5n_1q_1)) - d_1(9k_1 - 8l_1 - 7q_1)(3k_1 - q_1))b_1 + g_1(-d_1(3k_1 - q_1)(21k_1 - 17l_1 - 15q_1) + g_1(-37k_1m_1 - 16l_1m_1 + 7q_1m_1 + 19k_1n_1 + 16l_1n_1 - n_1q_1) + a_1(3k_1 - q_1)(39k_1 - 10l_1n_1 - 17q_1)z_1)) + b_1^2(3k_1 - q_1)(3g_1k_1 + 4d_1m_1 - 4d_1n_1 - g_1q_1) + g_1((3k_1 - q_1)(5k_1 - 3(l_1g_1$$

$$\begin{aligned}
& +q_1))d_1^2 + (g_1(6l_1(m_1 - n_1) + k_1(9m_1 - 3n_1) - (m_1 + n_1)q_1) - (18k_1 - 5l_1 - 8q_1)g_1(3k_1 \\
& - q_1)z_1)d_1 - 9h_2k_1^2 - h_2q_1^2 - m_2q_1^2 + n_2q_1^2 + 45k_1^2z_1^2 + 5q_1^2z_1^2 - 30k_1q_1z_1^2 - 6k_2l_1m_1 + k_1z_1 \\
& + 6k_1l_2m_1 - 3k_1^2m_2 + 6k_1l_1m_2 + 6k_2l_1n_1 - 6k_1l_2n_1 + 3k_1^2n_2 - 6k_1l_1n_2 - 2g_1^2(k_1 + l_1)(3k_1 \\
& - q_1) + 6h_2k_1q_1 - 2k_2m_1q_1 - 2l_2m_1q_1 + 4k_1m_2q_1 - 2l_1m_2q_1 + 2k_2n_1q_1 + 2l_2n_1q_1 + q_1^2w_2 \\
& - 4k_1n_2q_1 + 2l_1n_2q_1 + 2k_1m_1q_2 + 2l_1m_1q_2 - 2k_1n_1q_2 - 2l_1n_1q_2 + 9k_1^2w_2 - 6k_1q_1w_2 + g_1 \\
& (-10l_1(m_1 - n_1) + k_1(7n_1 - 13m_1) + (m_1 + n_1)q_1)z_1) + b_1((3k_1 - q_1)(3k_1d_1^2 + (g_1(25k_1 \\
& m_1 + 4l_1m_1 - 2(l_1 + q_1)) - 7q_1m_1 - 19k_1n_1 - 4l_1n_1 + 5n_1q_1) - 2(q_1 - 3k_1)^2z_1)d_1 + g_1(3 \\
& k_1 - q_1)(g_1(3k_1 - 5l_1 - 2q_1) + 10(n_1 - m_1)z_1))),
\end{aligned}$$

$$\begin{aligned}
A_4 = & \frac{1}{15g_1}(2(a_1(4b_1d_1g_1 + 6d_1g_1^2 + 3g_1k_2 - 3g_2k_1 - 4g_1l_2 + 4g_2l_1 - 3g_1q_2 + 3g_2q_1 - 6g_1^2z_1) \\
& + b_1(4(-g_1m_2 + g_2m_1 + g_1n_2 - g_2n_1 + g_1^3) - 2d_1^2g_1) + 3a_2g_1k_1 - 4a_2g_1l_1 - 3a_2g_1q_1 \\
& - 3a_1^2g_1^2 - 4b_2g_1m_1 + 4b_2g_1n_1 + 4b_1^2g_1^2 - 3d_2g_1k_1 - 3d_1g_1k_2 + 3d_1g_2k_1 + 2d_2g_1l_1 \\
& + 2d_1g_1l_2 - 2d_1g_2l_1 + 2d_2g_1q_1 + 2d_1g_1q_2 - 2d_1g_2q_1 + 2d_1g_1^2z_1 - 2d_1^2g_1^2 - 2g_1^2h_2 + 6g_1k_2 \\
& + 6g_1k_1z_2 - 6g_2k_1z_1 - 3g_1^2m_2 + 2g_1^2n_2 - 2g_1q_2z_1 - 2g_1q_1z_2 + 2g_2q_1z_1 + 3g_1^2w_2)),
\end{aligned}$$

$$\begin{aligned}
A_5 = & \frac{\pi}{8}(2a_2b_1 + 2a_1b_2 + 3a_2g_1 + 3a_1g_2 - b_1d_2 - b_2d_1 - d_2g_1 - d_1g_2 + g_2z_1 + g_1z_2 - 3k_3 \\
& + 3l_3 - p_3 + q_3).
\end{aligned}$$

Since the rank of the Jacobian matrix of the function $\mathcal{A} = (A_1, \dots, A_5, -\frac{2}{3}(2b_3 - c_3 + g_3), \pi\alpha_3, 2\delta_3)$ with respect to its parameters which appear in their expressions is maximal, i.e. it is 8. In view of Lemma 1.1, we conclude that the maximum number of real solutions of the equation $f_3(r) = 0$ is at most seven. Now by using Descartes Theorem we conclude that the function $f_3(r) = 0$ can have at most seven positive solutions. Therefore the averaging theory up to third order can provide at most seven limit cycles for the discontinuous piecewise differential system (4.1)–(4.2).

Now we consider the second case.

Case 2. $g_1 = 0$ and $q_1 \neq 3k_1$. Computing the function $f_2(r)$ we obtain

$$\begin{aligned}
f_2(r) = & \frac{1}{16}\pi r^5(h_1(q_1 - 3k_1) + k_1(-m_1 + n_1 + 3w_1) + 2l_1m_1 - 2l_1n_1 + m_1q_1 - n_1q_1 - q_1w_1) \\
& + \frac{2}{15}r^4(a_1(3k_1 - 4l_1 - 3q_1) - 4b_1m_1 + 4b_1n_1 + d_1(-3k_1 + 2l_1 + 2q_1) + 6k_1z_1 - 2q_1z_1) \\
& + \frac{1}{8}\pi r^3(a_1c_1 - b_1d_1 - 3k_2 + 3l_2 - p_2 + q_2) - \frac{2}{3}r^2(2b_2 - c_2 + g_2) + \pi\alpha_2r + 2\delta_2.
\end{aligned}$$

So the polynomial $f_2(r)$ can have at most five positive real roots which produce at most five limit cycles for the discontinuous piecewise differential system (4.1)–(4.2) when ε is sufficiently small. In order to apply the averaging theory of third order we put $f_2(r) \equiv 0$.

So we need to consider

$$\begin{aligned} c_2 &= 2b_2 + g_2, p_2 = a_1 c_1 - b_1 d_1 - 3k_2 + 3l_2 + q_2, \alpha_2 = 0, \delta_2 = 0, \\ w_1 &= \frac{1}{4b_1(3k_1 - q_1)}((k_1 - 2l_1 - q_1)(a_1(3k_1 - 4l_1 - 3q_1) + d_1(2(l_1 + q_1) - 3k_1) + 6k_1 z_1 - 2q_1 z_1) \\ &\quad + 4b_1 h_1(3k_1 - q_1)), \\ m_1 &= \frac{1}{4b_1}(a_1(3k_1 - 4l_1 - 3q_1) + 4b_1 n_1 + d_1(2(l_1 + q_1) - 3k_1) + 6k_1 z_1 - 2q_1 z_1). \end{aligned}$$

From the expression of $f_2(r)$ we distinguish immediately two subcases $b_1 \neq 0$ or $b_1 = 0$.

Subcase 2.1. $b_1 \neq 0$. Computing $f_3(r)$ we get

$$f_3(r) = B_1 r^7 + B_2 r^6 + B_3 r^5 + B_4 r^4 + B_5 r^3 - \frac{2}{3}(2b_3 - c_3 + g_3)r^2 + \pi \alpha_3 r + 2\delta_3.$$

Where

$$\begin{aligned} B_1 &= \frac{\pi}{512b_1^2(3k_1 - q_1)}(k_1 - 5l_1 - 2q_1)(-2a_1(3k_1 - 4l_1 - 3q_1)(b_1(h_1 - n_1)(3k_1 - q_1) + l_1(d_1 \\ &\quad (3k_1 - 2(l_1 + q_1)t) + 2z_1(q_1 - 3k_1))) + a_1^2 l_1(-3k_1 + 4l_1 + 3q_1)^2 + 8b_1^2(k_1 - l_1)(q_1 - 3k_1)^2 \\ &\quad + c_1 h_1 - n_1)(3k_1 - q_1)d_1(3k_1 - 2l_1 + q_1) + 2z_1 q_1 - 3k_1) + l_1(d_1(2(l_1 + q_1) - 3k_1) \\ &\quad + 6k_1 z_1 - 2q_1 z_1)^2), \\ B_2 &= \frac{1}{105b_1(3k_1 - q_1)}(-2a_1(b_1(h_1 - n_1)(-24k_1 q_1 + 27k_1^2 + 5q_1^2) + d_1(3k_1^2(8l_1 + q_1) - 3k_1 \\ &\quad (15l_1 q_1 + 5l_1^2 + 3q_1^2) + q_1(29l_1 q_1 + 25l_1^2 + 6q_1^2)) + z_1(3k_1 - q_1)(-33k_1 l_1 - 9k_1 q_1 + 3k_1^2 \\ &\quad + 29l_1 q_1 + 16l_1^2 + 6q_1^2)) + a_1^2(k_1^2(75l_1 + 36q_1) - 3k_1(50l_1 q_1 + 28l_1^2 + 15q_1^2) - 9k_1^3 + q_1(75 \\ &\quad l_1 q_1 + 68l_1^2 + 18q_1^2)) + 4b_1^2(q_1 - 3k_1)^2(9k_1 - 2(6l_1 + q_1)) + c_1(h_1 - n_1)(3k_1 - q_1)(d_1(9k_1 \\ &\quad - 4q_1) + 8z_1(q_1 - 3k_1)) + 90d_1 k_1 l_1 q_1 z_1 + 6d_1^2 k_1 l_1 q_1 - 54d_1 k_1^2 l_1 z_1 + 48d_1 k_1 l_1^2 z_1 - 15d_1^2 \\ &\quad k_1^2 l_1 + 6d_1^2 k_1 l_1^2 + 42d_1 k_1^2 q_1 z_1 - 12d_1 k_1 q_1^2 z_1 - 24d_1^2 k_1^2 q_1 + 12d_1^2 k_1 q_1^2 - 18d_1 k_1^3 z_1 + 9d_1^2 \\ &\quad k_1^3 - 24d_1 l_1 q_1^2 z_1 - 16d_1 l_1^2 q_1 z_1 + 8d_1^2 l_1 q_1^2 + 8d_1^2 l_1^2 q_1 - 96k_1 l_1 q_1 z_1^2 + 144k_1^2 l_1 z_1^2 + 16l_1 q_1^2), \\ B_3 &= \frac{-\pi}{64b_1(3k_1 - q_1)}(a_1(b_1(2z_1(3k_1 - q_1)(5k_1 - 4l_1 - 5q_1) - d_1(-26k_1 l_1 - 22k_1 q_1 + 9k_1^2 \\ &\quad + 22l_1 q_1 + 16l_1^2 + 9q_1^2)) + 8b_1^2(h_1 + n_1)(3k_1 - q_1) - 2(3k_1 - 4l_1 - 3q_1)(-k_2(3l_1 + q_1) \\ &\quad + 3k_1 l_2 + k_1 q_2 - l_2 q_1 + l_1 q_2)) + 4a_1^2 b_1(-5k_1(l_1 + q_1) + 3k_1^2 + 5l_1 q_1 + 4l_1^2 + 2q_1^2) + b_1 \\ &\quad (2d_1 z_1(3k_1 - q_1)(2k_1 + 2l_1 + q_1) + d_1^2(-8k_1 l_1 - 3k_1 q_1 - 3k_1^2 + 6l_1 q_1 + 4l_1^2 + 2q_1^2) + 4(3k_1 \end{aligned}$$

$$\begin{aligned}
& -q_1)(3h_2k_1 - h_2q_1 + k_1m_2 - k_1n_2 - 3k_1w_2 - 2l_1m_2 + 2l_1n_2 - m_2q_1 + n_2q_1 + q_1w_2)) \\
& -4b_1^2d_1(h_1 + n_1)(3k_1 - q_1) - 4b_1^3(q_1 - 3k_1)^2 + 2(k_2(3l_1 + q_1) - k_1(3l_2 + q_2) + l_2q_1 - l_1q_2) \\
& (d_1(2(l_1 + q_1) - 3k_1) + 6k_1z_1 - 2q_1z_1)), \\
B_4 = & \frac{1}{15b_1(3k_1 - q_1)}(a_1(8b_1^2d_1(3k_1 - q_1) + (3k_1 - 4l_1 - 3q_1)(-b_2(6k_1 - 2q_1) - 3g_2(k_1 + l_1))) \\
& + c_1(3k_1 - q_1)(3k_2 - 4l_2 - 3q_2)) + c_1(3k_1 - q_1)(a_2(3k_2 - 4l_1 - 3q_1) - 3d_1k_2 + 2d_1l_2 \\
& + 2d_1q_2 - 3d_2k_1 + 2d_2l_1 + 2d_2q_1 + g_2h_1 - n_1) + 6k_1z_2 + 6k_2z_1 - 2q_1z_2 - 2q_2z_1) + (b_2(6k_1 \\
& - 2q_1) + 3g_2(k_1 + l_1))(d_1(3k_1 - 2(l_1 + q_1)) + 2z_1(q_1 - 3k_1)) - 4b_1^2(3k_1 - q_1)(d_1^2 + 2m_2 \\
& - 2n_2)), \\
B_5 = & \frac{\pi}{8}(2a_1b_2 + 3a_1g_2 + a_2c_1 - b_2d_1 - b_1d_2 - d_1g_2 + g_2z_1 - 3k_3 + 3l_3 - p_3 + q_3).
\end{aligned}$$

In a similar way as in the proof of **Case 1** and according to Descartes Theorem, we know that the function $f_3(r)$ can have at most seven positive real roots, which provide at most seven limit cycles.

Subcase 2.2: If $b_1 = 0$ the polynomial function $f_2(r)$ becomes

$$\begin{aligned}
f_2(r) = & \frac{1}{16}\pi r^5(h_1(q_1 - 3k_1) + k_1(-m_1 + n_1 + 3w_1) + 2l_1m_1 - 2l_1n_1 + m_1q_1 - n_1q_1 - q_1w_1) \\
& + \frac{2}{15}r^4(a_1(3k_1 - 4l_1 - 3q_1) + d_1(-3k_1 + 2l_1 + 2q_1) + 6k_1z_1 - 2q_1z_1) + \frac{1}{8}\pi r^3(-3k_2 \\
& + 3l_2 - p_2 + q_2) - \frac{2}{3}r^2(2b_2 - c_2 + g_2) + \pi\alpha_2r + 2\delta_2.
\end{aligned}$$

This function can have at most five positive real roots. We should have $f_2(r) \equiv 0$ to apply the averaging theory of the third order. So we need to take

$$z_1 = \frac{a_1(-3k_1 + 4l_1 + 3q_1) + d_1(3k_1 - 2(l_1 + q_1))}{6k_1 - 2q_1}, \alpha_2 = 0, \delta_2 = 0,$$

$$c_2 = 2b_2 + g_2, p_2 = -3k_2 + 3l_2 + q_2, w_1 = h_1 + \frac{2(k_1 + l_1)(m_1 - n_1)}{q_1 - 3k_1} + m_1 - n_1.$$

Computing $f_3(r)$ we get

$$f_3(r) = C_1r^7 + C_2r^6 + C_3r^5 + C_4r^4 + C_5r^3 - \frac{2}{3}(2b_3 - c_3 + g_3)r^2 + \pi\alpha_3r + 2\delta_3.$$

Where

$$C_1 = \frac{1}{64(3k_1 - q_1)}(\pi(k_1 - 5l_1 - 2q_1)(k_1(-3h_1m_1 + 3h_1n_1 + 6l_1q_1 + 3m_1n_1 - 3n_1^2 + q_1^2) + q_1$$

$$(h_1 - n_1)(m_1 - n_1) - 3k_1^2(3l_1 + 2q_1) + 9k_1^3 + l_1(-4m_1n_1 + 2m_1^2 + 2n_1^2 - q_1^2))),$$

$$C_2 = \frac{1}{105(3k_1 - q_1)}(2(a_1(h_1(3k_1 - q_1))(3k_1 - 16l_1 - 7q_1) + 6k_1(3l_1m_1 + 5l_1n_1 + 3m_1q_1$$

$$\begin{aligned}
& +n_1q_1) - 3k_1^2(2m_1 + n_1) - 10l_1m_1q_1 + 32l_1^2m_1 - 6l_1n_1q_1 - 32l_1^2n_1 - 12m_1q_1^25n_1q_1^2) \\
& +d_1(-h_1(3k_1 - q_1)(3k_1 - 4(2l_1 + q_1)) + 3k_1(10l_1m_1 - 18l_1n_1 + 4m_1q_1 - 9n_1q_1) + k_1^2 \\
& (15n_1 - 6m_1) - 4(2l_1 + q_1)(2l_1m_1 - 2l_1n_1 - n_1q_1))), \\
C_3 = & -\frac{1}{64(3k_1 - q_1)}(\pi(-2a_1d_1(3k_1l_1 + q_1(3l_1 + 2q_1)) + a_1^2(k_1 - q_1)(3k_1 - 12l_1 - 7q_1) + d_1^2k_1 \\
& (-3k_1 + 6l_1 + 4q_1) - 4(h_2(q_1 - 3k_1)^2 + 2k_2(3l_1 + q_1)(m_1 - n_1) - 6k_1l_2m_1 - 6k_1l_1m_2 \\
& + 6k_1l_2n_1 + 6k_1l_1n_2 - 4k_1m_2q_1 - 2k_1m_1q_2 + 3k_1^2m_2 + 4k_1n_2q_1 + 2k_1n_1q_2 - 3k_1^2n_2 \\
& + 6k_1q_1w_2 - 9k_1^2w_2 + 2l_2m_1q_1 + 2l_1m_2q_1 - 2l_1m_1q_2 - 2l_2n_1q_1 - 2l_1n_2q_1 + 2l_1n_1q_2 \\
& + m_2q_1^2 - n_2q_1^2 - q_1^2w_2))), \\
C_4 = & -\frac{1}{(45k_1 - 15q_1)}(2(-a_2(3k_1 - q_1)(3k_1 - 4l_1 - 3q_1) + 12a_1k_1l_2 - 12a_1k_2l_1 + 6a_1k_1q_2 \\
& - 6a_1k_2q_1 - 4a_1l_2q_1 + 4a_1l_1q_2 + 12b_2k_1m_1 - 12b_2k_1n_1 - 4b_2m_1q_1 + 4b_2n_1q_1 - 6d_2k_1l_1 \\
& - 6d_1k_1l_2 + 6d_1k_2l_1 - 9d_2k_1q_1 - 3d_1k_1q_2 + 3d_1k_2q_1 + 9d_2k_1^2 + 2d_2l_1q_1 + 2d_1l_2q_1 \\
& - 2d_1l_1q_2 + 2d_2q_1^2 + g_2(h_1(q_1 - 3k_1) + 6k_1m_1 - 3k_1n_1 + 6l_1m_1 - 6l_1n_1 - n_1q_1) \\
& + 12k_1q_1z_2 - 18k_1^2z_2 - 2q_1^2z_2)), \\
C_5 = & \frac{1}{(48k_1 - 16q_1)}(\pi(a_1(12b_2k_1 - 4b_2q_1 + 15g_2k_1 + 4g_2l_1 - 3g_2q_1) + 2b_2d_1(q_1 - 3k_1) \\
& - 3d_1g_2k_1 - 2d_1g_2l_1 + 18k_1l_3 - 6k_1p_3 + 6k_1q_3 + 6k_3q_1 - 18k_3k_1 - 6l_3q_1 + 2p_3q_1 \\
& - 2q_1q_3)).
\end{aligned}$$

The polynomial $f_3(r)$ can have at most seven positive real roots, and generate when ε is sufficiently small at most seven limit cycles for the discontinuous piecewise differential system (4.1)–(4.2).

Case 3. $g_1 \neq 0$ and $q_1 = 3k_1$. The polynomial $f_2(r)$ is written as

$$\begin{aligned}
f_2(r) = & \frac{1}{8}\pi r^5(k_1 + l_1)(m_1 - n_1) - \frac{2}{15}r^4(6a_1k_1 + 4a_1l_1 + 4b_1m_1 - 4b_1n_1 - 3d_1k_1 - 2d_1l_1 \\
& + g_1(2h_1 + 3m_1 - 2n_1 - 3w_1)) + \frac{1}{8}\pi r^3(2a_1b_1 + 3a_1g_1 - b_1d_1 - d_1g_1 + g_1z_1 - 3k_2 \\
& + 3l_2 - p_2 + q_2) - \frac{2}{3}r^2(2b_2 - c_2 + g_2) + \pi\alpha_2r + 2\delta_2.
\end{aligned}$$

This polynomial can have at most five positive real roots. In order to apply the averaging theory of third order we must have $f_2(r) \equiv 0$ and in order to eliminate the coefficient of r^5 we need to have $m_1 = n_1$ or $k_1 = -l_1$. Here also we have two subcases

Subcase 3.1. We consider

$$z_1 = \frac{-a_1(2b_1 + 3g_1) + d_1(b_1 + g_1) + 3k_2 - 3l_2 + p_2 - q_2}{g_1}, \alpha_2 = 0, \delta_2 = 0,$$

$$w_1 = \frac{(2a_1 - d_1)(3k_1 + 2l_1) + g_1(2h_1 + n_1)}{3g_1}, k_1 \neq -l_1, m_1 = n_1, c_2 = 2b_2 + g_2.$$

Computing $f_3(r)$ we get

$$f_3(r) = D_1 r^6 + D_2 r^5 + D_3 r^4 + D_4 r^3 - \frac{2}{3}(2b_3 - c_3 + g_3)r^2 + \pi\alpha_3 r + 2\delta_3.$$

Where

$$D_1 = \frac{1}{315g_1} (2(-2g_1(2a_1 - d_1)(h_1 - m_1)(15k_1 + 8l_1) - 10l_1(d_1 - 2a_1)^2(2l_1 + q_1) + g_1^2(-8h_1m_1 + 4h_1^2 + 72k_1l_1 + 45k_1^2 + 72l_1^2 + 4m_1^2))),$$

$$D_2 = -\frac{1}{48g_1} (\pi(a_1(6b_1(2d_1l_1 + g_1(m_1 - h_1)) + d_1g_1(2l_1 - 15k_1) - 7g_1^2(h_1 - m_1) + 2(9k_2l_1 - 9k_1l_2 + 5l_1p_2 - 3l_1q_2 - 15l_2l_1 + p_2q_1)) + 2a_1^2(-6b_1l_1 + 15g_1k_1 + 2g_1l_1) - 3b_1(d_1g_1(m_1 - h_1t) + d_1^2l_1 - g_1^2(5l_1 + q_1)) + 2d_1g_1^2h_1 - 2d_1^2g_1l_1 - 9d_1k_2l_1 + 9d_1k_1l_2 - 3d_1k_1p_2 - 5d_1l_1p_2 + 15d_1l_1l_2 + d_1p_1q_2 + 18g_1h_1k_2 + 5g_1h_1p_2 - 6g_1h_1q_2 - 6g_1k_1m_2 + 6g_1k_1n_2 + 6g_1^3k_1 - 3g_1l_2m_1 - 6g_1l_1m_2 + 6g_1l_1n_2 + 6g_1^3l_1 + g_1m_1p_2 - 15g_1h_1l_2 - 2d_1g_1^2m_1)),$$

$$D_3 = \frac{1}{15g_1} (2(a_1(-2b_1(3d_1g_1 + 6k_2 - 2q_2) - 6d_1g_1^2 - 33g_1k_2 + 6g_2k_1 + 14g_1l_2 - 6g_1p_2 + 9g_1q_2) + 3a_1^2g_1(4b_1 + 5g_1) - 6a_2g_1k_1 - 4a_2g_1l_1 + b_1(6d_1k_2 - 2d_1q_2 - 4g_1m_2 + 4g_1n_2 + 4g_1^3) + 4b_1^2g_1^2 - 3d_1g_2k_1 + 9d_1g_1k_2 + 2d_2g_1l_1 - 2d_1g_2l_1 - 4d_1g_1l_2 + 2d_1g_1p_2 - 2d_1g_1q_2 + d_2g_1q_1 - 2g_1^2h_2 - 3g_1^2m_2 + 2g_1^2n_2 + 3g_1^2w_2 - 18k_2l_2 + 6k_2p_2 - 12k_2q_2 + 18k_2^2 + 6l_2q_2 - 2p_2q_2 + 2q_2^2 + 4g_2l_1)),$$

$$D_4 = \frac{1}{8g_1} (\pi(2a_1b_2g_1 + a_2g_1(2b_1 + 3g_1) - 2a_1b_1g_2 - b_2d_1g_1 - b_1d_2g_1 + b_1d_1g_2 - d_2g_1^2 - 3g_1k_3 + 3g_2k_2 + 3g_1l_3 - 3g_2l_2 - g_1p_3 + g_2p_2 + g_1q_3 - g_2q_2 + g_1^2z_2)).$$

This polynomial can have at most six positive real roots, which produce at most six limit cycles.

Now we analyze the second subcase.

Subcase 3.2. We consider the following values of the parameters of the function $f_3(r)$

$$z_1 = \frac{-a_1(2b_1 + 3g_1) + d_1(b_1 + g_1) + 3k_2 - 3l_2 + p_2 - q_2}{g_1}, k_1 = -l_1, c_2 = 2b_2 + g_2,$$

$$w_1 = \frac{-2a_1l_1 - 2n_1(2b_1 + g_1) + 4b_1m_1 + d_1l_1 + 2g_1h_1 + 3g_1m_1}{3g_1}, \alpha_2 = 0, \delta_2 = 0, m_1 \neq n_1.$$

$f_3(r)$ becomes

$$f_3(r) = F_1 r^7 + F_2 r^6 + F_3 r^5 + F_4 r^4 + F_5 r^3 - \frac{2}{3}(2b_3 - c_3 + g_3)r^2 + \pi\alpha_3 r + 2\delta_2.$$

Where

$$F_1 = \frac{\pi l_1}{192g_1}((m_1 - n_1)(5(-2a_1 l_1 + 4b_1 m_1 - 4b_1 n_1 + d_1 l_1) + g_1(-5h_1 + 12m_1 - 7n_1))),$$

$$F_2 = \frac{1}{315g_1}(2(2g_1(2a_1 l_1(7h_1 - 45m_1 + 38n_1) - 8b_1(m_1 - n_1)(2h_1 + 3m_1 - 5n_1) + d_1 l_1(-7h_1 + 24m_1 - 17n_1)) + 2(-4a_1 l_1(17b_1(m_1 - n_1) + 5d_1 l_1) + 20a_1^2 l_1^2 + 34b_1 d_1 l_1(m_1 - n_1) - 8(m_1 - n_1)(5b_1^2(m_1 - n_1) - 9k_2 l_1 + 3l_1(3l_2 - p_2 + q_2)) + 5d_1^2 l_1^2) + g_1^2(-8h_1(3m_1 - 2n_1) + 4h_1^2 + 45l_1^2 + 4n_1(6m_1 - 5n_1)))),$$

$$F_3 = \frac{1}{48g_1}(\pi(a_1(-2b_1(6d_1 l_1 + g_1(-3h_1 + 2m_1 + n_1)) + 12b_1^2(m_1 - n_1) - 17d_1 g_1 l_1 + g_1^2(7h_1 - 12m_1 + 5n_1) + 2l_1(-9k_2 + 6l_2 - 2p_2 + 3q_2)) + 2a_1^2 l_1(6b_1 + 13g_1) + b_1(d_1 g_1(-3h_1 - 4m_1 + 7n_1) + 3d_1^2 l_1 - 2(3g_1^2 l_1 + (m_1 - n_1)(9k_2 - 15l_2 + 5p_2 - 3q_2))) + 6b_1^2 d_1(n_1 - m_1)15g_1 - 2d_1 g_1^2 h_1 + 2d_1^2 g_1 l_1 + 2d_1 g_1^2 n_1 + 9d_1 k_2 l_1 + 2d_1 l_1 p_2 - 3d_1 l_1 q_2 - 6d_1 l_1 l_2 - 18g_1 h_1 k_2 + 15g_1 h_1 l_2 - 5g_1 h_1 p_2 + 6g_1 h_1 q_2 - 3g_1 k_2 m_1 + 3g_1 k_2 n_1 + 15g_1 l_2 m_1 - 12g_1 l_2 n_1 - 3g_1 m_1 p_2 + 3g_1 m_1 q_2 + 2g_1 n_1 p_2 - 3g_1 n_1 q_2)),$$

$$F_4 = \frac{1}{15g_1}(2(-a_1(2b_1(3d_1 g_1 + 6k_2 - 2q_2) + 6d_1 g_1^2 + 33g_1 k_2 - 14g_1 l_2 + 2g_2 l_1 + 6g_1 p_2 - 9g_1 q_2) + 3a_1^2 g_1(4b_1 + 5g_1) + 2a_2 g_1 l_1 + b_1(6d_1 k_2 - 2d_1 q_2 - 4g_1 m_2 + 4g_2 m_1 + 4g_1 n_2 - 4g_2 n_1 + 4g_1^3) - 4b_2 g_1 m_1 + 4b_2 g_1 n_1 + 4b_1^2 g_1^2 + 9d_1 g_1 k_2 - d_2 g_1 l_1 + d_1 g_2 l_1 - 4d_1 g_1 l_2 + 2d_1 g_1 p_2 - 2d_1 g_1 q_2 - 2g_1^2 h_2 - 3g_1^2 m_2 + 2g_1^2 n_2 + 3g_1^2 w_2 - 18k_2 l_2 + 6k_2 p_2 - 12k_2 q_2 + 18k_2^2 + 6l_2 q_2 - 2p_2 q_2 + 2q_2^2),$$

$$F_5 = \frac{1}{8g_1}(\pi(2a_1 b_2 g_1 + a_2 g_1(2b_1 + 3g_1) - 2a_1 b_1 g_2 - b_2 d_1 g_1 - b_1 d_2 g_1 + b_1 d_1 g_2 - d_2 g_1^2 - 3g_1 k_3 + 3g_2 k_2 + 3g_1 l_3 - 3g_2 l_2 - g_1 p_3 + g_2 p_2 + g_1 q_3 - g_2 q_2 + g_1^2 z_2).$$

Then the polynomial $f_3(r)$ can have at most seven positive real roots.

Case 4. $g_1 = 0$ and $q_1 = 3k_1$. Computing the function $f_2(r)$ we obtain

$$f_2(r) = \frac{1}{8}\pi r^5(k_1 + l_1)(m_1 - n_1) - \frac{2}{15}r^4(6a_1 k_1 + 4a_1 l_1 + 4b_1 m_1 - 4b_1 n_1 - 3d_1 k_1 - 2d_1 l_1) + \frac{1}{8}\pi r^3(a_1 c_1 - b_1 d_1 - 3k_2 + 3l_2 - p_2 + q_2) - \frac{2}{3}r^2(2b_2 - c_2 + g_2) + \pi\alpha_2 r + 2\delta_2.$$

This polynomial can have at most five positive real roots. Now we apply the averaging

theory of third order by considering $f_2(r) \equiv 0$. We see that to remove the coefficient of r^5 we need to take $k_1 = -l_1$ or $m_1 = n_1$. Here we also have two subcases.

Subcase 4.1. We consider $k_1 = -l_1$, $c_2 = 2b_2 + g$, $q_2 = -2a_1b_1 + b_1d_1 + 3k_2 - 3l_2 + p_2$, $m_1 = \frac{l_1(2a_1 - d_1)}{4b_1} + n_1$, $\alpha_2 = 0$, $\delta_2 = 0$, $b_1 \neq 0$, $m_1 \neq n_1$, and we distinguish another two subcases $b_1 \neq 0$ or $b_1 = 0$.

4.1.1: For $b_1 \neq 0$. Computing $f_3(r)$ we get

$$f_3(r) = G_1r^7 + G_2r^6 + G_3r^5 + G_4r^4 + G_5r^3 - \frac{2}{3}(2b_3 - c_3 + g_3)r^2 + \pi\alpha_3r + 2\delta_3.$$

Where

$$\begin{aligned} G_1 &= \frac{1}{1024b_1^2}(-\pi l_1^2(2a_1 - d_1)(l_1(2a_1 - d_1) + 20b_1(h_1 - w_1))), \\ G_2 &= \frac{1}{210b_1}(l_1(2a_1 - d_1)(l_1(10a_1 - 11d_1 + 16z_1) + 12b_1(4h_1 + n_1 - 5w_1))), \\ G_3 &= -\frac{1}{64b_1}\pi(2a_1(b_1(6l_1z_1 - 5d_1l_1) + 4b_1^2(h_1 + n_1) + l_1(-2k_2 + l_2 - p_2)) + 8a_1^2b_1l_1 + b_1 \\ &\quad (-6d_1l_1z_1 + d_1^2p_1 + 4(h_1 - w_1)(3l_2 - p_2)) - 4b_1^2d_1(h_1 + n_1) + d_1l_1(2k_2 - l_2 + p_2)), \\ G_4 &= \frac{1}{30b_1}(-2a_1(b_1^2(6d_1 - 8z_1) + l_1(4b_2 + 3g_2)) + c_1(6k_2 - 5l_2 + 3p_2)) - 4b_1(-2a_2l_1 - 3d_1k_2 \\ &\quad + d_2l_1 + 4d_1l_2 - 2d_1p_2 + g_2(2h_1 + n_1 - 3w_1) - 6l_2z_1 + 2p_2z_1) + 24a_1^2b_1^2 + d_1l_1(4b_2 + 3g_2) \\ &\quad - 8b_1^2(d_1z_1 + 2m_2 - 2n_2)), \\ G_5 &= \frac{1}{8}\pi(2a_1b_2 + 3a_1g_2 + a_2c_1 - b_2d_1 - b_1d_2 - d_1g_2 + g_2z_1 - 3k_3 + 3l_3 - p_3 + q_3)). \end{aligned}$$

This polynomial can have at most seven positive real roots, consequently at most seven limit cycles for the discontinuous piecewise differential system (4.1)–(4.2).

4.1.2. If $b_1 = 0$ the polynomial $f_2(r)$ is written as

$$\begin{aligned} f_2(r) &= \frac{1}{8}\pi r^5(k_1 + l_1)(m_1 - n_1) - \frac{2}{15}r^4(2a_1 - d_1)(3k_1 + 2l_1) + \frac{1}{8}\pi r^3(-3k_2 + 3l_2 - p_2 + q_2) \\ &\quad - \frac{2}{3}r^2(2b_2 - c_2 + g_2) + \pi\alpha_2r + 2\delta_2. \end{aligned}$$

In this case the function $f_2(r)$ can have at most five positive real roots. We set $f_2(r) \equiv 0$, and to delete the coefficients of r^4 we need another two subcases $3k_1 + 2l_1 = 0$ or $d_1 = 2a_1$. We start with the first subcase $3k_1 + 2l_1 = 0$.

4.1.2.1. $c_2 = 2b_2 + g_2$, $p_2 = -3k_2 + 3l_2 + q_2$, $\alpha_2 = 0$, $\delta_2 = 0$, $l_1 = 0$, $k_1 = 0$ and $d_1 \neq 2a_1$.

Computing the function $f_3(r)$ we obtain

$$f_3(r) = \frac{1}{16}\pi r^5(h_1(q_2 - 3k_2) + k_2(-m_1 + n_1 + 3w_1) + 2l_2m_1 - 2l_2n_1 + m_1q_2 - n_1q_2 - q_2w_1) \\ + \frac{2}{15}r^4(a_1(3k_2 - 4l_2 - 3q_2) - 4b_2m_1 + 4b_2n_1 - 3d_1k_2 + 2d_1l_2 + 2d_1q_2 + g_2(-2h_1 - 3m_1 \\ + 2n_1 + 3w_1) + 6k_2z_1 - 2q_2z_1) + \frac{1}{8}\pi r^3(2a_1b_2 + 3a_1g_2 - b_2d_1 - d_1g_2 + g_2z_1 - 3k_3 + 3l_3 \\ - p_3 + q_3) - r^2\left(\frac{4}{3}b_3 - \frac{2}{3}c_3 + \frac{2}{3}g_3\right) + \pi\alpha_3r + 2\delta_3.$$

Then the polynomial $f_3(r)$ can have at most five positive real roots.

Now we compute $f_3(r)$ for the second case $d_1 = 2a_1$.

4.1.2.2. $c_2 = 2b_2 + g_2$, $\alpha_2 = 0$, $c_2 = 2b_2 + g_2$, $\delta_2 = 0$, $d_1 = 2a_1$, $k_1 = -l_1$ and $3k_1 + 2l_1 \neq 0$.

Computing the function $f_3(r)$ we obtain

$$f_3(r) = -\frac{1}{64}\pi l_1 r^7(m_1 - n_1)(5h_1 + m_1 - n_1 - 5w_1) - \frac{8}{105}l_1 r^6(3a_1 - 4z_1)(m_1 - n_1) + \frac{1}{16}\pi r^5 \\ (h_1(q_2 - 3k_2) + k_2(-m_1 + n_1 + 3w_1) + 2l_2m_1 - 2l_2n_1 + m_1q_2 - n_1q_2 - q_2w_1) - \frac{2}{15}r^4 \\ (3a_1k_2 - 2a_2l_1 - a_1q_2 + 4b_2m_1 - 4b_2n_1 + d_2l_1 + g_2(2h_1 + 3m_1 - 2n_1 - 3w_1) - 6k_2z_1 \\ + 2q_2z_1) + \frac{1}{8}\pi r^3(a_1g_2 + g_2z_1 - 3k_3 + 3l_3 - p_3 + q_3) - \frac{2}{3}r^2(2b_3 - c_3 + g_3) + \pi\alpha_3r + 2\delta_3.$$

This polynomial function can have at most seven positive real roots. Now taking the second subcase $m_1 = n_1$.

Subcase 4.2. $m_1 = n_1$, $c_2 = 2b_2 + g_2$, $p_2 = 2a_1b_1 - b_1d_1 - 3k_2 + 3l_2 + q_2$, $\alpha_2 = 0$, $\delta_2 = 0$ and $k_1 = -\frac{2l_1}{3}$. Computing $f_3(r)$ we get

$$f_3(r) = \frac{4}{105}l_1 r^6(2a_1 - d_1)(4h_1 + n_1 - 5w_1) - \frac{1}{48}\pi r^5(a_1(6(b_1(n_1 + w_1) + l_1z_1) - 3d_1l_1) \\ + 2a_1^2l_1 - 3b_1d_1n_1 - 3b_1d_1w_1 - 3d_1l_1z_1 + d_1^2l_1 + h_1(9k_2 - 3q_2) - 9k_2w_1 - 2l_1m_2 \\ + 2l_1n_2 + 3q_2w_1) - \frac{2}{15}r^4(a_1(-4b_1d_1 - 3k_2 + 4l_2 + 3q_2) + 2b_1(d_1^2 + 2m_2 - 2n_2) \\ + 3d_1k_2 - 2d_1l_2 - 2d_1q_2 + 2g_2h_1 + g_2n_1 - 3g_2w_1 - 6k_2z_1 + 2q_2z_1) + \frac{1}{8}\pi r^3(2a_2b_1 \\ + 2a_1b_2 + 3a_1g_2 - b_1d_2 - b_2d_1 - d_1g_2 + g_2z_1 - 3k_3 + 3l_3 - p_3 + q_3) - \frac{2}{3}r^2(2b_3 - c_3 \\ + g_3) + \pi\alpha_3r + 2\delta_3.$$

This polynomial can have at most six positive real roots. In general, in all the cases mentioned above, the polynomials $f_i(r)$, with $i = 1, 2, 3$ can have at most 3 or 5 or 6 or 7 real positive roots. Thus the maximum number of limit cycles that can be obtained via the averaging theory up to third order is at most seven.

Now we are going to reach our result by giving an example with exactly seven limit cycles

Example with exactly seven limit cycles

In the half plane $y \geq 0$, we consider the linear differential system (4.5) with the values $\{\alpha_1, \beta_1, \gamma_1, \delta_1, \alpha_2, \beta_2, \gamma_2, \delta_2, \alpha_3, \beta_3, \gamma_3, \delta_3\} \rightarrow \{0, 1, 2, 0, 0, 1, 1, 0, 13068/\pi, -1, -1, -2520\}$.

Now in the half plane $y \leq 0$, we consider the cubic weak focus or center (4.6) with

$\{a_1, b_1, d_1, m_1, g_1, k_1, l_1, c_1, n_1, p_1, q_1, h_1, w_1, z_1, a_2, m_2, b_2, c_2, k_2, d_2, g_2, h_2, l_2, w_2, n_2, p_2, q_2, z_2, a_3, b_3, q_3, c_3, d_3, g_3, k_3, m_3, z_3, n_3, h_3, p_3, l_3, w_3\} \rightarrow \{0, H_1/K_1, H_1/K_1+1, 0, 1, -2\sqrt{25-9+\frac{64}{\pi}}, 2, 0, 1, 1, (-5\pi-\sqrt{\pi(64+25\pi)})/(2\pi), (7\pi-\sqrt{\pi(25\pi+64)})/(2\pi), -2\sqrt{25+\frac{64}{\pi}}-9, 2, 0, 1, 1, 1, -1, -1, -1302.26, 0, \frac{1}{2}, -\frac{1}{2}, 3907.78, -1, 163.431, -1, 1, -20, 0, -1, 19738, -1, 1, 1, -1, -1, -54152/\pi, H_2/K_2, -2, 1\}$, with $H_1 = -23\sqrt{\pi(64+25\pi)} - 880\pi - 128$, $K_1 = 8(5\pi + 4 + \sqrt{\pi(64+25\pi)})$, $H_2 = 9(\sqrt{\pi(64+25\pi)} - 80\pi)$ and $K_2 = 8(\sqrt{\pi(64+25\pi)} + 5\pi + 4)$.

An exhausting computation shows that $f_1(r) \equiv f_2(r) \equiv 0$ and

$$f_3(r) = (r-1)(r-2)(r-3)(r-4)(r-5)(r-6)(r-7).$$

Then for these systems we have exactly seven limit cycles bifurcating from the periodic orbits of the discontinuous piecewise differential system (4.1)-(4.2).

Moreover, in polar coordinates (r, θ) the periodic orbits that bifurcate are $r = 1, 2, 3, 4, 5, 6, 7$.

This completes the proof of the Theorem 4.2.

Global Phase Portraits of Piecewise Quadratic Differential Systems with a Pseudo-Focus

This chapter is devoted to investigate the global dynamics of planar piecewise smooth differential systems consisting of two different vector fields separated by one straight line passing through the origin. From a quasi-canonical family of piecewise quadratic differential system with a pseudo-focus point at the origin, which has six parameters, we investigate the subfamilies where the origin is indeed a pseudo-center. For such subfamilies, we classify their global phase portraits in the Poincaré disk and the associated bifurcation sets.

We start by considering non-trivial piecewise quadratic system with a pseudo-focus at the origin written in the quasi-canonical form. Following [24].

$$\begin{cases} \dot{x} = t_-x - y + \delta_-y^2, \\ \dot{y} = -1 + d_-x, \end{cases} \text{ if } x \leq 0, \quad \begin{cases} \dot{x} = t_+x - y + \delta_+y^2, \\ \dot{y} = 1 + d_+x, \end{cases} \text{ if } x \geq 0. \quad (5.1)$$

System (5.1) can be abridged to the more compact expression

$$\begin{cases} \dot{x} = t_{\pm}x - y + \delta_{\pm}y^2, \\ \dot{y} = \pm 1 + d_{\pm}x, \end{cases} \text{ for } \pm x \geq 0, \quad (5.2)$$

and we remark that, for the ambiguities appearing when regarding orbits starting at or

arriving at the discontinuity manifold

$$\Sigma = \{(x, y) : x = 0\},$$

we should resort to the Filippov convention, see [27].

Note that this family has six parameters $(t_{\pm}, d_{\pm}, \delta_{\pm})$ but only one quadratic term in the vector field, while the first component is already in the canonical normal form proposed in [24], the second component has an extra term $(d_{\pm}x)$ with respect to such a normal form.

The following lemma, whose proof is direct, will be useful to reduce the taxonomy of different cases.

LEMMA 5.1 *Regarding system (5.1), the following statements hold.*

(a) *If we consider the change of variables and time $(X, Y, \theta) = (x, -y, -\tau)$, then we get the equivalent system*

$$\begin{cases} \dot{X} = -t_{\pm}X - Y - \delta_{\pm}Y^2, \\ \dot{Y} = \pm 1 + d_{\pm}X, \end{cases} \text{ for } \pm X \geq 0, \quad (5.3)$$

that is, the behavior for the parameter set $(t_{-}, d_{-}, \delta_{-}, t_{+}, d_{+}, \delta_{+})$ is equivalent to the exhibited by that with parameters $(-t_{-}, d_{-}, -\delta_{-}, -t_{+}, d_{+}, -\delta_{+})$, since the only effect is to get the symmetrical phase portrait with respect to the horizontal axis, keeping the anti-clockwise sense of rotation for orbits around the origin.

(b) *If we consider the change of variables and time $(X, Y, \theta) = (-x, y, -\tau)$, then we get the equivalent system*

$$\begin{cases} \dot{X} = -t_{\mp}X - Y + \delta_{\mp}Y^2, \\ \dot{Y} = \pm 1 + d_{\mp}X, \end{cases} \text{ for } \pm X \geq 0, \quad (5.4)$$

that is, the behavior for the parameter set $(t_{-}, d_{-}, \delta_{-}, t_{+}, d_{+}, \delta_{+})$ is equivalent to the exhibited by that with parameters $(-t_{+}, d_{+}, \delta_{+}, -t_{-}, d_{-}, \delta_{-})$, since the only effect is to get the symmetrical phase portrait with respect to the vertical axis, keeping the anti-clockwise sense of rotation for orbits around the origin.

(c) If we consider the change of variables $(X, Y) = (-x, -y)$, then we get the equivalent system

$$\begin{cases} \dot{X} = t_{\mp}X - Y - \delta_{\mp}Y^2, \\ \dot{Y} = \pm 1 + d_{\mp}X, \end{cases} \text{ for } \pm X \geq 0, \quad (5.5)$$

that is, the behavior for the parameter set $(t_-, d_-, \delta_-, t_+, d_+, \delta_+)$ is equivalent to the exhibited by that with parameters $(t_+, d_+, -\delta_+, t_-, d_-, -\delta_-)$, since the only effect is to get the symmetrical phase portrait with respect to the origin, keeping the anti-clockwise sense of rotation for orbits around the origin.

Section 5.1 Subfamilies with a pseudo-center at the origin

Starting from system (5.1), and computing the half-return maps around the origin, see [24], it is possible to determine the subfamilies for which the origin is indeed a *pseudo-center*, that is, the origin is surrounded by a periodic annulus filled by periodic orbits.

According to statement (b.ii) of Proposition 11 of Esteban *et al.* [24], a first specific case for system (5.1) exhibiting a pseudo-center at the origin is the one-parameter family of linear-quadratic system

$$\begin{cases} \dot{x} = \delta x - y, \\ \dot{y} = -1, \end{cases} \text{ if } x \leq 0, \quad \begin{cases} \dot{x} = -2\delta x - y + \delta y^2, \\ \dot{y} = 1, \end{cases} \text{ if } x \geq 0, \quad (5.6)$$

that is, we have $t_- = \delta_+ = \delta$, $d_- = d_+ = \delta_- = 0$, and $t_+ = -2\delta$ in (5.1).

A second family from system (5.1) possessing a pseudo-center is given by the discontinuous bi-parametric differential system

$$\begin{cases} \dot{x} = -y + \delta y^2, \\ \dot{y} = -1 + dx, \end{cases} \text{ if } x \leq 0, \quad \begin{cases} \dot{x} = \delta x - y, \\ \dot{y} = 1 - 2\delta^2 x, \end{cases} \text{ if } x \geq 0, \quad (5.7)$$

so that we have $t_- = \delta_+ = 0$, $t_+ = \delta_- = \delta$, $d_- = d$, and $d_+ = -2\delta^2$. This is the dual case of Proposition 11(b.i) in Esteban *et al.* [24].

As a third family of system (5.1) with a pseudo-center, taking $t_- = t_+ = 0$ and $\delta_- =$

$\delta_+ = \delta$ in (5.1), we consider the piecewise quadratic Hamiltonian family of system

$$\begin{cases} \dot{x} = -y + \delta y^2, \\ \dot{y} = -1 + d_- x, \end{cases} \text{ if } x \leq 0, \quad \begin{cases} \dot{x} = -y + \delta y^2, \\ \dot{y} = 1 + d_+ x, \end{cases} \text{ if } x \geq 0, \quad (5.8)$$

with three parameters, namely d_- , d_+ , and δ .

As our last piecewise quadratic set of system with a pseudo-center, we consider the Σ -reversible quadratic family

$$\begin{cases} \dot{x} = \pm t x - y + \delta y^2, \\ \dot{y} = \pm 1 + d x, \end{cases} \text{ for } \pm x \geq 0, \quad (5.9)$$

which comes from (5.1) by putting $t_+ = -t_- = t$, $d_+ = d_- = d$, and $\delta_+ = \delta_- = \delta$. These system has a phase portrait which is symmetric with respect to the y -axis, as a consequence of their invariance under the transformation $(x, y, \tau) \rightarrow (-x, y, -\tau)$. Furthermore, there cannot appear any sliding set. Using the change in Lemma 5.1(a) if necessary, we can assume $\delta > 0$, to make again the change of variables and time $(X, Y, \theta) = (\delta^2 x, \delta y, \delta \tau)$, so that system (5.9) is transformed into

$$\begin{cases} \dot{X} = \pm \tilde{t} X - Y + Y^2, \\ \dot{Y} = \pm 1 + \tilde{d} X, \end{cases} \text{ for } \pm X \geq 0, \quad (5.10)$$

where $\tilde{t} = t/\delta$ and $\tilde{d} = d/\delta^2$ are the only two parameters involved.

5.1.1 Finite and infinite singular points

To study the global phase portraits of the piecewise differential system with a pseudo-centers previously mentioned, we have to compute the finite and infinite singular points.

Finite singular points. We identify the finite singular (or simply **SP**) points of the piecewise differential system (5.6), (5.7), (5.8) and (5.10) in the following Proposition.

PROPOSITION 5.1 *The following statements hold.*

(i) *System (5.6) has no finite SP.*

(ii) The right subsystem of system (5.7) has a real saddle $(x, y) = \left(\frac{1}{2\delta^2}, \frac{1}{2\delta}\right)$ for $\delta \neq 0$, and no real singularity for $\delta = 0$. The left subsystem of system (5.7) has two **SP**, $(x, y) = \left(\frac{1}{d}, 0\right)$ which is a real saddle for $d < 0$ and a virtual center for $d > 0$, the second singularity at $(x, y) = \left(\frac{1}{d}, \frac{1}{\delta}\right)$ which is a virtual saddle for $d > 0$ and a real center for $d < 0$, and if $\delta = 0$ the system has $(x, y) = \left(\frac{1}{d}, 0\right)$ as a **SP** with the same local behavior mentioned previously.

(iii) For system (5.8) we only studied the right subsystem because we have the same results in the left one. The right subsystem of system (5.8) has two **SP**, $(x, y) = \left(-\frac{1}{d_+}, 0\right)$ which is a real saddle for $d_+ < 0$ and a virtual center for $d_+ > 0$, and $(x, y) = \left(-\frac{1}{d_+}, \frac{1}{\delta}\right)$ which is a virtual saddle for $d_+ > 0$ and a real center for $d_+ < 0$, and if $\delta = 0$ the unique **SP** is $(x, y) = \left(-\frac{1}{d_+}, 0\right)$.

(iv) Because of the reversibility we studied only the right subsystem. If $\Delta = \frac{4\tilde{t}}{\tilde{d}} + 1 > 0$ and $d < 0$ the right subsystem of (5.10) has two real **SP**, $p_L = (X_L, Y_L) = \left(-\frac{1}{\tilde{d}}, \frac{1 - \sqrt{\Delta}}{2}\right)$ which is a real saddle, and the second singularity at $p_U = (X_U, Y_U) = \left(-\frac{1}{\tilde{d}}, \frac{1 + \sqrt{\Delta}}{2}\right)$ which is a real node if $\tilde{t}^2 + 4\tilde{d}\sqrt{\Delta} > 0$ and a real focus if $\tilde{t}^2 + 4\tilde{d}\sqrt{\Delta} < 0$, where the subscripts L and U stand for lower and upper, respectively. If $\Delta > 0$ and $d > 0$ the right subsystem of (5.10) has two virtual **SP**, $p_L = (X_L, Y_L) = \left(-\frac{1}{\tilde{d}}, \frac{1 - \sqrt{\Delta}}{2}\right)$ which is a node if $\tilde{t}^2 - 4\tilde{d}\sqrt{\Delta} > 0$ and a focus if $\tilde{t}^2 - 4\tilde{d}\sqrt{\Delta} < 0$, and a saddle at $p_U = (X_U, Y_U) = \left(-\frac{1}{\tilde{d}}, \frac{1 + \sqrt{\Delta}}{2}\right)$ if $\tilde{t}^2 + 4\tilde{d}\sqrt{\Delta} > 0$.

If $\Delta = 0$ then the unique **SP** of the right subsystem is $(x, y) = \left(-\frac{1}{\tilde{d}}, \frac{1}{2}\right)$, which is a real (virtual) saddle-node for $d < 0$ ($d > 0$).

If $\Delta < 0$ system (5.10) has no singularity.

Proof.

Proof of statement (i) of Proposition 5.1. It is clear that system (5.6) has no finite singularity.

Proof of statement (ii) of Proposition 5.1. For $x \geq 0$ system (5.7) has one singularity at $\left(\frac{1}{2\delta^2}, \frac{1}{2\delta}\right)$ with eigenvalues $-\delta$ and 2δ , then it's is a real saddle if $\delta \neq 0$. For $x \leq 0$ system (5.7) has two singularities, $\left(\frac{1}{d}, 0\right)$ which is a real saddle if $d < 0$ with eigenvalues $\pm\sqrt{-d}$ and

a virtual centre with eigenvalues $\pm i\sqrt{d}$ if $d > 0$, the second point is $(\frac{1}{d}, \frac{1}{\delta})$ which is a virtual saddle with eigenvalues $\pm\sqrt{-d}$ if $d < 0$ and a real centre with eigenvalues $\pm i\sqrt{d}$ if $d > 0$.

Proof of statement (iii) of Proposition 5.1. For $x \geq 0$ system (5.8) has two singularities, $(-\frac{1}{d_+}, 0)$ which is a real saddle with eigenvalues $\pm\sqrt{-d_+}$ if $d_+ < 0$ and a virtual centre with eigenvalues $\pm i\sqrt{d_+}$ if $d_+ > 0$, the second singularity is $(-\frac{1}{d_+}, \frac{1}{\delta})$ which is a virtual saddle with eigenvalues $\pm\sqrt{-d_+}$ if $d_+ < 0$ and a real center with eigenvalues $\pm i\sqrt{d_+}$ if $d_+ > 0$.

Proof of statement (iv) of Proposition 5.1. Since the Jacobian matrix of the right subsystem is

$$J(X, Y) = \begin{pmatrix} \tilde{t} & 2Y - 1 \\ \tilde{d} & 0 \end{pmatrix},$$

we get

$$J(X_L, Y_L) = \begin{pmatrix} \tilde{t} & -\sqrt{\Delta} \\ \tilde{d} & 0 \end{pmatrix} \quad \text{and} \quad J(X_U, Y_U) = \begin{pmatrix} \tilde{t} & \sqrt{\Delta} \\ \tilde{d} & 0 \end{pmatrix},$$

and then we can easily conclude that if $d < 0$ the equilibrium p_L is always a real saddle with eigenvalues $\frac{1}{2}(\tilde{t} \pm \sqrt{\tilde{t}^2 - 4\tilde{d}\sqrt{\Delta}})$ and if $d > 0$ p_L is a virtual node or focus. The second singularity at p_U with eigenvalues $\frac{1}{2}(\tilde{t} \pm \sqrt{\tilde{t}^2 + 4\tilde{d}\sqrt{\Delta}})$ which is a real node if $\tilde{t}^2 + 4\tilde{d}\sqrt{\Delta} > 0$ and $d < 0$, a real focus if $\tilde{t}^2 + 4\tilde{d}\sqrt{\Delta} < 0$ and $d < 0$ and a virtual saddle if $\tilde{t}^2 + 4\tilde{d}\sqrt{\Delta} > 0$ and $d > 0$. If $\Delta = 0$ it has one singularity $(-\frac{1}{d}, \frac{1}{2})$ with eigenvalues $-\frac{d}{4}$ and 0. In order to obtain the local phase portrait at this point we use Theorem 2.19 of [27], and we conclude that it's a saddle-node.

Infinite singular points. By using the preliminaries given in chapter 1 we study the infinite singular points and their nature in the Poincaré disc. Note that in this work we must take into account that the vector field (P, Q) has different expressions depending on the sign of x_1 . In particular, when computing the flows in the charts U_2 and V_2 , we must compute two different vector fields on each side of the straight line $u = 0$. Thus, even when for these charts the origin is not a singular point for each subsystem, the combined action of the two vector fields along the equator $v = 0$ can transform it in a pseudo-equilibrium point; otherwise, we must speak of the origin as a crossing point. We begin by analyzing the simpler cases when $\delta = 0$ in the different families under study.

PROPOSITION 5.2 *Under the hypothesis $\delta = 0$, the following statements hold for the relevant local charts of the corresponding Poincaré compactification.*

- (i) *In system (5.6), both for the chart U_1 and the chart V_1 , the only singular point is the origin, which becomes a semi-hyperbolic point with one hyperbolic sector and one elliptic sector. In the charts U_2 and V_2 the origin is a standard crossing point.*
- (ii) *In system (5.7), for the chart U_1 the only singular point is the origin, which becomes a semi-hyperbolic saddle-node. Regarding the equator $v = 0$ of the chart V_1 there are no singular points for $d > 0$, one semi-hyperbolic saddle-node at the origin when $d = 0$, and for $d = -\kappa^2 < 0$ there appear two hyperbolic singular points, namely a stable node at $(-\kappa, 0)$ and an unstable node at $(\kappa, 0)$. In the charts U_2 and V_2 the origin is a standard crossing point.*
- (iii) *In system (5.8), the singular points with $v = 0$ for both charts U_1 and V_1 behave exactly as for V_1 in statement (ii), by substituting $d = d_+$ or $d = d_-$, respectively. Again, in the charts U_2 and V_2 the origin is a standard crossing point.*
- (iv) *Keeping $\delta = 0$, consider system (5.9) with the additional hypothesis $t \neq 0$. In the equator $v = 0$ of the charts U_1 and V_1 , if $t^2 - 4d > 0$ then there are two singular points, just one when $t^2 - 4d = 0$ and none when $t^2 - 4d < 0$. The origin of the charts U_2 and V_2 is not a singularity.*

Proof.

Proof of statement (i) of Proposition 5.2. According to (1.6) with $n = 1$, the flow in the chart U_1 is ruled by the differential equations

$$\dot{u} = v + u^2, \quad \dot{v} = uv. \quad (5.11)$$

Accordingly, the origin is a nilpotent singular point and we are in the situation of statement (iii2) of Theorem 3.5 of [23], that is, the origin has one hyperbolic and one elliptic sector. Note that for all $v > 0$ we have $\dot{u} > 0$ so that the elliptic sector appears for $v < 0$ and it will not be visible in the Poincaré disk. The same is true for V_1 since then the only change in the equations is that now $\dot{u} = -v + u^2$, so that the elliptic sector now appears for $v < 0$. From (1.7), the flow

in the chart U_2 is given by the differential equations

$$\dot{u} = -1 \pm uv, \quad \dot{v} = \mp v^2, \quad (5.12)$$

for $\pm u \geq 0$, and so the two flows concatenate in a natural way at the origin, which is not a singular point. The same is true for the chart V_2 .

Proof of statement (ii) of Proposition 5.2. The flow in the chart U_1 is exactly the same than in statement (i). The flow in the chart V_1 now depends on the value of d because it given as

$$\dot{u} = d - v + u^2, \quad \dot{v} = uv. \quad (5.13)$$

Clearly, for $d > 0$ there are no singular points in the equator $v = 0$, we reproduce the situation of statement (i) for $d = 0$, and for $d = -\kappa^2 < 0$ we get, apart from the singular point $(0, d)$ of saddle type, the two singular points $(\pm\kappa, 0)$. A simple analysis shows that $(\kappa, 0)$ is an unstable node and $(-\kappa, 0)$ is a stable node.

Regarding the chart U_2 , we must combine the vector field given in (5.12) for $u \geq 0$ with the given by

$$\dot{u} = -1 - du^2 + uv, \quad \dot{v} = -v(du - v), \quad (5.14)$$

for $u \leq 0$. We see that at the origin $\dot{u} = -1$ from both sides, it is a standard crossing point. The same is true for V_2 .

Proof of statement (iii) of Proposition 5.2. Here, we obtain for U_1 the flow

$$\dot{u} = d_+ + v + u^2, \quad \dot{v} = uv, \quad (5.15)$$

and similarly, for V_1 , we have

$$\dot{u} = d_- - v + u^2, \quad \dot{v} = uv, \quad (5.16)$$

and the conclusions for these two charts follow by reasoning as in statement (ii) for the chart V_1 . Regarding the chart U_2 , we must combine the two flows given by

$$\dot{u} = -1 - d_{\pm}u^2 \mp uv, \quad \dot{v} = -v(d_{\pm}u \pm v), \quad (5.17)$$

for $\pm u \geq 0$, where we see that the origin is not a singular point. Obviously, the same is true for V_2 .

Proof of statement (iv) of Proposition 5.2. we obtain for U_1 the flow

$$\dot{u} = d - tu + v + u^2, \quad \dot{v} = v(u - t), \quad (5.18)$$

and similarly, for V_1 , we have

$$\dot{u} = d + tu - v + u^2, \quad \dot{v} = v(u + t), \quad (5.19)$$

and in both cases the number and topological type of possible equilibria at the equator $v = 0$ are associated with the real roots of the quadratic equation $u^2 \pm tu + d = 0$. Thus, if $t^2 - 4d > 0$, we are in saddle or node cases and two singular points appear. For $t^2 - 4d = 0$ there appears only one singular point (improper node case) and none in the focus case ($t^2 - 4d < 0$).

Regarding the chart U_2 , we must combine the two flows

$$\dot{u} = -1 \pm tu - du^2 \mp uv, \quad \dot{v} = -v(du \pm v), \quad (5.20)$$

and we see that the origin is not a singular point, becoming a crossing point. The same is true for the chart V_2 . ■

Next, by using the same techniques, we consider the more involved cases with $\delta > 0$.

PROPOSITION 5.3 *Under the hypothesis $\delta > 0$, the following statements hold for the relevant local charts of the corresponding Poincaré compactification.*

- (i) *For system (5.6), its chart U_1 has a degenerate **SP** at the origin with vanishing linear part, where its local phase portrait consists of one hyperbolic, one elliptic and two parabolic sectors. Regarding its chart V_1 system (5.6) has two **SP**, the origin of coordinates $q_1 = (0, 0)$, which is a hyperbolic stable improper node, and $q_2 = (\delta, 0)$, which is a semi-hyperbolic saddle-node. On the other hand, the origin of the chart U_2 is not a singularity for any vector field in the half-planes, but taking into account the sliding vector field in Σ^{rs} , and that the flows go in opposite directions at such a point when $v = 0$, it behaves like an unstable pseudo-node. However, the origin of the chart V_2 behaves like a regular point.*
- (ii) *For system (5.7), in the chart U_1 there are two **SP** with $v = 0$, namely the point $q_3 = (-\delta, 0)$, which is an hyperbolic stable node and the point $q_4 = (2\delta, 0)$, which is*

a hyperbolic unstable node. In the chart V_1 , there is one nilpotent node at the origin of coordinates. The origin of the chart U_2 is now a stable pseudo-node while for the chart V_2 the origin is not a singularity.

(iii) For system (5.8), in the chart U_1 there is one nilpotent node at the origin of coordinates, as it also happens in chart V_1 . The origin, both for the chart U_2 and V_2 is not a singularity.

(iv) For system (5.10), in the charts U_1 and V_1 there is one nilpotent node at the origin of coordinates, but such a point in the charts U_2 and V_2 is not a singularity.

Proof.

Proof of statement (i) of Proposition 5.3. According to (1.6) with $n = 2$, system (5.6) has a Poincaré compactification whose local chart U_1 becomes

$$\begin{aligned}\dot{u} &= -\delta u^3 + u^2 v + 2\delta u v + v^2, \\ \dot{v} &= v(-\delta u^2 + u v + 2\delta v).\end{aligned}\tag{5.21}$$

This system has a degenerate **SP** at the origin with a vanishing linear part. In order to know the nature of this singularity, we do a blow-up of the form $v = u^2 w$ to describe its local phase portrait. After eliminating the common factor u^2 of \dot{u} and \dot{w} , via the rescaling of the independent variable such that $ds = u^2 d\tau$, we obtain the system

$$\begin{aligned}\dot{u} &= -\delta u + u^2 w + 2\delta u w + u^2 w^2, \\ \dot{w} &= -2u w^3 - u w^2 - 2\delta w^2 + \delta w.\end{aligned}\tag{5.22}$$

For $u = 0$ this system has two singularities, a hyperbolic saddle at the origin with eigenvalues $-\delta$ and δ and a semi-hyperbolic saddle-node at $(0, 1/2)$. Going back through the changes of variables and time, and by taking into account the direction of the flow of the system on the axes of coordinates, we obtain that the local phase portrait at the origin of system (5.21) is formed by one hyperbolic, one elliptic and two parabolic sectors.

In the chart V_1 system (5.6) is given by

$$\dot{u} = u^2 - \delta u - v, \quad \dot{v} = v(u - \delta).\tag{5.23}$$

This system has two **SP**, namely a hyperbolic stable node at $q_1 = (0, 0)$, with a double eigenvalues $-\delta$, and a semi-hyperbolic singularity $q_2 = (\delta, 0)$, with eigenvalues δ and 0 . By using

Theorem 2.19 of [23], we know that q_2 is a saddle-node.

We study now the chart U_2 , and note that for that we must combine two vector fields, one for each side of the line $x = 0$. Regarding (1.7) with $n = 2$, and using the definition for $x \geq 0$, system (5.6) has a Poincaré compactification whose local chart U_2 becomes

$$\dot{u} = \delta - v - 2\delta uv - uv^2, \quad \dot{v} = -v^3, \quad (5.24)$$

so that $\dot{u}|_{v=0} = \delta > 0$. However, if we use instead the definition for $x \leq 0$ and $n = 1$, we get for the local chart V_2 the system

$$\dot{u} = \delta u - 1 + uv, \quad \dot{v} = v^2, \quad (5.25)$$

so that $\dot{u}|_{v=0} = \delta u - 1$, which is negative for small u , getting so a pseudo-equilibrium point at the origin in V_2 . Its typification as an unstable pseudo-node comes from the study of directions on $v = 0$ and by considering the sliding vector field on Σ^{rs} .

Note that in the chart V_2 the two vector fields to be combined near the origin are the one in (5.25), which requires $n = 1$, and the opposite to the given in (5.24) because here $n = 2$. Therefore, now the directions of the flow along the equator $v = 0$ near the origin coincide, so such a point becomes a standard crossing point.

Proof of statement (ii) of Proposition 5.3. System (5.7) in the chart U_1 becomes

$$\dot{u} = -2\delta^2 - \delta u + v + u^2, \quad \dot{v} = v(u - \delta). \quad (5.26)$$

This system has an hyperbolic stable node at $q_3 = (-\delta, 0)$ with eigenvalues -3δ and -2δ and an hyperbolic unstable node at $q_4 = (2\delta, 0)$ with eigenvalues δ and 3δ . For the chart V_1 , we get

$$\dot{u} = dv - v^2 + u^2v - \delta u^3, \quad \dot{v} = uv(v - u\delta). \quad (5.27)$$

The origin is the unique singularity of the differential system (5.27) when $v = 0$, and it has a nilpotent linear part. By transforming this system into its normal form and by applying Theorem 3.5 of [23], we know this singular point is a node.

Regarding the chart U_2 for system (5.7), we proceed as in the proof of statement (i) by computing (1.7). For the definition when $x \geq 0$ with $n = 1$, we get

$$\dot{u} = -1 + u(\delta - v) + 2\delta^2 u^2, \quad \dot{v} = -v(v - 2\delta^2 u), \quad (5.28)$$

to be considered for $u \geq 0$, while for $x \leq 0$ with $n = 2$ we get

$$\dot{u} = \delta - v(du^2 + 1) + uv^2, \quad \dot{v} = v^2(v - du), \quad (5.29)$$

to be considered for $u \leq 0$. In a similar way to what happens for statement (i), we see that the origin in the chart U_2 behaves like a pseudo-node. Effectively, even it is not a singular point for any of the vector fields (5.28) and (5.29), we have that the flow on $v = 0$ satisfies $\dot{u} = 2\delta^2u^2 + \delta u - 1$, which is negative for small $u > 0$, while $\dot{u} = \delta > 0$ for $u < 0$. Now, by taking into account the sliding vector field given in (1.2), we conclude that the origin behaves like a stable pseudo-node. Again, however, the origin in the chart V_2 is a standard crossing point.

Proof of statement (iii) of Proposition 5.3. Here, we can take advantage of the study made for statement (ii) regarding there the chart V_1 , just by making in (5.27) the substitution $d = d_+$ and changing one sign. Thus, the expression of system (5.8) in the chart U_1 is

$$\dot{u} = d_+v + v^2 + u^2v - \delta u^3, \quad \dot{v} = uv(v - \delta u). \quad (5.30)$$

Accordingly, the only singularity with $v = 0$ is the origin, which is a nilpotent node, after applying Theorem 3.5 of [23]. The same is true for the chart V_1 by making in (5.27) the substitution $d = d_-$.

To analyze the origin in the chart U_2 , we must combine the two vector fields

$$\dot{u} = \delta - v(d_{\pm}u^2 + 1) \mp uv^2, \quad \dot{v} = -v^2(d_{\pm}u \pm v), \quad (5.31)$$

for $\pm u \geq 0$. It is clear that the origin of the chart U_2 is not an equilibrium and that the two flows concatenate in a natural way. The case of V_2 is similar.

Proof of statement (iv) of Proposition 5.3. In the chart U_1 , we have

$$\dot{u} = \tilde{d}v + v^2 - \tilde{t}uv + u^2v - u^3, \quad \dot{v} = -v(\tilde{t}v + u^2 - uv). \quad (5.32)$$

while for the chart V_1 we obtain

$$\dot{u} = \tilde{d}v - v^2 + \tilde{t}uv + u^2v - u^3, \quad \dot{v} = -v(-\tilde{t}v + u^2 - uv). \quad (5.33)$$

As in statement (iii), these system has in the equator $v = 0$ a unique **SP**, which is a nilpotent node at the origin.

In the local chart U_2 , we must combine the two flows

$$\dot{u} = v(-\tilde{d}u^2 \pm \tilde{t}u \mp 1) \mp uv^2 + 1, \quad \dot{v} = -v^2(\tilde{d}u \pm v), \quad (5.34)$$

for $\pm u \geq 0$. Clearly, the origin is not a **SP** and the two flows concatenate; therefore, it is a crossing point. The same occurs in V_2 . ■

Section 5.2 Main results

The objective of this chapter is to classify all the global phase portraits of the linear-quadratic and quadratic-quadratic piecewise differential system with a pseudo-center point at the origin.

5.2.1 Linear-quadratic differential system

We provide the global phase portraits in the Poincaré disc of the piecewise linear-quadratic differential system (5.6). Here, the case $\delta = 0$ could be excluded from our discussion, since then we should have the trivial piecewise linear case $\dot{x} = -y$, $\dot{y} = \pm 1$ for $\pm x > 0$, leading to a global pseudo-center, invariant under every transformation of Lemma 5.1, see Figure 5.1(a). When $\delta \neq 0$, using Lemma 5.1(b), we can assume $\delta > 0$ without loss of generality and discard the Σ -symmetric configuration. Furthermore, we can obtain a canonical representant for all the system in the family with $\delta > 0$ by making the change of variables and time $(X, Y, \theta) = (\delta^2 x, \delta y, \delta \tau)$. Effectively, system (5.6) becomes

$$\begin{cases} \dot{X} = X - Y, \\ \dot{Y} = -1, \end{cases} \text{ if } X \leq 0, \quad \begin{cases} \dot{X} = -2X - Y + Y^2, \\ \dot{Y} = 1, \end{cases} \text{ if } X \geq 0, \quad (5.35)$$

where the dot now denotes derivatives with respect to the new time θ . The above system is linear-quadratic and apart from the origin, it has another tangency point at $(x, y) = (0, 1)$ for the right subsystem. Note that there are no real nor virtual equilibrium points, but there appears a pseudo-saddle point at $(x, y) = (0, 2)$, see Figure 5.1(b). For this simple case, we can state the following result.

THEOREM 5.1 System (5.6) has, modulo the symmetries described in Lemma 5.1, only 2 topologically distinct global phase portraits, as depicted in Figure 5.1 for $\delta \geq 0$.

Thus, for $\delta = 0$ the full plane is filled by crossing periodic orbits, so that the origin becomes a global pseudo-center, see the phase portrait of Figure 5.1(a). When $\delta > 0$ there appears a pseudo-center whose periodic annulus is also unbounded, but confined into the region

$$\{(x, y) : \delta y < 1 + \delta^2 x, x \leq 0\} \cup \{(x, y) : \delta y < 1 - \delta\sqrt{2x}, x > 0\},$$

see Figure 5.1(b). In this last case, apart from a visible tangency point at $(0, 1/\delta)$ for the right subsystem, we also have a pseudo-saddle point at $(0, 2/\delta)$, which belongs to the repulsive sliding set $\Sigma^{rs} = \{(x, y) : x = 0, y > 1/\delta\}$.

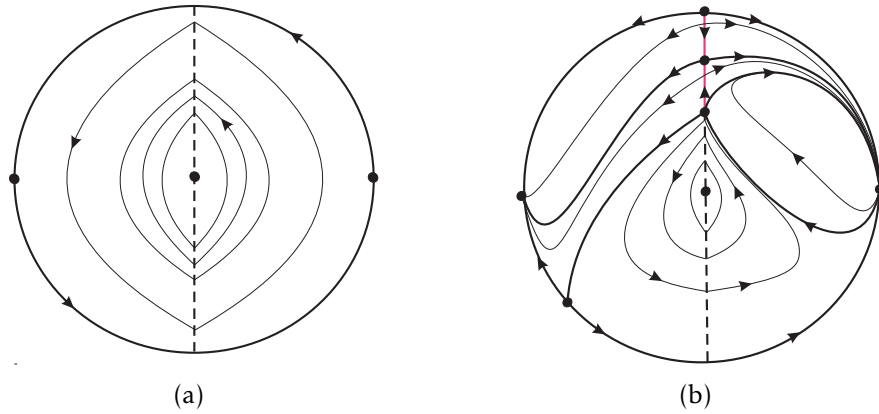


Figure 5.1: The global phase portraits of system (5.6) when (a) $\delta = 0$ and (b) $\delta > 0$.

Proof.

Proof of Theorem 5.1. If $\delta = 0$ then system (5.6) becomes the trivial, piecewise Hamiltonian, and Σ -reversible system $\dot{x} = -y$, $\dot{y} = \pm 1$, for $\pm x \geq 0$. Excepting the origin, where we have a double invisible tangency point, all the points in Σ are crossing points. By integrating the vector field, we see that the orbits in the half-plane $x \geq 0$ are the parabolas in the family $2x = \kappa^2 - y^2$ for $\kappa \geq 0$, each one of them joining the points $(0, -\kappa)$ and $(0, \kappa)$ in Σ . These parabolas, along with the corresponding parabolas $2x = y^2 - \kappa^2$ in the half-plane $x \leq 0$, determine the crossing periodic orbits that fill the whole plane. Taking into account statement (i) of Propositions 5.1 and 5.2, we obtain the global phase portrait of Figure 5.1(a).

When $\delta > 0$, apart from the double invisible tangency point at the origin, system (5.6) has for $x \geq 0$ a visible tangency at $(0, 1/\delta)$, which is the lower endpoint of an unbounded repulsive

sliding set Σ^{rs} . Thus, by using (1.2), for $x = 0$ and $y > 1/\delta$, the sliding vector field is

$$\begin{cases} \dot{x} = 0, \\ \dot{y} = g(y) = \frac{2y - \delta y^2}{\delta y^2}. \end{cases} \quad (5.36)$$

Then $(x, y) = (0, 2/\delta)$ is a pseudo equilibrium for the sliding vector field with $g'(2/\delta) < 0$, that is with stable dynamics in the sliding set, and since $X_1^+(0, 2/\delta) = 2 X_1^-(0, 2/\delta) = -2/\delta < 0$, it turns out to be a pseudo-saddle. Integrating the left vector field, we obtain that the orbits for $x \leq 0$ satisfy the expression

$$\delta^2 x + \kappa e^{-\delta y} - \delta y + 1 = 0,$$

for some constant κ . From the above orbits, there are two distinguished ones, namely the invariant straight line $\delta^2 x - \delta y + 1 = 0$ arriving at $(0, 1/\delta)$ and the curve

$$\delta^2 x + e^{2-\delta y} - \delta y + 1 = 0,$$

which arrives at the pseudo-saddle point $(0, 2/\delta)$ from the left and can be thought as a part of its unstable manifold. If we integrate the vector field for $x \geq 0$, then we get that the orbits satisfy the expression

$$2\delta^2 x + \kappa e^{-2\delta y} - (\delta y - 1)^2 = 0,$$

for some constant κ . Then the distinguished orbits are given by

$$2\delta^2 x + e^{2(2-\delta y)} - (\delta y - 1)^2 = 0,$$

which can be thought as another part of the unstable manifold of the pseudo-saddle $(0, 2/\delta)$, and the one with $\kappa = 0$, which is the parabola $2x = (y - 1/\delta)^2$, which is tangent to Σ at the point $(0, 1/\delta)$. The lower half of this parabola is given by $\delta y = 1 - \delta\sqrt{2x}$ for $x \geq 0$, and joining it with the straight line $\delta y = \delta^2 x + 1$ for $x \leq 0$, we obtain the upper boundary of the periodic annulus corresponding to the pseudo-center at the origin. By resorting now to statement (i) of Propositions 5.1 and 5.3, the global phase portrait of system (5.6) for $\delta > 0$ is as drawn in Figure 5.1(b). ■

5.2.2 Bi-parametric differential system

We provide the global phase portraits in the Poincaré disc of the piecewise linear- quadratic differential system (5.7). If $\delta = 0$, then we have the piecewise linear Hamiltonian system

$$\dot{x} = -y, \quad \dot{y} = \begin{cases} -1 + dx, & \text{if } x \leq 0, \\ 1 & \text{if } x \geq 0, \end{cases}$$

so that for $d = 0$ we are again in the trivial case of Figure 5.1(a). When $d \neq 0$, we note that while for $d > 0$ there appears a virtual center at $(x, y) = (1/d, 0)$ that does not introduce any qualitative change in the global phase portrait, for $d < 0$ such equilibrium becomes a real saddle whose invariant manifolds bound the periodic annulus of the pseudo-center at the origin, see Figures 5.2(a) and 5.2(b), respectively.

When $\delta \neq 0$ in system (5.7), the situation is much more involved, since there appears a visible tangency point for the left subsystem at $(x, y) = (0, 1/\delta)$ and a real saddle for the right subsystem at $(x, y) = (1/(2\delta^2), 1/(2\delta))$. From Lemma 5.1, we can assume without loss of generality that $\delta > 0$, and then the change of variables and time $(X, Y, \theta) = (\delta^2 x, \delta y, \delta \tau)$ provides us the one-parameter canonical representative family

$$\begin{cases} \dot{X} = -Y + Y^2, \\ \dot{Y} = -1 + \tilde{d}X, \end{cases} \text{ if } X \leq 0, \quad \begin{cases} \dot{X} = X - Y, \\ \dot{Y} = 1 - 2X, \end{cases} \text{ if } X \geq 0, \quad (5.37)$$

where $\delta^2 \tilde{d} = d$, and the dot now denotes derivatives with respect to the new time θ . The right subsystem has now the real saddle at $(x, y) = (1/2, 1/2)$, with eigenvalues -1 and 2 . For this more interesting case, we have the following result.

THEOREM 5.2 *System (5.7) has, modulo the symmetries described in Lemma 5.1, the six topologically distinct global phase portraits shown in Figure 5.2, according to the bifurcation set of Figure 5.3. More precisely, we have the following cases for $\delta \geq 0$.*

- (i) *If $\delta = 0$ and $d \geq 0$ then the origin is a global pseudo-center with no more equilibrium points. The system has the global phase portrait of Figure 5.2(a).*
- (ii) *If $\delta = 0$ and $d < 0$ then there is a real saddle at $(x, y) = (1/d, 0)$ whose invariant manifolds bound the periodic annulus associated with the pseudo-center at the origin,*

and the system has the global phase portrait of Figure 5.2(b).

(iii) If $\delta > 0$ then the right subsystem has a real saddle at $(x, y) = (1/(2\delta^2), 1/(2\delta))$. For $d < 0$ the left subsystem has a real saddle at $(x, y) = (1/d, 0)$ and a real center at $(x, y) = (1/d, 1/\delta)$ so that when $-3\delta^2 < d < 0$ the periodic annulus of the pseudo-center at the origin is bounded by the invariant manifolds of the right saddle, see Figure 5.2(c), while when $d \leq -3\delta^2 < 0$ the periodic annulus is bounded by the ones of the left saddle, see Figures 5.2(d) and 5.2(e).

(iv) If $\delta > 0$ and $d \geq 0$ then the right saddle is the only real equilibrium point and the global phase portrait of the system appears in Figure 5.2(f).

Whenever $\delta > 0$, the left subsystem has a visible tangency point at $(x, y) = (0, 1/\delta)$, and there exists an attractive sliding set $\Sigma^{as} = \{(x, y) : x = 0, y > 1/\delta\}$, with a pseudo-saddle at $(x, y) = (0, 2/\delta)$.

We organized the above cases for $\delta > 0$ in a bifurcation set in the plane (d, δ) as shown in Figure 5.3

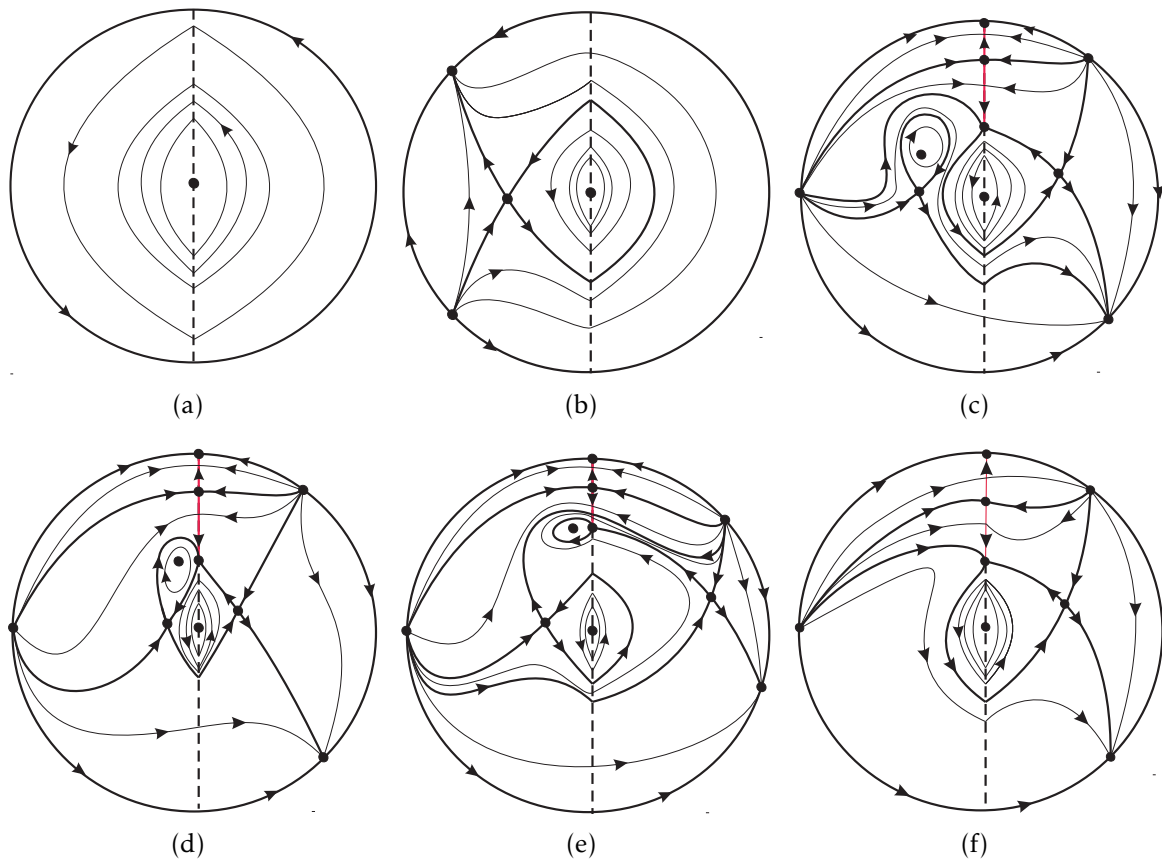


Figure 5.2: The global phase portraits of system (5.7). The cases (a) and (b) correspond with $\delta = 0$, while the remaining pictures are for $\delta > 0$.

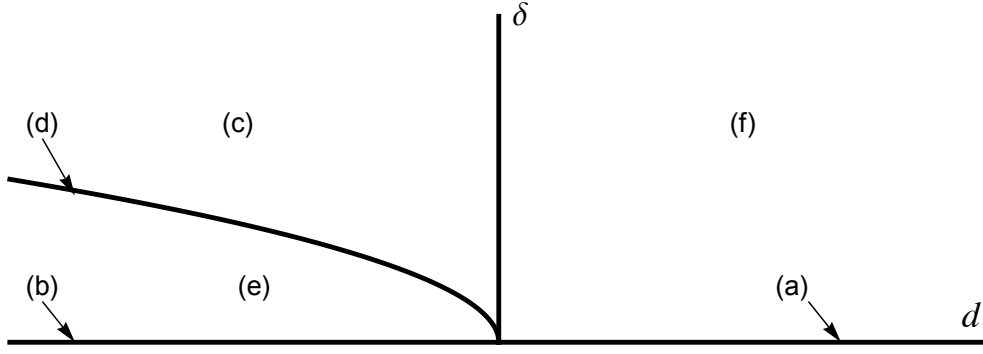


Figure 5.3: The bifurcation set in the plane (d, δ) for system (5.7) when $\delta \geq 0$. The labels in lines or open regions indicate the different global phase portraits, according to Figure 5.2. Note the bifurcation curve given by $d = -3\delta^2$, whose points correspond to the global phase portrait of Figure 5.2(d), separating the ones of Figures 5.2(c) and 5.2(e).

Proof.

Proof of Theorem 5.2.

If $\delta = 0$ then system (5.7) equals to system (5.6) under the same hypothesis but with an extra term dx in the second component of the left vector field. Thus, when $d = 0$ statement (i) is a direct consequence of Theorem 5.1. If $\delta = 0$ and $d > 0$, then the left vector field has a virtual center at $(1/d, 0)$ and each orbit in the half-plane $x \leq 0$ is an arc of the ellipse

$$dx^2 - 2x + y^2 = \kappa^2,$$

for some constant $\kappa \geq 0$, joining the points $(0, \kappa)$ and $(0, -\kappa)$. The global phase portrait is completely similar to the previous case, except that here the semi-hyperbolic point at the origin in the chart V_1 does not appear, see statement (ii) of Propositions 5.1 and 5.2. If $\delta = 0$ and $d = -\kappa^2 < 0$, then the left vector field has a real saddle at $(1/d, 0)$ with eigenvalues $\pm\kappa$, and each orbit in the half-plane $x \leq 0$ is an arc of the hyperbola

$$y^2 - \kappa^2 x^2 - 2x = C,$$

for some constant C ; in the particular case $C = 1/\kappa^2$ we get the two straight lines $\kappa^2 x \pm \kappa y + 1 = 0$ that determine the invariant manifolds of the saddle, which intersect Σ at two symmetric points. The global phase portrait is as depicted in Figure 5.2(b) and statement (ii) is shown.

For $\delta > 0$ the analysis is more involved. Apart from the double invisible tangency point at the origin, system (5.7) has for $x \leq 0$ a visible tangency at $(0, 1/\delta)$, which is the lower endpoint of an unbounded attractive sliding set Σ^{as} . Thus, by using (1.2), for $x = 0$ and $y > 1/\delta$, the

sliding vector field is

$$\begin{cases} \dot{x} = 0, \\ \dot{y} = g(y) = \frac{\delta y^2 - 2y}{\delta y^2}. \end{cases} \quad (5.38)$$

The point $(x, y) = (0, 2/\delta)$ is a pseudo equilibrium of $g(y)$ with $g'(2/\delta) > 0$, that is with unstable dynamics in the sliding set, and since $X_1^+(0, 2/\delta) = -2/\delta < 0$ $X_1^-(0, 2/\delta) = 2/\delta > 0$, it turns out to be a pseudo-saddle.

Since $\delta > 0$, the right subsystem has a real saddle at $(1/(2\delta^2), 1/(2\delta))$. Their invariant manifolds are the two straight lines $\delta^2 x + \delta y - 1 = 0$ and $4\delta^2 x - 2\delta y - 1 = 0$, which intersect Σ at the point $(0, 1/\delta)$ (the lower endpoint of the sliding set) and $(0, -1/(2\delta))$, respectively. Regarding the left subsystem, possible equilibria for $d \neq 0$ are $(1/d, 0)$ and $(1/d, 1/\delta)$, to be both real only if $d < 0$; in such a case, the first one is a saddle, while the second is a center. In fact, we see that a first integral for this subsystem is the function

$$H(x, y) = 6x - 3dx^2 - 3y^2 + 2\delta y^3. \quad (5.39)$$

The level curve of this function containing the saddle $(x, y) = (1/d, 0)$ is given by the condition $H(x, y) = 3/d$. The above equality can be written in the form

$$3d\left(x - \frac{1}{d}\right)^2 + (3 - 2\delta y)y^2 = 0,$$

which allows to justify the existence of a loop in such a level curve, symmetric with respect to the vertical line $x = 1/d$, located in the band between the horizontal straight lines $y = 0$ and $y = 3/2\delta$. Always supposing $\delta < 0$, this loop can be entirely located in the half-plane $x < 0$ or, on the contrary, have two points in Σ . The intermediate situation between the above two possibilities appears when the loop is tangent to Σ , necessarily at the visible tangency point $(0, 1/\delta)$. Since $H(0, 1/\delta) = -1/\delta^2$, the loop contained in $H(x, y) = 3/d$ becomes tangent when $3/d = -1/\delta^2$, that is, $d = -3\delta^2$. Thus, we should consider three different cases for $d < 0$, namely $-3\delta^2 < d < 0$, $d = -3\delta^2$, and $d < -3\delta^2 < 0$, see Figure 5.3. Note that the level curve $H(x, y) = -1/\delta^2$ which becomes tangent to Σ at $(0, 1/\delta)$ can be written as

$$6\delta^2 x - 3\delta^2 dx^2 + (2\delta y + 1)(\delta y - 1)^2 = 0,$$

and so this level curve also includes the point $(0, -1/(2\delta))$, and that such a point and $(0, 1/\delta)$ are precisely the intersection points with Σ for the invariant manifolds of the right saddle.

Taking into account the above facts, and using statement (ii) of Proposition 5.3, we conclude that for $d < 0$ the global phase portraits are topologically equivalent to the shown in Figure 5.2(c) when $-3\delta^2 < d < 0$; to the one in Figure 5.2(d) when $d = -3\delta^2$ and to the given in Figure 5.2(e) when $d < -3\delta^2 < 0$. Statement (iii) follows.

For $\delta > 0$ and $d \geq 0$ the situation is much simpler, since the only real equilibrium point is $(1/2\delta^2, 1/2\delta)$. System (5.7) has three infinite SP, as described in statement (ii) of Proposition 5.3. Thus, the global phase portrait of the system is topologically equivalent to the one shown in Figure 5.2 (f). Statement (iv) is shown and the proof is complete. ■

5.2.3 Quadratic Hamiltonian differential system

We classify all the global phase portraits in the Poincaré disc of the piecewise quadratic-quadratic differential system (5.8).

In the particular case $\delta = 0$, we get a piecewise linear dynamical system that can have, depending on the sign of d_- and d_+ , two real saddles (one in each half-plane, see Figures 5.4(a) and 5.4(b)), only one (see Figure 5.4(c)), or none (as in Figure 5.2(a)).

For $\delta \neq 0$ in system (5.8), we can assume as before from Lemma 5.1 that $\delta > 0$, and reduce the number of parameters by making the change of variables and time $(X, Y, \theta) = (\delta^2 x, \delta y, \delta \tau)$. Effectively, we get

$$\begin{cases} \dot{X} = -Y + Y^2, \\ \dot{Y} = -1 + \tilde{d}_- X, \end{cases} \text{ if } X \leq 0, \quad \begin{cases} \dot{X} = -Y + Y^2, \\ \dot{Y} = 1 + \tilde{d}_+ X, \end{cases} \text{ if } X \geq 0, \quad (5.40)$$

where $\delta^2 \tilde{d}_\pm = d_\pm$ and the dot now denotes derivatives with respect to the new time θ .

We summarize the analysis of system (5.8) in the following result.

THEOREM 5.3 *System (5.8) has, modulo the symmetries described in Lemma 5.1, sixteen topologically distinct global phase portraits, namely the global pseudo-center of Figure 5.2(a) or one of the fifteen phase portraits shown in Figure 5.4. More precisely, we have the following cases for $\delta \geq 0$.*

- (i) *If $\delta = 0$ and $d_-, d_+ \geq 0$ then we are in the trivial case of global pseudo-center of Figure 5.2(a) without any other equilibria.*

- (ii) If $\delta = 0$ and $d_-, d_+ < 0$ then, apart from the pseudo-center at the origin, we have two real saddles whose invariant manifolds bound the periodic annulus of the origin. For the Σ -reversible case $d_- = d_+ < 0$ see Figure 5.4(a), and for instance when $d_+ < d_- < 0$ they are the invariant manifolds of the right subsystem who bound the periodic annulus, see Figure 5.4(b). If $\delta = 0$ and for instance $d_- < 0$ but $d_+ \geq 0$ then we have only one real saddle along with the bounded pseudo-center, see Figure 5.4(c).
- (iii) If $\delta > 0$ and both $d_-, d_+ < 0$ then, apart from the pseudo-center at the origin, we have two real saddles and two real centers, which organize the phase portrait. For instance, when $-3\delta^2 < d_- < 0$ and $-3\delta^2 < d_+ < 0$ we have the situation of Figure 5.4(d) if $d_- = d_+$, and Figure 5.4(e) if $d_- \neq d_+$; when $-3\delta^2 = d_- = d_+ < 0$ we have the Σ -reversible situation shown in Figure 5.4(f); when $d_- = -3\delta^2$ and $-3\delta^2 < d_+ < 0$, see Figure 5.4(g); when $d_- < -3\delta^2$ but $d_+ = -3\delta^2$, see Figure 5.4(h); when $d_- < -3\delta^2$ and $d_+ < -3\delta^2$, see Figure 5.4(i) if $d_- = d_+$, and Figure 5.4(j) if $d_- \neq d_+$; when $d_- < -3\delta^2$ but $-3\delta^2 < d_+ < 0$, see Figure 5.4(k).
- (iv) If $\delta > 0$ but not both parameters d_-, d_+ are strictly negative, new cases arise. For instance, when $d_- < -3\delta^2$ and $d_+ \geq 0$, see Figure 5.4(l); when $d_- = d_+ = 0$, see Figure 5.4(m); when $-3\delta^2 < d_- < 0$ and $d_+ \geq 0$, see Figure 5.4(n); and finally, when $d_- = -3\delta^2$ and $d_+ \geq 0$, see Figure 5.4(o).

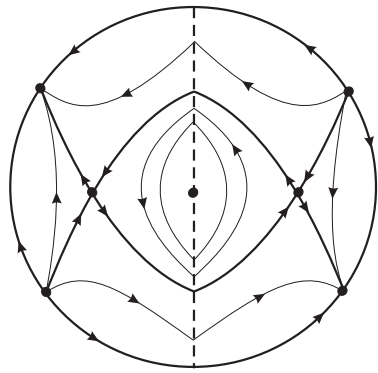
Whenever $\delta > 0$, although there is no proper sliding set, there appears an isolated pseudo-saddle at $(x, y) = (0, 1/\delta)$, which becomes a visible-visible double tangency point.

All the above cases for $\delta > 0$ can be organized in a bifurcation set, see Figure 5.5.

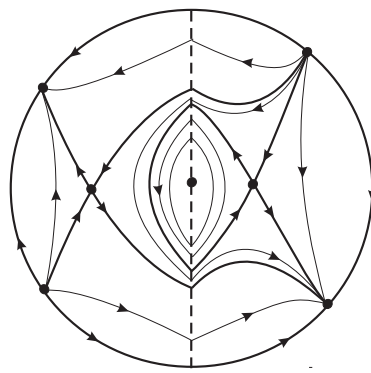
Proof.

Proof of Theorem 5.3. Here the study made for the left system in Theorem 5.2 is completely valid just by substituting there $d = d_-$. Furthermore, the right subsystem is in an analogous situation now with $d = d_+$, so that one can obtain all the orbits by such study just by using the transformation $(x, y, \tau) \rightarrow (-x, y, -\tau)$, and making all the possible combinations playing with the different qualitative ranges for d_- and d_+ . Clearly, whenever $d_- = d_+$, we will have a Σ -reversible global phase portrait. Since the visible tangency point $(0, 1/\delta)$ does not depend on d_{\pm} , it becomes a double visible tangency point leading to a pseudo-saddle in all cases. Again, there not appear any proper sliding set.

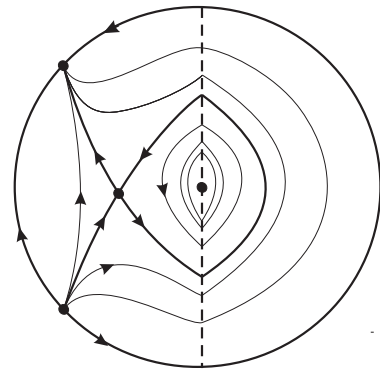
For $\delta = 0$ and $d_-, d_+ \geq 0$ then system (5.8) becomes equal to system (5.7) with $d = d_-$ in the second component of the left vector field and under the transformation $(x, y, \tau) \rightarrow (-x, y, -\tau)$



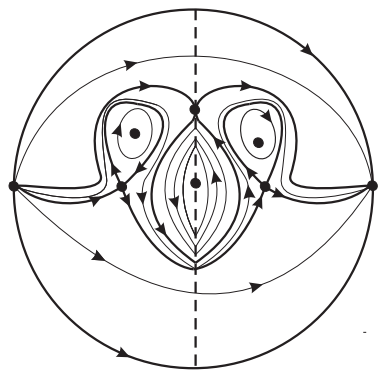
(a)



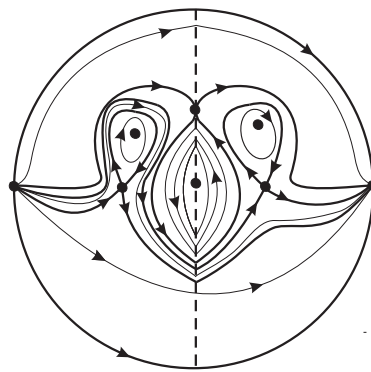
(b)



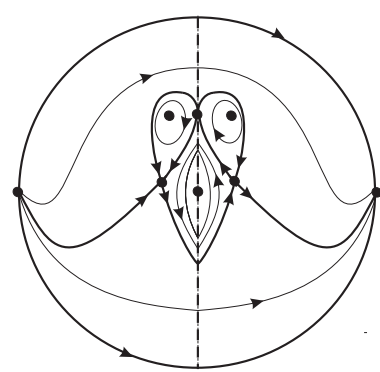
(c)



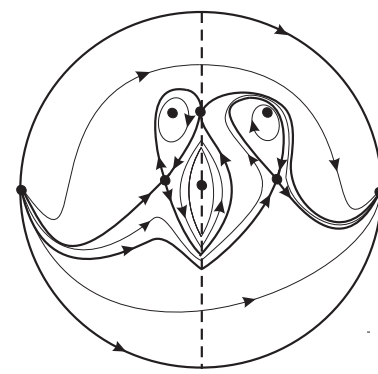
(d)



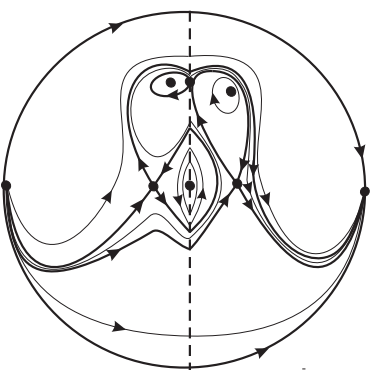
(e)



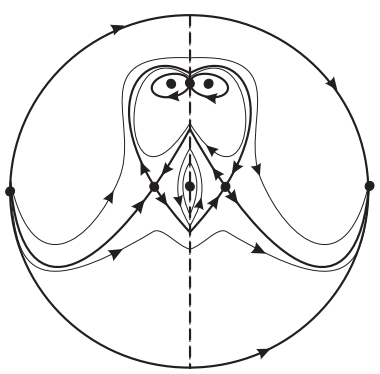
(f)



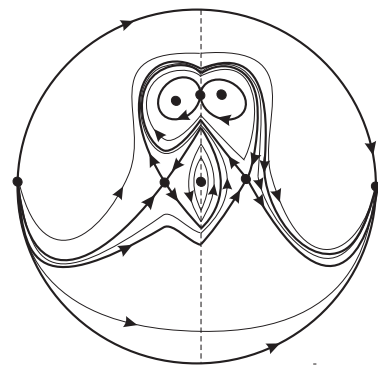
(g)



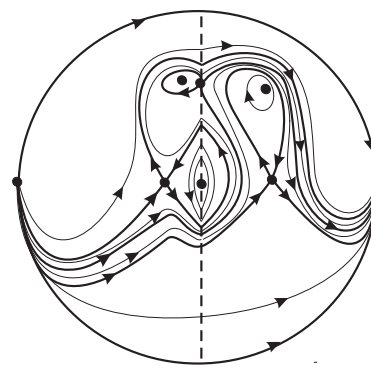
(h)



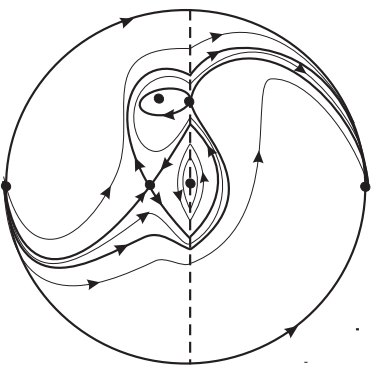
(i)



(j)



(k)



(l)

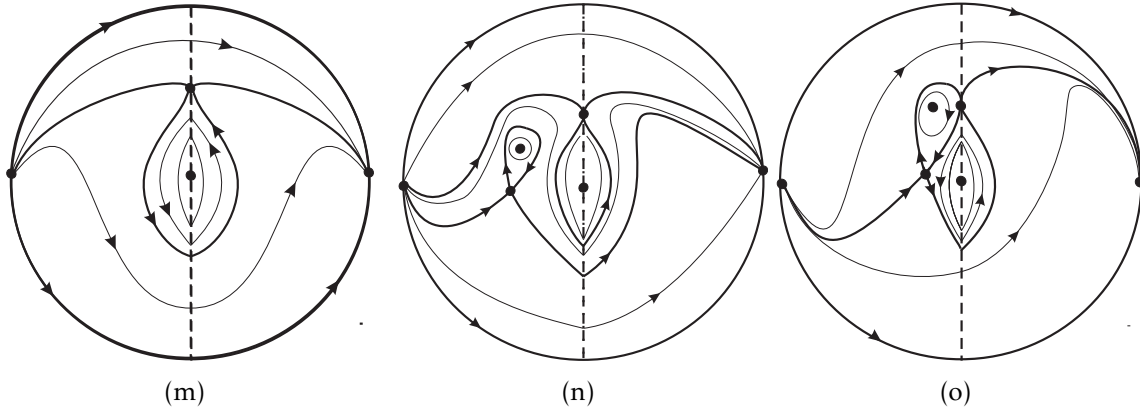


Figure 5.4: The different global phase portraits of system (5.8). The cases (a)-(c) correspond with $\delta = 0$, while the remaining pictures are for $\delta > 0$ and correspond to the different regions of Figure 5.5.

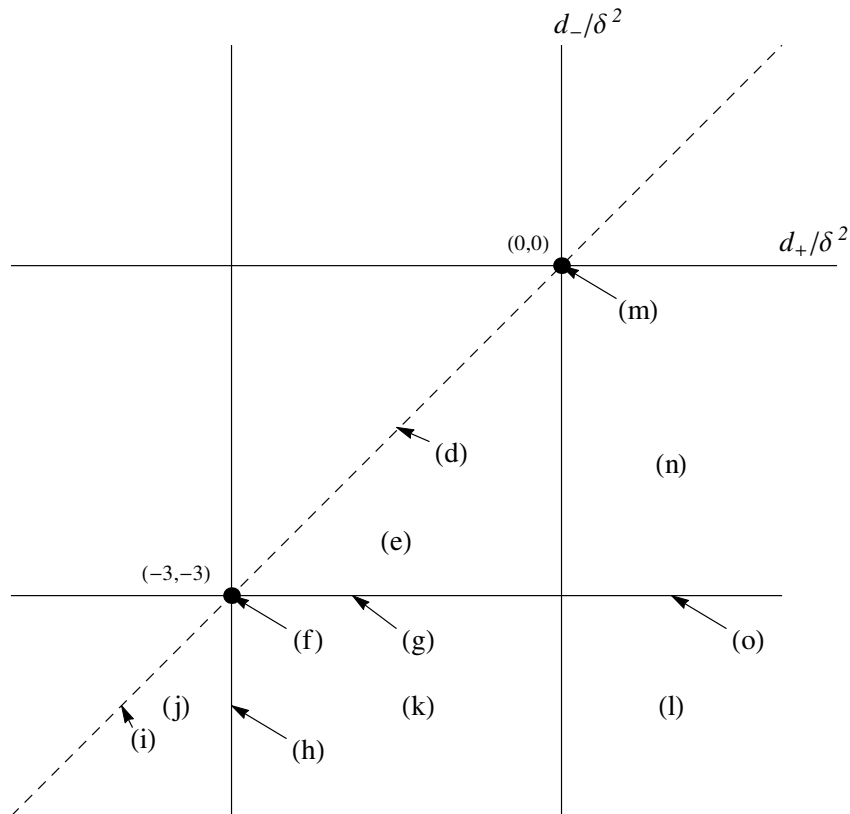


Figure 5.5: Bifurcation set of system (5.8) for $\delta > 0$. Note that by using Lemma 5.1(b), it is immediate to deduce the global phase portraits for the portion of the diagram which is symmetric with respect to the dashed main diagonal.

and $d = d_+$ in the right ones. Thus statement (i) is a direct consequence of statement (i) of Theorem 5.2.

If $\delta = 0$ and $d_- = -\kappa^2$ and $d_+ = -\nu^2$ with $-\nu^2 < -\kappa^2 < 0$ then system (5.8) has two real saddles at $(1/d_-, 0)$ and $(-1/d_+, 0)$ with eigenvalues $\pm\kappa$ and $\pm\nu$ respectively. and each orbit in the plane is an arc of the hyperbola

$$y^2 - \kappa^2 x^2 - 2x = C,$$

for $x \leq 0$, and the hyperbola

$$y^2 - \nu^2 x^2 + 2x = K,$$

for $x \geq 0$. Using the same proof method of statement (ii) Theorem 5.2 then the global phase portrait is as depicted in Figure 5.4(a) when $d_- = d_+ < 0$; Figure 5.4(b) when $d_+ < d_- < 0$ and Figure 5.4(c) when $d_- < 0$ and $d_+ \geq 0$. So statement (ii) follows.

If $\delta > 0$ and both $d_-, d_+ < 0$. for both regions we use the same technique used in the proof of statement (iii) of Theorem 5.2. Hence statement (iii) holds.

For $\delta > 0$, $d_- < 0$ and $d_+ \geq 0$ the left subsystem of system (5.8) has two real equilibrium $(1/d_-, 0)$ and $(1/d_-, 1/\delta)$ and the right one has only virtual equilibrium points when $d_+ > 0$. By using statement (iii) of Proposition 5.3 and the proof of statement (iii) of Theorem 5.2 the global phase portraits of system (5.8) are topologically equivalent to Figure 5.4(l) when $d_- < -3\delta^2$ and $d_+ \geq 0$; Figure 5.4(n) when $-3\delta^2 < d_- < 0$ and $d_+ \geq 0$ and Figure 5.4(o) when $d_- = -3\delta^2$ and $d_+ \geq 0$. If $d_- = d_+ = 0$ the situation is match simpler, since we have no real equilibrium points, system (5.8) has two infinite **SP**, as described in statement (iii) Proposition 5.3. Thus the global phase portrait is equivalent to the one shown in Figure 5.4(m). Statement (iv) follows and the proof is complete. ■

5.2.4 Reversible quadratic differential system

As our last case we consider the more generic case (5.9). We note first that when $t = 0$ system (5.9) becomes the Σ -reversible case ($d_+ = d_- = d$) of the piecewise Hamiltonian system (5.8). In such a degenerate situation, Theorem 5.3 applies, and we could reproduce for system (5.9) the global phase portraits of Figures 5.2(a), 5.4(a), and every case corresponding to points at the main diagonal in the bifurcation set of Figure 5.5. In short, the global phase portraits of Figures 5.2(a), 5.4(a), 5.4(d), 5.4(f), 5.4(i), and 5.4(m) are also admissible for system (5.9).

If $t \neq 0$ and $\delta = 0$ then from Lemma 5.1(a) there is no loss of generality in assuming $t > 0$. Thus, we get again a piecewise linear Σ -reversible family and several cases arise depending on the value of d , see the bifurcation set of Figure 5.7. When $d < 0$ (the saddle case S in Figure 5.7 we have again a phase portrait similar to the one of Figure 5.4(a), this time in a non-Hamiltonian situation. Other possible global phase portraits for system $t > 0$ and $\delta = 0$ appear for the singular case $d = 0$, see Figure 5.6(a), for the node case $0 < d < t^2/4$, see Figure 5.6(b), and for the improper node case $0 < d = t^2/4$, see Figure 5.6(c), while for the focus case $t^2/4 < d$ we have a global non-conservative pseudo-center, similar to the one of Figure 5.1(a). In the characterization of these phase portraits, we have used statement (iv) of Proposition 5.2.

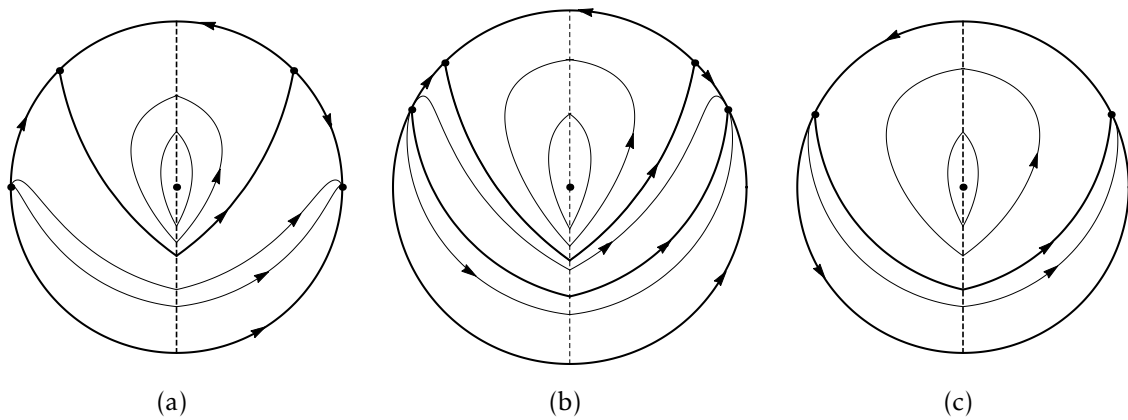


Figure 5.6: According to the bifurcation set of Figure 5.7, for $\delta = 0$ and $d \geq 0$ we have an unbounded periodic annulus. If we except the focus case (not shown), then such periodic annulus is limited from below because of the existence of invariant straight lines. We represent in (a) the singular case $d = 0$, in (b) the node case $0 < d < t^2/4$, and in (c) the improper node case $0 < d = t^2/4$.

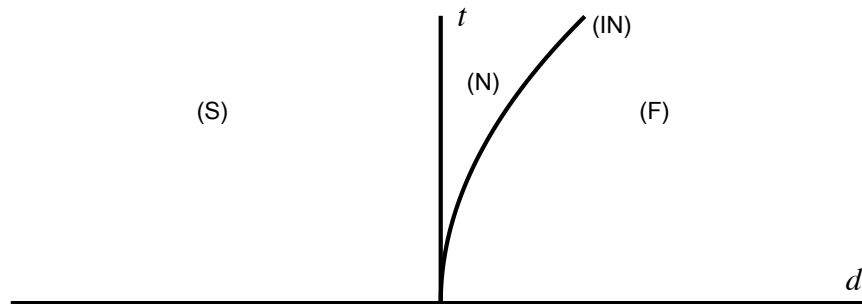


Figure 5.7: Bifurcation set of system (5.9) for $\delta = 0$ in the half-plane (d, t) with $t \geq 0$. We indicate the saddle region R, the node region N, the improper node curve IN and the focus region F.

If both $t \neq 0$ and $\delta \neq 0$ then we have in general three parameters. We observe that for system (5.10) there appears again the pseudo-saddle point at $(X, Y) = (0, 1)$, because it is

a double visible tangency point.

Possible real equilibria for system (5.10) can be analyzed by considering just the right subsystem because of the reversibility. We can conclude that when $\delta > 0$ and $d \geq 0$ in system (5.9) then there are no real equilibria, and global phase portraits in these cases are topologically equivalent to the one in Figure 5.4(m).

When in system (5.10) we have $d < 0$, the existence of equilibria for system (5.10), to be located at the line $X = -1/\tilde{d} > 0$, requires the existence of real roots for the quadratic equation $Y^2 - Y - \tilde{t}/\tilde{d} = 0$, with discriminant

$$\Delta = 1 + \frac{4\tilde{t}}{\tilde{d}} = 1 + \frac{4\delta t}{d}. \quad (5.41)$$

This discriminant changes its sign passing from negative to positive values in two different situations, both leading to saddle-node bifurcations of equilibria, where we pass from no equilibria to two of them (a saddle and a node, which emerge from a non-hyperbolic equilibrium point) or vice versa. Firstly, such saddle-node bifurcation appears for $\tilde{d} = -4\tilde{t}$ under the assumption $\tilde{t} > 0$, where the non-hyperbolic equilibrium point appears at $(X, Y) = (-1/\tilde{d}, 1/2)$. In the second place, when for $\tilde{t} < 0$ the value of \tilde{d} goes from a small positive value to a negative value passing through zero; then the saddle-node bifurcation comes from a singular point at infinity. When $\Delta > 0$ the two singular points are p_L and p_U , being both in the same vertical line.

Unfortunately, apart from the local bifurcations depicted in Figure 5.9, for $\delta > 0$ and in the presence of real equilibria there appear other bifurcation curves of global character that are associated to the relative position of the invariant manifolds of the saddle with respect to the orbits of the contact point $(X, Y) = (0, 1)$, where we have a double visible tangency. In fact, for the parameter values $(\tilde{t}, \tilde{d}) = (0, -3)$ we can take advantage of the Hamiltonian character of the system to compute the invariant algebraic curve

$$6X + 3\tilde{d}X^2 + 3Y^2 - 2Y^3 - 1 = 0,$$

which contains a homoclinic orbit to the saddle at $(X, Y) = (1/3, 0)$ and becomes tangent to the Y -axis precisely at the point $(X, Y) = (0, 1)$, see Figure 5.4(f). It can be conjectured that from the point $(0, -3)$ indicated in the bifurcation set of Figure 5.9 there should emerge some bifurcation curves for $\tilde{t} > 0$ and maybe some other for $\tilde{t} < 0$ where once broken the homoclinic orbit for $t \neq 0$, the tangent orbit at $(X, Y) = (0, 1)$ coincides either

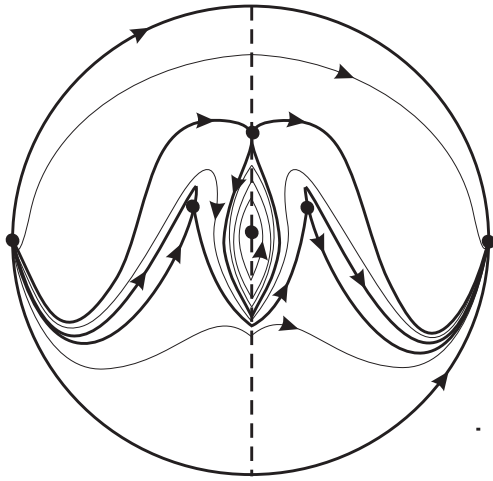
with one stable invariant manifold or with one unstable manifold of the saddle.

Since for $t \neq 0$ we cannot have analytical expressions for solutions, the mentioned global bifurcation curves should be obtained numerically, by continuation procedures. Therefore, the complete bifurcation set organizing all the possible global phase portraits of system (5.9) cannot be obtained by analytical methods and so it turns out to be beyond the scope of this paper. We will finish by showing some representative global phase portraits we have already detected for system (5.9), under the assumptions $\delta > 0$, $0 < 4\delta t \leq -d$, see Figure 5.8, so that the discriminant Δ in (5.41) is non-negative and we have real equilibria. For sake of convenience, we will refer to the equivalent system (5.10) with normalized parameters \tilde{t} and \tilde{d} .

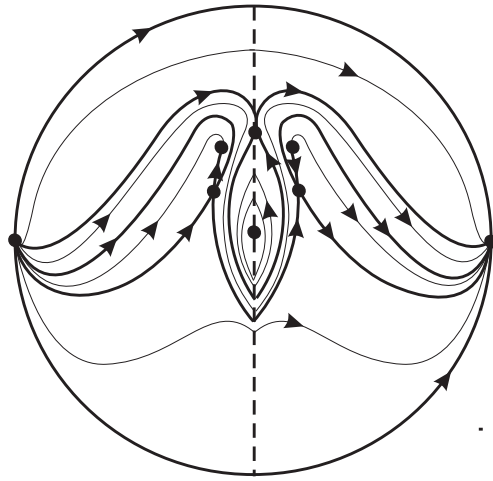
In Figure 5.8(a), we show a global phase portrait of our Σ -reversible family (5.10) for $0 < 4\tilde{t} = -\tilde{d}$, so that $\Delta = 0$ and we have a real non-hyperbolic saddle-node at $(X, Y) = (1/\tilde{d}, 1/2)$. The pseudo-center at the origin is bounded by the orbits passing through the contact point $(X, Y) = (0, 1)$. The drawn phase plane corresponds to the values $(\tilde{t}, \tilde{d}) = (\text{values})$.

If $0 < 4\tilde{t} < -\tilde{d}$, so that $\Delta > 0$, and $\tilde{t}^2 + 4\tilde{d}\sqrt{\Delta} > 0$, then system (5.10) has a real saddle at (X_L, Y_L) and a real unstable node at (X_U, Y_U) . In this case, the system has the global phase portraits of Figure 5.8(b), Figure 5.8(c) and Figure 5.8(d), where for drawing them we have used some representative values for (\tilde{t}, \tilde{d}) . For instance, fixed the value $\tilde{t} = 2$ and $-8.12 \leq \tilde{d} < -8$, we have the situation of Figure 5.8(b); if $\tilde{t} = 2.4$ and $-9.81 \leq \tilde{d} \leq -9.77$, we have the situation of Figure 5.8(c); finally, when $\tilde{t} = 2.46$ and $-10.06 \leq \tilde{d} \leq -10.05$, we have the situation of Figure 5.8(d).

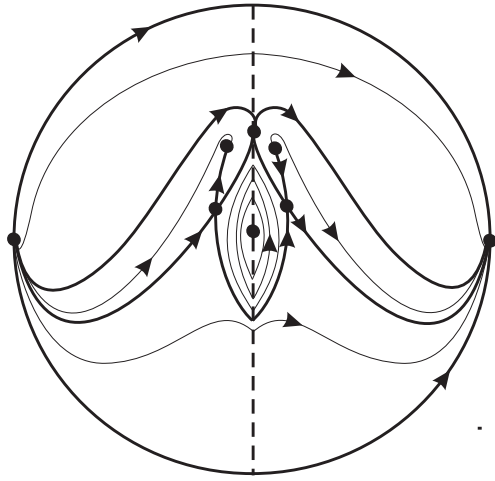
If $0 < 4\tilde{t} < -\tilde{d}$, so that $\Delta > 0$, but $\tilde{t}^2 + 4\tilde{d}\sqrt{\Delta} < 0$, then the real equilibria at (X_U, Y_U) is an unstable focus, which organizes the phase portraits. For instance, keeping fixed the value of $\tilde{t} = 0.1$, we note that when $\tilde{d} = -2.5$, we have the situation of Figure 5.8(e); when $\tilde{d} = -3.1$ we have the situation of Figure 5.8(f); for $\tilde{d} = -3.5$ we have the phase portrait Figure 5.8(g); the phase portrait of Figure 5.8(h) appears for $\tilde{d} = -4.2$; finally, when $\tilde{d} = -5$ we have the situation of Figure 5.8(i). Note that in this last case, we detect a second periodic annulus of crossing type that surrounds the two real foci, which makes such configuration specially interesting. Clearly, even we have shown its main different global phase portraits, system (5.10) deserves further research in order to complete its bifurcation set, in the sense we have mentioned before.



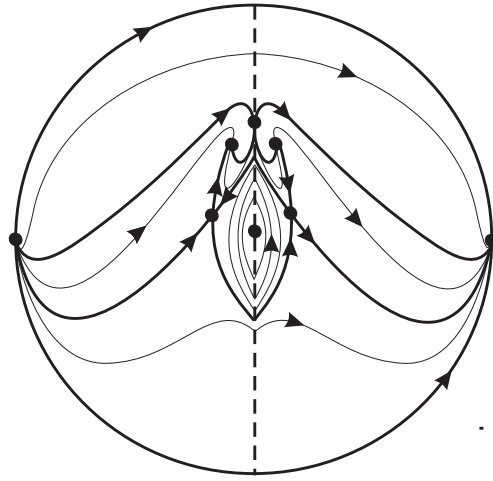
(a)



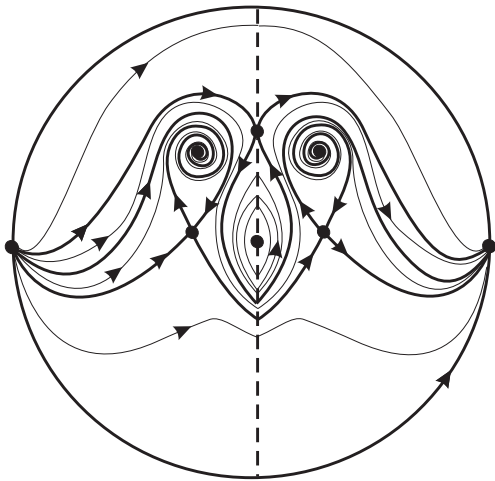
(b)



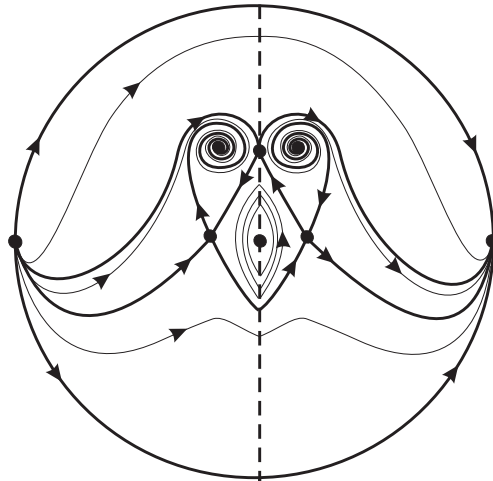
(c)



(d)



(e)



(f)

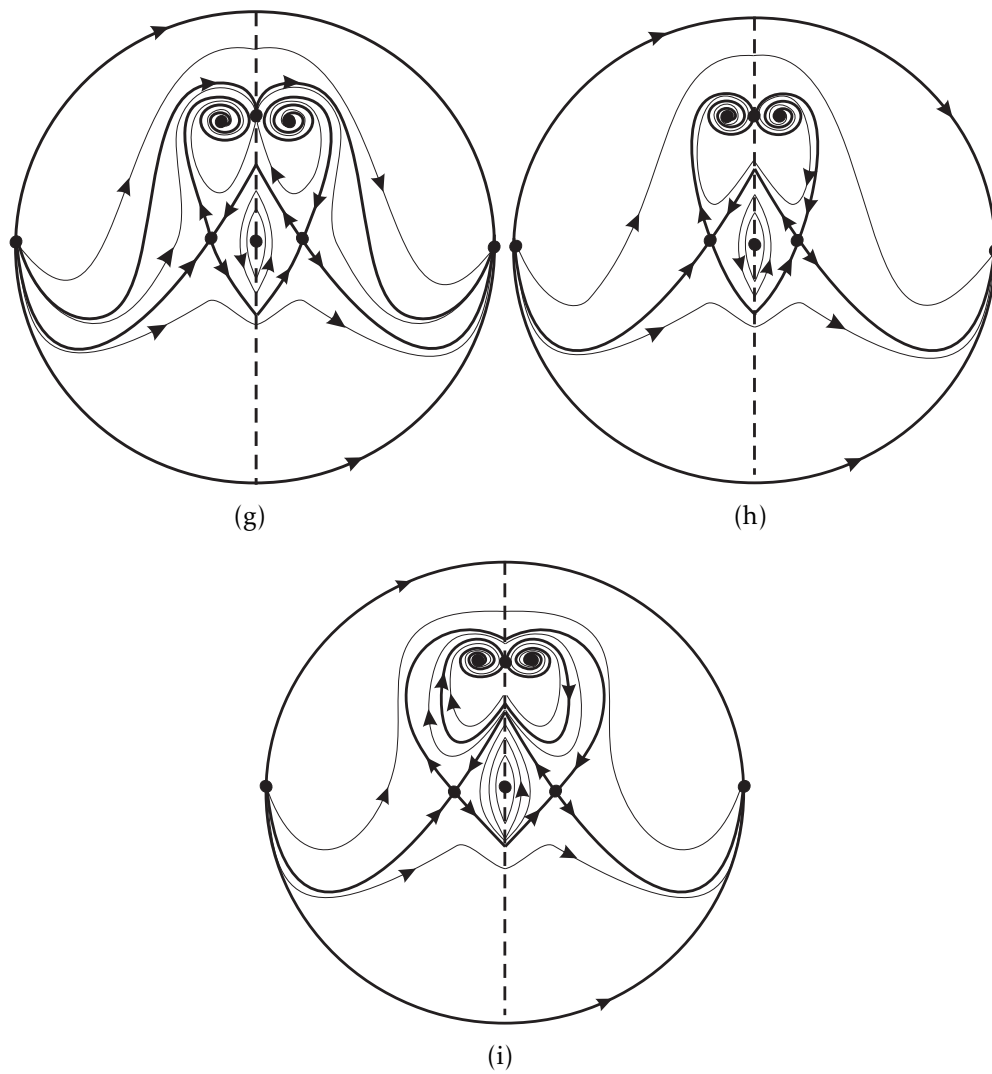


Figure 5.8: Some global phase portraits of system (5.10), where we assume $t > 0$, $d < 0$, and $\delta > 0$. The case (a) corresponds to $\delta > 0$, $d < 0$ and $4\delta t + d = 0$ (at the right saddle-node bifurcation straight line of Figure 5.9).

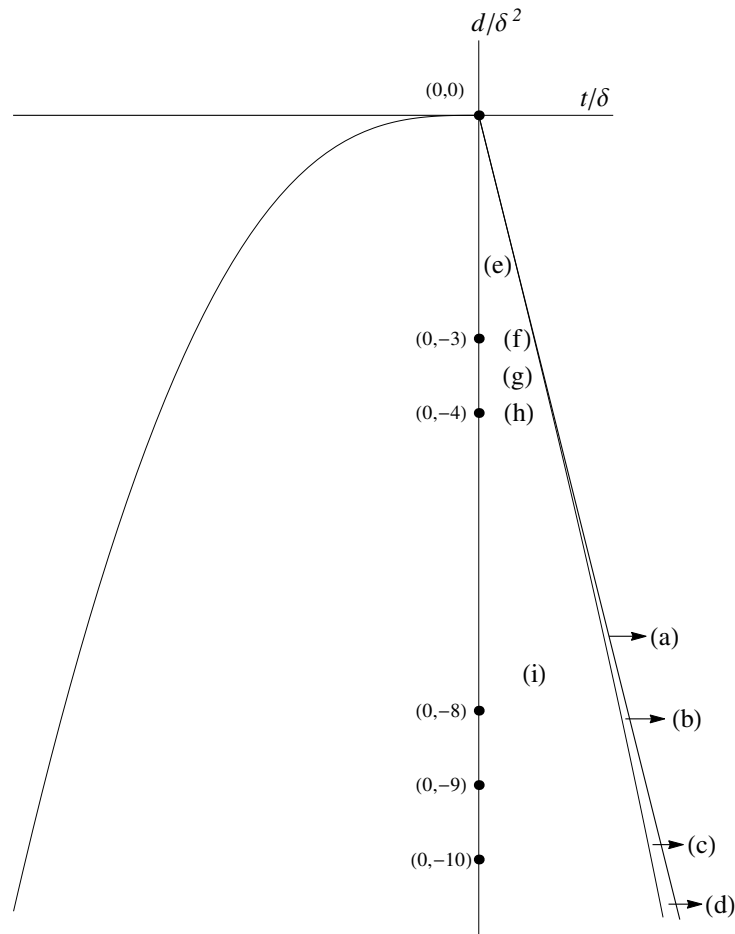


Figure 5.9: Partial bifurcation set of system (5.10) in the parameter plane $(\tilde{t}, \tilde{d}) = (t/\delta, d/\delta^2)$ when $\delta > 0$. The two thick half-straight lines emanating from the origin are saddle-node bifurcation curves, and we also show two nearby curves where the node becomes a focus. At the vertical axis we have $t = 0$, so that the system becomes piecewise-Hamiltonian, leading to the particular case $d_+ = d_- = d$, which is within the previous family (5.8).

Conclusion

In this work, firstly, we have solved the extension of the second part of the 16th Hilbert problem to some families of discontinuous piecewise differential systems. The first one is formed by linear center and a class of Hamiltonian isochronous global center of degree n separated by straight line. The second family is formed by linear and cubic isochronous centers separated by irregular line.

Secondly, we applied the averaging theory up to third order to finding the upper bound for the maximum number of limit cycles for the discontinuous piecewise differential systems formed by a linear focus or center and a cubic weak focus or center separated by the straight line $y = 0$.

Finally, we dealt with the global dynamics of planar piecewise quadratic differential systems with a pseudo-center at the origin. We classified there global phase portraits and there associated bifurcation sets.

Bibliography

- [1] Andronov, A., Vitt, A., Khaikin, S.: Theory of Oscillations. Pergamon Press. Oxford (1966)
- [2] Artés, J.C., Llibre, J., Medrado, J.C., Teixeira, M.A.: Piecewise linear differential systems with two real saddles. *Math. Comput. Simul.* **95**, 13-22 (2013)
- [3] Artés, J.C., Rezende, A.C., Oliveira, R.D.S.: Global phase portraits of quadratic polynomial differential systems with a semi-elemental triple node. *Int. J. Bifur. Chaos.* **23**, 1350140 (2013)
- [4] Barkat, M., Benterki, R., Llibre, J.: The extended 16th Hilbert problem for a class of discontinuous piecewise differential systems. *Nonlinear Dyn.* **111**, 1475–1484 (2023)
- [5] Barkat, M., Benterki, R.: Limit cycles of discontinuous piecewise differential systems formed by linear and cubic centers via averaging theory. *Differ Equ Dyn Syst* (2024)
- [6] Barkat, M., Benterki, R., Enrique, p.: Global phase portraits of piecewise quadratic differential systems with a pseudo-center. *Int. J. Bifur. Chaos.* **34**. No. 03, 2450032 (2024)
- [7] Belfar, A., Benterki, R., Llibre, J.: Limit cycles of planar discontinuous piecewise linear Hamiltonian systems without equilibrium points and separated by irreducible cubics. *Dyn. Contin. Discr. Impuls. Syst. Series B: Applications and Algorithms.* **28**. 399-421 (2021)
- [8] Belousov, B. H.: A periodic reaction and its mechanism. A collection of short papers on radiation medicine for 1958. Moscow. Med. Publ. in Russian (1959)

- [9] Benterki, R., Barkat, M.: Limit cycles of discontinuous piecewise differential systems formed by linear and cubic isochronous centers. *J. Math. Comput. Sci.* **12** (2022)
- [10] Benterki, R., Llibre, J.: The solution of the second part of the 16th Hilbert problem for nine families of discontinuous piecewise differential systems. *Nonlinear Dyn.* **102**, 2453–2466 (2020)
- [11] Benterki, R., Llibre, J.: Crossing limit cycles of planar piecewise linear Hamiltonian systems without equilibrium points. *Mathematics* 8. No. 5, Article No. 755, 14 pp (2020)
- [12] Benterki, R., Llibre, J.: Phase portraits of quadratic polynomial differential systems having as solution some classical planar algebraic curves of degree 4. *Electron. J. Differ. Equ.* 2019, Paper No. 15, 25 p (2019)
- [13] Benterki, R., Jimenez, J., Llibre, J.: Limit cycles of planar discontinuous piecewise linear Hamiltonian systems without equilibria separated by reducible cubics. *Electron. J. Differ. Equ.* **69**, 1-38 (2021)
- [14] Bernardo, M. di., Budd, C.J., Champneys, A. R., Kowalczyk, P.: Piecewise smooth dynamical systems. Theory and Applications. *Appl. Math. Sci. Series 163*. Springer-Verlag. London (2008)
- [15] Berezin, I., Zhidkov, N.: Computing methods. Pergamon Press. Volume II Oxford (1964)
- [16] Bogoliubov, N., Krylov, N.: The application of methods of nonlinear mechanics in the theory of stationary oscillations. *Publ. 8 of the Ukrainian Acad. Sci. Kiev* (1934)
- [17] Braga, D. C., Fonseca, A.F., Gonçalves, L.F., Mello, L.F.: Lyapunov coefficients for an invisible fold-fold singularity in planar piecewise Hamiltonian systems, *J Dyn Control Syst* **27**, 179–204 (2021)
- [18] Braga, D. C., Mello, L. F.: Limit cycles in a family of discontinuous piecewise linear differential systems with two zones in the plane, *Nonlinear Dyn.* **73**, 1283–1288 (2013)
- [19] Buzzi, C., Pessoa, C., Torregrosa, J.: Piecewise linear perturbations of a linear center. *Discrete Contin. Dyn. Syst.* **33**, 3915–3936 (2013)

- [20] Chavarriga, J., Sabatini, M.: A survey on isochronous centers. *Qual. Theory Dyn. Syst.* **1**, 1-70 (1999)
- [21] Chen, H., Wei, F., Xia, Y., Xiao, D.: Global dynamics of an asymmetry piecewise linear differential system. *Theory and Applications. Bull. Sci. Math.* **160**, 102858 (2020)
- [22] De Bustos, M. T., Guirao, J. L. G., Llibre, J., Vera, J. A.: New families of periodic orbits for a galactic potential. *Chaos Solitons Fractals.* **82**, 97–102 (2016)
- [23] Dumortier, F., Llibre, J., Artés, J.C.: *Qualitative theory of planar differential systems.* Springer. New York (2006)
- [24] Esteban, M., Freire, E., Ponce, E., Torres, F.: On normal forms and return maps for pseudo-focus points. *J. Math. Anal. Appl.* **507**, 125774 (2022)
- [25] Euzébio, R.D., Llibre, J.: On the number of limit cycles in discontinuous piecewise linear differential systems with two pieces separated by a straight line. *J. Math. Anal. Appl.* **424**(1), 475-486 (2015)
- [26] Fatou, P.: Sur le mouvement d'un système soumis à des forces à courte période. *Bull. Soc. Math. France.* **56**, 98–139 (1928)
- [27] Filippov, A.F.: *Differential equations with discontinuous right-hand sides.* translated from Russian. *Mathematics and its Applications. (Soviet Series) vol. 18,* Kluwer Academic Publishers Group, Dordrecht (1988)
- [28] Fonseca, A. F., Llibre, J., Mello, L. F.: Limit cycles in planar piecewise linear Hamiltonian systems with three zones without equilibrium points. *Int. J. Bifur. Chaos Appl. Sci. Engrg.* **30**. No. **11**, 2050157, 8 pp (2020)
- [29] Freire, E., Ponce, E., Rodrigo, F., Torres, F.: Bifurcation sets of continuous piecewise linear systems with two zones. *Int. J. Bifur. Chaos.* **8**, 2073-2097 (1998)
- [30] Freire, E., Ponce, E., Torres, F.: A general mechanism to generate three limit cycles in planar Filippov systems with two zones. *Nonlinear Dyn.* **78**, 251–263 (2014)
- [31] Giannakopoulos, F., Pliete, K.: Planar systems of piecewise linear differential equations with a line of discontinuity. *Nonlinearity.* **14**, 1611–1632 (2001)

- [32] Han, M., Yang, J.: The maximum number of zeros of functions with parameters and application to differential equations. *J. Nonlinear Model. Anal.* **3**, 13–34 (2021)
- [33] Han, M.: On the maximum number of periodic solutions of piecewise smooth periodic equations by average method. *J. Appl. Anal. Comput.* **7**(2), 788–794 (2017)
- [34] Han, M., Zhang, W.: On hopf bifurcation in non-smooth planar systems. *J. Differential Equations.* **248** (9), 2399–2416 (2010)
- [35] Hilbert, D.: *Mathematische Probleme. Lecture. Second Internat. Congr. Math. (Paris, 1900).* *Nachr. Ges. Wiss. Göttingen Math. Phys. Kl.*, 253-297 (1900) English transl. *Bull. Amer. Math. Soc.* **8**, 437-479 (1902) *Bull. (New Series) Amer. Math. Soc.* **37**, 407–436 (2000)
- [36] Ilyashenko, Yu.: Centennial history of Hilbert’s 16th problem. *Bull. (New Series) Amer. Math. Soc.* **39**, 301-354 (2002)
- [37] Itikawa, J., Llibre, J., Novaes, D.D.: A new result on averaging theory for a class of discontinuous planar differential systems with applications. *Rev. Mat. Iberoam.* **33**, 1247–1265 (2017)
- [38] Li, J.: Hilbert’s 16th problem and bifurcations of planar polynomial vector fields. *Int. J. Bifur. Chaos Appl. Sci. Engrg.* **13**, 47-106 (2003)
- [39] Li, L.: Three crossing limit cycles in planar piecewise linear systems with saddle-focus type. *Electron. J. Qual. Theory Differ. Equ.* No. **70**, 1–14 (2014)
- [40] Li, S., Llibre, J.: Phase portraits of piecewise linear continuous differential systems with two zones separated by a straight line. *J. Differ. Equ.* **266**, 8094–8109 (2019)
- [41] Llibre, J., Mereu, A.C., Novaes, D.D.: Averaging theory for discontinuous piecewise differential systems. *J. Differ. Equ.* **258**(11), 4007–4032 (2015)
- [42] Llibre, J., Novaes, D.D., Rodrigues, C.A.B.: Averaging theory at any order for computing limit cycles of discontinuous piecewise differential systems with many zones. *Phys. D Nonlinear Phenom.* **353**, 1–10 (2017)
- [43] Llibre, J., Novaes, D.D., Teixeira, M.A.: Higher order averaging theory for finding periodic solutions via Brouwer degree. *Nonlinearity.* **27**, 563-583 (2014)

- [44] Llibre, J., Novaes, D.D., Teixeira, M.A.: On the birth of limit cycles for non-smooth dynamical systems. *Bull. Sci. Math.* **139**(3), 229–244 (2015)
- [45] Llibre, J., Novaes, D. D., Teixeira, M. A.: Maximum number of limit cycles for certain piecewise linear dynamical systems. *Nonlinear Dyn.* **82**, No. 3, 1159–1175 (2015)
- [46] Llibre, J., Ponce, E.: Three nested limit cycles in discontinuous piecewise linear differential systems with two zones. *Dyn. Contin. Discr. Impul. Syst., Ser. B, Appl. Algorithms* **19**, 325–335 (2012)
- [47] Llibre, J., Ponce, E., Torres, F.: On the existence and uniqueness of limit cycles in Liénard differential equations allowing discontinuities, *Nonlinearity*. **21**, 2121–2142 (2008)
- [48] Llibre, J., Świrszcz, G.: On the limit cycles of polynomial vector fields., *Dyn. Contin. Discrete Impuls. Syst. Ser. A Math. Anal.* **18**, 203-214 (2011)
- [49] Llibre, J., Teixeira, M.A.: Piecewise linear differential systems with only centers can create limit cycles ?. *Nonlinear Dyn.* **91**, 249-255 (2018)
- [50] Llibre, J., Teruel, A. E.: Introduction to the qualitative theory of differential systems. Planar. symmetric and continuous piecewise linear systems. *Birkhäuser Advanced Texts. Basler Lehrbücher.* Basel: Birkhäuser/Springer (ISBN 978-3-0348-0656-5/hbk; 978-3-0348-0657-2/ebook). xiii, 289 p (2014)
- [51] Llibre, J., Yu, J.: Global phase portraits of quadratic systems with an ellipse and a straight line as algebraic curves, *Electron. J. Differ. Equ. Paper No.* **314**, 14 p (2015)
- [52] Makarenkov, O., Lamb, J.S.W.: Dynamics and bifurcations of nonsmooth systems. a survey. *Phys. D.* **241**, 1826–1844 (2012)
- [53] Mañosas, F., Villadelprat, J.: Area-preserving normalizations for centers of planar Hamiltonian systems. *J. Differ. Equ.* **197**, 625-646 (2002)
- [54] Perko, L.: Differential equations and dynamical system. *Texts in Applied Mathematics.* 7. Springer. xiv. New York. NY. 553 p (2001)
- [55] Poincaré, M.: Mémoire sur les courbes définies par une équations différentielle. IV. *J. Math, Pures Appl, Sér.* **4**(2), 155-217 (1886)

- [56] Reyn, J.: Phase portraits of planar quadratic systems. Mathematics and its Applications. 583. Springer. New York (2007)
- [57] Sabatini, M.: A connection between isochronous Hamiltonian centers and the Jacobian conjecture. Nonlinear Analysis. **34**, 829-838 (1998)
- [58] Shao, Y., Guan, H., Li, S., Fu, H.: The global dynamics of linear refracting systems of focus-node or center-node type. Nonlinear Analysis: Real World Applications. **71**, 103826 (2023)
- [59] Shao, Y., Li, S., Zhang, X.: Limit cycles and global dynamics of planar piecewise linear refracting systems of focus-focus type. Nonlinear Analysis. Real World Applications. **58**, 103228 (2021)
- [60] Simpson, D.J.W.: Bifurcations in piecewise-smooth continuous systems. World Scientific Series on Nonlinear Science A. vol. **69**. World Scientific. Singapore (2010)
- [61] Uribe, M., Movasati., H.: Limit cycles. Abelian integral and Hilbert's sixteenth Problem. Publicações Matemáticas do IMPA. Rio de Janeiro: Instituto Nacional de Matemática Pura Aplicada (IMPA) (ISBN 978-85-244-0437-5/pbk). **106** p. openaccess (2017)
- [62] Van Der Pol, B.: On relaxation-oscillations. The London. Edinburgh and Dublin ppil. Mag. and J. of Sci. **2**, pp, 978–992 (1926)
- [63] Wei, L., Zhang, X.: Averaging theory of arbitrary order for piecewise smooth differential systems and its application. J. Dyn. Differ. Equ. **30** , 55–79 (2018)
- [64] Xiu, Q., Pi, D.: Bifurcation analysis of a class of planar piecewise smooth linear-quadratic system. Annals of Applied Mathematics. **36**, 282-308 (2021)
- [65] Xiong, L., Wu, K., Li, S.: Phase portraits of the discontinuous planar piecewise linear differential systems of focus-center type. Qual. Theory Differ. syst. **21**:78 (2022)
- [66] Zhao, H., Wu, K., Shao, Y.: Global dynamics of a planar piecewise linear refracting system of node-node types. Int. J. Bifur. Chaos. **32**, 2250201 (2022)

ملخص:

تناولنا في هذه الأطروحة دراسة بعض الأنظمة الغير خطية و المنفصلة حيث أننا قمنا بحل الجزء الثاني من مسألة هيلبرت السادسة عشر لفئة من الأنظمة التفاضلية باستعمال التكاملات الأولى لها. كما ركزنا على إيجاد الحد الأقصى لعدد الدورات الحدية عن طريق استخدام نظرية المتوسط، و في الاخير تمكنا من إيجاد الحلول الهندسية في قرص بوانكاريه للأنظمة التفاضلية التربيعية المتقطعة والتي تتميز بوجود مركز زائف.

الكلمات المفتاحية:

أنظمة تفاضلية منفصلة، النظام المركزي الخطي، المركز العالمي الايزوكروني، نظرية المتوسط، المركز الزائف، صور المرحلة.

Abstract:

Our thesis is divided in three parts, the first part consists in solving the second part of the extended 16th Hilbert problem for a class of discontinuous piecewise differential systems. The second part focuses on finding the maximum number of limit cycles of small amplitude which is called the cyclicity problem, and the third part we were able to find the global phase portraits and the bifurcation sets for some specific families of discontinuous piecewise quadratic differential systems, characterized by having a pseudo-center at the origin.

Keywords:

Piecewise differential system, Linear center, Hamiltonian isochronous global center, Averaging theory, Pseudo-center, Phase portrait.

Résumé:

Notre thèse est divisée en trois parties. La première partie consiste à résoudre la deuxième partie du seizième problème d'Hilbert pour une classe de systèmes différentiels discontinus par morceaux. La deuxième partie se focalise sur la recherche du nombre maximal de cycles limites de petite amplitude, appelé problème de cyclicité. Enfin, dans la troisième partie, nous avons réussi à trouver les portraits de phase globaux et les ensembles de bifurcation pour certaines familles de systèmes différentiels quadratiques discontinus par morceaux, avec un pseudo-centre à l'origine.

Mots clés:

Systèmes différentiels par morceaux, centre linéaire, Centre global isochrone Hamiltonien, Théorie de la moyenne, Pseudo-centre, Portrait de phase.